PUBLICATIONS OF
THE UNIVERSITY OF EASTERN FINLAND

Dissertations in Forestry and Natural Sciences

ABHISEK BHATTARAI

NOVEL DUAL-CONTRAST COMPUTED TOMOGRAPHY TECHNIQUE FOR DETECTION OF CARTILAGE INJURIES

NOVEL DUAL-CONTRAST COMPUTED TOMOGRAPHY TECHNIQUE FOR DETECTION OF CARTILAGE INJURIES

PUBLICATIONS OF THE UNIVERSITY OF EASTERN FINLAND
DISSERTATIONS IN FORESTRY AND NATURAL SCIENCES

N:o 392

Abhisek Bhattarai

NOVEL DUAL-CONTRAST COMPUTED TOMOGRAPHY TECHNIQUE FOR DETECTION OF CARTILAGE INJURIES

ACADEMIC DISSERTATION

To be presented by the permission of the Faculty of Science and Forestry for public examination in the Auditorium SN200 in the Snellmania Building at the University of Eastern Finland, Kuopio, on 16th October 2020, at 15 o'clock.

University of Eastern Finland
Department of Applied Physics
Kuopio 2020

Grano Oy
Jyväskylä, 2020
Editors: Pertti Pasanen, Raine Kortet,
Jukka Tuomela, Matti Tedre

Distribution:
University of Eastern Finland / Sales of publications
http://www.uef.fi/kirjasto

ISBN: 978-952-61-3576-2 (nid.)
ISSNL: 1798-5668
ISSN: 1798-5668
ISBN: 978-952-61-3577-9 (pdf)
ISSNL: 1798-5668
ISSN: 1798-5676

Author's address: University of Eastern Finland
Department of Applied Physics
P.O. Box 1627, 70211 Kuopio, Finland
email: abhisek.bhattarai@uef.fi, abhisek89@hotmail.com

Supervisors: Professor Juha Töyräs
University of Eastern Finland
Department of Applied Physics
Kuopio, Finland
The University of Queensland
School of Information Technology and
Electrical Engineering
Brisbane, Australia
email: juha.toyras@uef.fi

Dean Jukka Jurvelin
University of Eastern Finland
Faculty of Forestry and Natural Sciences
Kuopio, Finland
email: jukka.jurvelin@uef.fi

Janne Mäkelä, Ph.D.
University of Eastern Finland
Department of Applied Physics
Kuopio, Finland
email: janne.makela@uef.fi

Behdad Pouran, Ph.D.
Utrecht University
Utrecht, The Netherlands
email: b.pouran@umcutrecht.nl

Reviewers: Associate Professor Greet Kerckhofs
Institute of Mechanics, Materials, and Civil Engineering
UCLouvain, Louvain-la-Neuve; Belgium
email: greet.kerckhofs@uclouvain.be

Assistant Professor Adam Wang
Department of Radiology
Stanford University
email: adamwang@stanford.edu

Opponent: Assistant Professor, Sarah Manske
McCaig Institute for Bone and Joint Health
Department of Radiology
Cumming School of Medicine
University of Calgary
email: smanske@ucalgary.ca

Bhattarai, Abhisek
NOVEL DUAL-CONTRAST COMPUTED TOMOGRAPHY TECHNIQUE FOR DETECTION OF CARTILAGE INJURIES
Kuopio: University of Eastern Finland, 2020
Publications of the University of Eastern Finland
Dissertations in Forestry and Natural Sciences 2020; 392

ABSTRACT

The early detection of cartilage injuries is important for preventing further tissue degeneration leading to post-traumatic osteoarthritis (PTOA). However, the currently available diagnostic techniques such as magnetic resonance imaging, ultrasound imaging, and radiography lack sensitivity in making a reliable detection of either acute injuries or the initial signs of post-traumatic degeneration surrounding the original injury. Contrast-enhanced computed tomography enables the detection of cartilage loss at lesion sites, segmentation of articulating tissues, and information on the diffusion of contrast agents into tissues. The diffusion of the contrast agent is controlled by cartilage composition and integrity, thus providing information on the lesion severity and the possible initiation of post-traumatic damage. Novel cationic contrast agents have shown superior diagnostic sensitivities at diffusion equilibrium as compared to conventional anionic agents. However, the cartilage degeneration related loss in the proteoglycan content, and the increase in the water content, diminish the sensitivity of cationic agents at clinically relevant early diffusion time-points.

The overall aim of this thesis project was to develop a quantitative dual-energy computed tomography technique (QDECT) for cartilage diagnostics; the first hypothesis was that the diagnostic sensitivity of a cationic agent could be enhanced by determining the diffusion that would be only related to the PG content and in that way it could nullify the contribution of the tissue water content and permeability to diffusion. To achieve this aim, a cationic iodine-based agent (CA4+), sensitive to the proteoglycan content, was used simultaneously with a non-ionic gadolinium-based agent (gadoteridol), sensitive to the water content and permeability. The second hypothesis was that the simultaneous quantification of iodine and gadolinium-based contrast agent would be possible with the use of dual-energy CT. Based on the diffusion of both contrast agents, it would be possible to separately quantify the contents of two important constituents of cartilage (i.e., PG and water). Further, it was hypothesized that normalization of the partition of a cationic contrast agent with that of a non-ionic agent would enhance the sensitivity of the cationic agent to

quantify the PG content, potentially improving cartilage diagnostics beyond the reach of the conventional techniques.

In study I, a dual-contrast technique was developed to quantify cationic and non-ionic contrast agent partitions in cartilage after immersion (72 h) in a mixture of CA4+ and gadoteridol, using a high-resolution microtomography scanner. In study II, we evaluated the potential of the dual-contrast technique to assess quantitatively both the biomechanical and histological characteristics of human articular cartilage. In study III, the effect of depth-dependent variation in cartilage constituents on the diffusion of contrast agents (CA4+ and gadoteridol) was examined.

In study I, CA4+ partition in bulk tissue, normalized or non-normalized by gadoteridol partition, correlated significantly with the cartilage equilibrium, instantaneous, and dynamic moduli, and the histological tissue ICRS grade. When inspecting the top 500 μm layer of cartilage, the normalized CA4+ partition with gadoteridol partition revealed a higher correlation with the cartilage equilibrium modulus. In study II, the correlation coefficient between the CA4+ partition and cartilage PG content improved as the diffusion time increased (10 min to 72 h). The normalized CA4+ partition correlated significantly with the PG content at earlier time-points, as compared with the non-normalized CA4+. When calculated at all time-points, the normalized partition correlated significantly with the histopathological-histochemical grade, i.e., the Mankin score. In study III, the CA4+ partition was found to be inversely controlled ($p < 0.05$) by the water content in superficial and mid-cartilage. In mid- and deep cartilage, PGs controlled ($p < 0.05$) the CA4+ partition. Throughout the cartilage thickness, the gadoteridol partition correlated inversely ($p < 0.05$) with the collagen concentration. Cartilage degeneration substantially increased the time for CA4+ to reach the bone-cartilage interface, whereas tissue degeneration decreased the diffusion time of gadoteridol.

To conclude, the QDECT technique enables simultaneous quantitative evaluation of cartilage PG and water contents, and characterization of cartilage structural and functional status. The present results are valuable in the development of novel contrast agents or optimizing the timing of delayed contrast-enhanced imaging of joints. This work also clarified the diffusion mechanisms of two different contrast agents and indicated the depth- and time-dependent relations of diffusion characteristics with articular cartilage constituents, PGs, collagen and water The QDECT technique has the potential to be exploited in the sensitive diagnostics of various joint conditions, especially the extent of articular cartilage degeneration. However, the technique is far from being ready for clinical application and warrants further research.

National Library of Medicine Classification: *QT 36, WN 160, WN 206, WE 300, WE 348, WE 870, WE 872*

Medical Subject Headings: *Cartilage, Articular/diagnostic imaging; Cartilage, Articular/injuries; Knee Joint; Osteoarthritis/diagnosis; Proteoglycans; Collagen; Water; Tomography, X-Ray Computed; Contrast Media; Diffusion; Permeability; Iodine Compounds; Gadolinium; Humans*

Yleinen suomalainen ontologia: *nivelrusto; nivelrikko; polvet; proteoglykaanit; kollageenit; vesi; kuvantaminen; tietokonetomografia; varjoainetutkimus; diffuusio; läpäisevyys*

ACKNOWLEDGEMENTS

The study was carried out during the years 2016-2020 in the Department of Applied Physics, University of Eastern Finland.

First and foremost, I would like to extend my deepest gratitude and special thanks to my principal supervisor Professor Juha Töyräs, Ph.D. for his valuable guidance and encouragement throughout the studies. His work ethic, discipline, and passion were a great motivating factor in completing the Ph.D. thesis. I extend my deepest gratitude towards my supervisor Dean Jukka Jurvelin, Ph.D. for giving me the opportunity to work in the BBC group. His support during the studies has been unparalleled. I also wish to extend my gratitude and thanks to my supervisor Janne Mäkelä, Ph.D. for his guidance and support throughout the studies. I am grateful to my supervisor Behdad Pouran for his support during the studies, especially during the diffusion experiments.

I would like to thank the official reviewers of this thesis, Associate Professor Greet Kerckhofs, Ph.D., and Assistant Professor Adam Wang Ph.D., for their professional review and constructive comments. I am grateful to all my co-authors for their significant contributions. Special thanks to Professor Mark Grinstaff, Ph.D. and Mikael Turunen, Ph.D. for their guidance and sharing innovative ideas.

It has been a privilege to interact and work with colleagues in the Biophysics of Bone and Cartilage (BBC) research group (names in alphabetical order): Aapo, Ali, Amigo (Gustavo), Amir, Annina, Ari, Atte, Christina, Chuby, Elvis, Ervin, Hans, Heta, Jari, Juuso, Kata, Lauri, Lasse, Lingwei, Markus, Mika M., Mikko F., Mikko N., Miitu, Mimmi, Mithilesh, Mohammad, Niina, Olli, Petri T., Petri P., Petro, Rubina, Sami, Satu, Simo, Teemu, Tulashi, and Tuomas. Cheers to my friends and coaches of Crossfit Kuopio, and players of our weekly floorball and basketball games at the University. Thanks to Juha for introducing me to alpine skiing, scuba diving, and for organizing international gatherings. It helped in keeping the spirit of the team high. Cheers to Rami for reminding us the summer has arrived by organizing the legendary Ranch parties.

I also wish to thank The Academy of Finland, Kuopio University Hospital, Department of Applied Physics, and Instrumentarium Science Foundation for supporting my thesis.

I thank my family and friends for the continuous support and encouragement throughout. I am tremendously grateful to my parents and sister for always believing in me. Last, but certainly not least, my beloved wife. Thank you for your patience

and the understanding you have expressed during these long working hours and for your continuous support.

In memory of my Grandparents,
Kuopio, 28th September 2020
Abhisek

LIST OF ORIGINAL PUBLICATIONS

This thesis is based on data presented in the following articles, referred to in the text by the Roman numerals I-III.

I. Bhattarai A, Honkanen JTJ, Myller KAH, Prakash M, Korhonen M, Saukko AEA, Viren T, Joukainen A, Patwa AN, Kröger H, Grinstaff MW, Jurvelin JS, Töyräs J. "Quantitative Dual Contrast CT Technique for Evaluation of Articular Cartilage Properties." *Annals of Biomedical Engineering,* 2018. 46(7):1038-1046.

II. Bhattarai A, Pouran B, Mäkelä JTA, Shaikh R, Honkanen MKM, Prakash M, Kröger H, Grinstaff MW, Weinans H, Jurvelin JS, Töyräs J. "Dual Contrast in Computed Tomography Allows Earlier Characterization of Articular Cartilage over Single Contrast." *Journal of Orthopaedic Research,* 2020.38(10):2230-2238.

III. Bhattarai A, Mäkelä JTA, Pouran B, Weinans H, Kröger H, Grinstaff MW, Töyräs J, Turunen MJ. "Effect of Human Articular Cartilage Constituents on Simultaneous Diffusion of Cationic and Non-ionic Contrast Agents." *Journal of Orthopaedic Research,* 2020 in press.

Throughout the thesis, these papers are referred to by Roman numerals. The original articles have been reproduced with the permission of copyright holders.

AUTHOR'S CONTRIBUTION

The publications in this dissertation are original research papers on quantitative dual-energy computed tomography of human articular cartilage. The author has been the main contributor to the planning and design of each paper. The author carried out all the contrast agent diffusion experiments and analysis and is the main writer of each paper. The collaboration and contribution of the co-authors in all of the studies have been substantial.

CONTENTS

LIST OF ABBREVIATIONS

2D	Two-dimensional
3D	Three-dimensional
CA4+	Contrast agent bearing four positive charges
CT	Computed tomography
DD	Digital densitometry
dGEMRIC	Delayed gadolinium enhanced magnetic resonance imaging of cartilage
ECM	Extracellular matrix
EDTA	Ethylenediaminetetraacetic acid disodium salt
FCD	Fixed Charge Density
FTIR	Fourier transform infrared spectroscopy
GAG	Glycosaminoglycan
ICRS	International Cartilage Repair Society
NaI	Sodium Iodide
NCP	Non-collagenous protein
microCT	X-ray microtomography
MRI	Magnetic resonance imaging
OA	Osteoarthritis
OARSI	Osteoarthritis Research Society International
OD	Optical density
PBS	Phosphate buffered saline
PG	Proteoglycan
PTOA	Post-traumatic osteoarthritis
QDECT	Quantitative dual-energy computed tomography
SD	Standard deviation
SNR	Signal-to-noise ratio

SYMBOLS AND NOTATIONS

α	X-ray attenuation
C	Solute concentration
C_{max}	Concentration maximum
D	Diffusion coefficient
E	Energy
$E_{equilibrium}$	Equilibrium modulus
$E_{instantaneous}$	Instantaneous modulus
Gd	Gadolinium
h	Thickness of the tissue
I	Intensity
I_o	Initial intensity
I	Iodine
J	Diffusion flux
M	Magnification
μ	Mass attenuation coefficient
n	Number of samples
O	Original object
O_i	Magnified object
p	Level of statistical significance
q	Electric charge
R	Gas constant
ρ	Spearman's rho
T	Temperature
t	Time
x	Distance
z	Valence of the ion
Z	Atomic number

1 INTRODUCTION

Articular cartilage is a connective tissue covering the ends of the articulating bones; it enables smooth nearly frictionless motion and distributes contact loads evenly throughout the joint [1,2]. Cartilage is aneural and avascular. It is primarily composed of collagen, proteoglycans (PGs), chondrocytes, and interstitial water. These are the essential constituents of cartilage, and any disruption of the components alters the tissue functioning. Trauma or a fall may lead to joint pain, swelling, and difficulty in locomotion, potentially initiating the development of post-traumatic osteoarthritis (PTOA). Cartilage bruising from a fall or a sports accident is a common injury affecting millions of people [3]. In the United States alone, 5 million adults are affected by PTOA [4]. The development of PTOA after cartilage damage, or ligament instability (chronic/acute), or a combination of both, is common [4]. Osteoarthritis (OA) is characterized by the deterioration of the cartilage and the subchondral bone, impairing the smooth movement between the bones in joints, and the distribution of the load. The degradation of the tissue is typically unnoticed until the patient is at a later stage of the disease when he/she starts to feel pain. Unfortunately, current diagnostic techniques have only a limited ability to detect cartilage injuries in its early stages. Therefore, effective intervention to hinder the development of PTOA becomes challenging. Consequently, in order to identify cartilage injuries at the early stages of PTOA, the development of new diagnostic methods is imperative.

Native X-ray imaging is commonly used for the clinical evaluation of joint integrity. The diagnosis of OA is based on the evaluation of joint space and alterations in the structure of subchondral bone [5]. Soft-tissues are hardly visible in native radiographs, and joint space narrowing and alterations in the structure of bone occur in the latest stages of OA [6]. The diagnosis can be confirmed with ultrasound, contrast-enhanced CT, MRI, or arthroscopy [6,7]. Arthroscopic ultrasound can identify mechanically degraded cartilage and distinguish differences between healthy and arthritic cartilage [8–10]. However, the natural curvature of the articular cartilage surface can lead to an increase in the ultrasound beam angle (i.e., > 5º), leading to unreliable results [7]. MRI provides sufficient soft-tissue contrast and serves as the gold standard in assessing hyaline cartilage [7]. However, MRI scanners are expensive, and patients often face long queue times [7]. Computed tomography (CT) is a more readily available alternative to MRI. The image acquisition time of a clinical CT is short with excellent image resolution compared to MRI. Specialized coils and sequences are not needed in CT, but if one wishes to evaluate the condition

of soft tissues (e.g., cartilage), then the use of contrast agents is necessary. However, a major advantage of contrast-enhanced CT is the simultaneous imaging of cartilage and bone, which is crucial in the diagnosis of arthritic conditions [11,12].

The early signs of cartilage degeneration include disruption of superficial collagen, loss of PGs, and increase in water content [13]. Delayed gadolinium-enhanced magnetic resonance imaging of cartilage (dGEMRIC) and delayed contrast-enhanced computed tomography (dCECT) assess cartilage health by reflecting these early changes [14–18]. The degeneration of the solid constituents (PG, collagen) and the increased water content (swelling) increase permeability, which affects the diffusion of contrast agents into cartilage [19–22]. Thus, by quantifying the diffusion of the contrast agent into cartilage using dCECT, acute injuries, lesions and areas undergoing macroscopic changes can be identified [21,23–25]. The diffusion of anionic and cationic agents into cartilage is inversely and directly proportional to the fixed charge density that the PG creates inside the tissue, respectively. Cationic agent, such as iodine (I)-based CA4+, is significantly more sensitive to the PG loss than its anionic counterparts [23,26–29]. However, the loss of the PGs and the increased permeability occur simultaneously, having opposite effects on cationic agent diffusion, leading to a reduced sensitivity to detect alterations before diffusion equilibrium has been reached inside the tissue, i.e., during the first hours after an intra-articular administration [16]. This limitation of the CA4+ could be overcome by nullifying the effect of the tissue permeability and water content to the diffusion, i.e., determining the agent uptake only due to the cartilage PG content. It was hypothesized that this could be achieved by combining CA4+ with a non-ionic contrast agent, such as the gadolinium-based agent, gadoteridol. Gadoteridol has no electrical affinity for the negatively charged PGs and diffuses freely based on the tissue permeability and water content [29,30]. Hence, by normalizing (i.e., dividing) the partition of CA4+ in cartilage with that of gadoteridol, the sensitivity of CA4+ to quantify PG content could be improved [30,31].

This thesis focuses on the development of a quantitative technique to assess cartilage PG and water contents, by simultaneously determining the partitions of iodine-based cationic and gadolinium-based non-ionic contrast agents. It is recognized that iodine and gadolinium have well-separated photoelectric absorption edges. Therefore, by scanning using two separate X-ray energies, it should be possible to make a simultaneous quantitative evaluation of the partition of both agents in cartilage. As water and PG contents are major indicators of cartilage health, this quantitative dual-energy computed tomography (QDECT) technique may improve diagnostic sensitivity, allowing for the early detection of minor or more acute cartilage injuries. This is not possible with the diagnostic techniques currently

available in clinics. The thesis comprises three independent studies: In study **I**, the potential of the QDECT technique to assess the depth-wise molar concentration of CA4+ and gadoteridol in human articular cartilage plugs is explored, after 72 h of immersion in a bath mixture of the contrast agents. The concentrations were used to examine the sensitivity of the technique to probe changes in the biomechanical properties of cartilage. Study **II** examines the effectiveness of the method with different durations of diffusion of the contrast agents (ranging from 10 min to 72 h). The partitions of the contrast agent were compared against the structural and functional properties of cartilage, determined using by classical methods i.e. biomechanical testing, histological measurements, and histopathological scoring. Study **III** focuses on the effects of cartilage degeneration, i.e., alterations in water, collagen, and PG content on the diffusion of the contrast agents in a time- and depth-dependent manner.

2 KNEE JOINT AND OSTEOARTHRITIS

The knee is a load-bearing synovial joint connecting femur, tibia, and patella, allowing these structures to articulate with minimal friction. Ligaments, tendons, and menisci help in stabilizing and supporting the movement of the knee joint (Figure 2.1). Articular cartilage is a specialized connective tissue that covers and protects the ends of the articulating bones [2,32]. Menisci help to ensure a uniform distribution of the load from the femur to tibia and thus protect the articular cartilage from excessive local mechanical stresses.

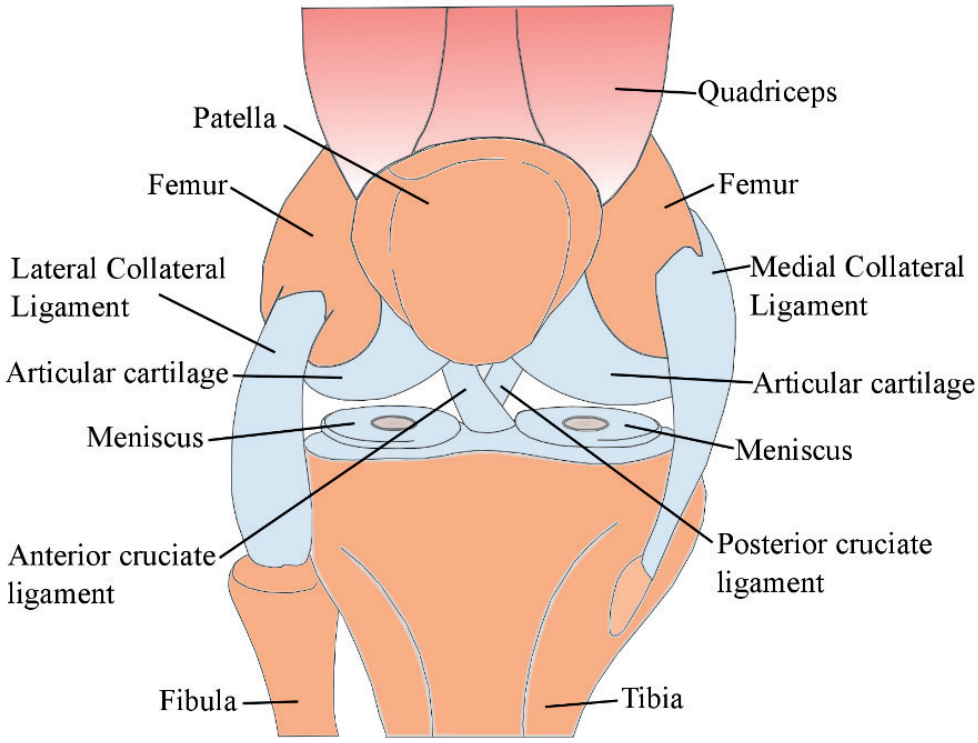

Figure 2.1: A Knee joint.

ARTICULAR CARTILAGE

Articular cartilage, in conjunction with synovial fluid, allows nearly frictionless movement of the articulating bones. Cartilage is an aneural and avascular tissue that

is subjected to major dynamic and static stresses between the articulating bones. Small impact injuries and lesions in cartilage, e.g., followed by cyclic mechanical loading and unloading, can potentially lead to further tissue degeneration due to the limited self-repair capability of the tissue [32].

2.1 STRUCTURE AND COMPOSITION

The main constituents of articular cartilage are water, collagen, proteoglycans (PGs), and the cartilage cells, i.e., chondrocytes [1,2,33]. Articular cartilage can be divided into three depth-wise zones. The arrangement and distribution of the collagen fibers, PGs, and the chondrocytes differ in the superficial, middle, and deep zones. The collagen fibrils are structured in an arch-like orientation (Figure 2.2), whereas the PG content increases towards deep cartilage [34]. This leads to an altered arrangement of the chondrocytes, each zone having different metabolic and synthetic activities [35].

2.1.1 Chondrocytes

Chondrocytes constitute 1-5% of articular cartilage volume and are responsible for the synthesis of the collagen fibrils and the PGs [1,36]. As cartilage is avascular, nutrients reach chondrocytes through diffusion and convective transport. The variation in shape, size, and density of chondrocytes in cartilage is depth-dependent. Chondrocytes in the surface are flatter and oriented in parallel to the articulating surface. In deeper cartilage, chondrocytes are spheroid and oriented in perpendicular to the cartilage-bone interface [37,38]. The structure of the extracellular matrix (ECM) protects the chondrocytes from excess mechanical loading i.e., enabling chondrocytes to function efficiently to ensure the proper maintenance of the tissue matrix. [1,39–41].

2.1.2 Collagen

Collagen is the main solid component of the cartilage ECM. Collagen fibers create a 3D arcade network, providing cartilage with its tensile stiffness and strength, as well as contributing to dynamic compressive stiffness [42,43]. Collagen type II is the most abundant collagen (accounting for 90-95% of the total collagen present in ECM) [36]. Some of the other collagen types are numbered III, VI, X, XI, XII, and XIV [42]. The fibers are arranged in parallel to the articulating surface, forming a wear-resistant mesh. In the middle zone, the fiber arrangement can be considered as random, while

in the deep zone, the fibers are perpendicular to the cartilage bone interface, providing a strong bond between the subchondral bone and cartilage.

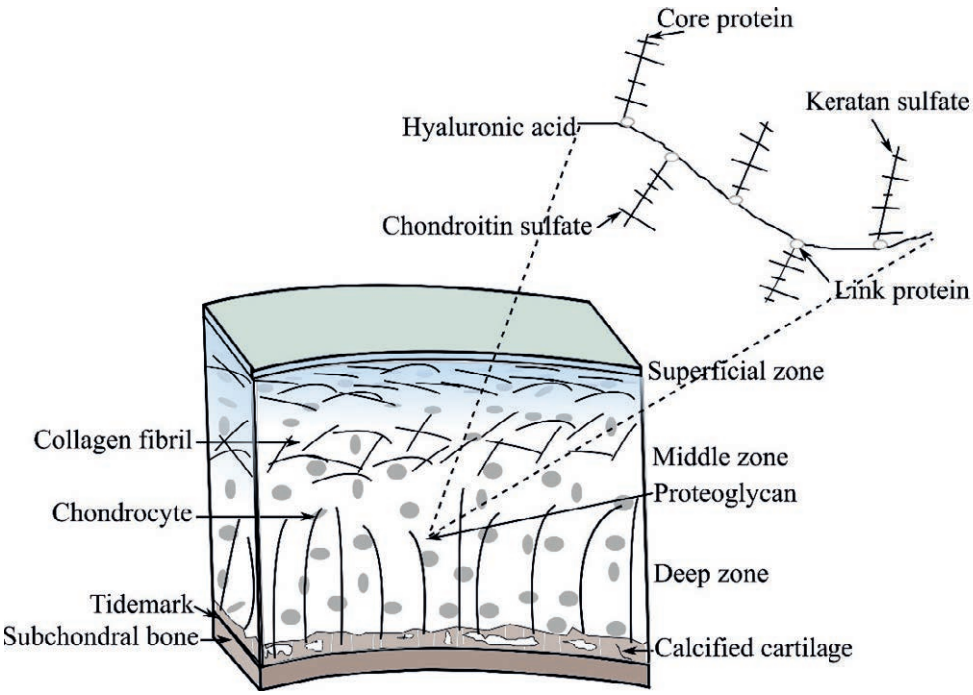

Figure 2.2: Simplified illustration of an articular cartilage structure. The superficial, middle, and deep zones can be differentiated based on the parallel, random, and perpendicular orientation of the collagen fibrils with respect to the surface of articular cartilage, respectively.

2.1.3 Proteoglycans

Proteoglycans are macromolecules, with a core protein to which polysaccharide glycosaminoglycan (GAG) chains are attached. The GAG molecules have a fixed negative charge due to their carboxyl and sulfate groups [44]. PGs form large aggregates and are bound to one end of the hyaluronic acid chain [1,45]. PG aggregates are immobilized and enclosed in the ECM. The fixed negative charge in cartilage creates an imbalance in the osmotic pressure in the ECM, attracting water, which results in a swelling of the tissue. Furthermore, the fixed charge densities (FCDs) in cartilage determine the total counter ion concentration, which governs the Donnan osmotic pressure in the tissue. This osmotic pressure contributes up to 50% of the cartilage compressive stiffness [1,45]. The non-covalent interaction between the

collagen network and PGs forms a fiber-reinforced composite solid, where the collagen network and PG content provide tensile and compressive stiffness, respectively.

2.1.4 Interstitial fluid

Interstitial fluid is a major constituent of cartilage; it is composed of water, proteins, and dissolved electrolytes. The porous cartilage structure entraps the fluid and also allows its free movement within the tissue [36]. The water content in cartilage is depth-dependent, and decreases from 85% in the superficial zone to 60% in the deep cartilage [1]. The water content in cartilage is influenced by the fixed charge density present due to the PGs and the organization of the collagen network. The hydrophilic nature of PGs attracts water, and the resulting swelling of the tissue is resisted by the collagen fiber network.

2.2 MECHANICAL PROPERTIES

From a mechanical perspective, articular cartilage can be considered to be a porous viscoelastic fibril reinforced tissue, and the interaction between collagen, PGs, and interstitial water determines its functional integrity. The ability of articular cartilage to withstand high and variable stresses, from loading and unloading in the knee joint, is attributed to its multiphasic (solid, liquid, and ionic phase) nature [46,47]. A fine balance exists between the swelling pressure exerted by the negatively charged GAGs and the restraining property of the collagen network. These properties enable cartilage to function in this high loading environment [11,48,49].

The compressive stiffness of cartilage decreases with increasing water content [50,51]. This decrease in stiffness (i.e., modulus) results from the decrease in the cartilage solid matrix, especially PGs, to resist the compressive load. Further, tensile and shear properties of cartilage are attributable to the collagen fibril mesh [52]. Cartilage is functionally anisotropic and exhibits a depth-dependent variation in compressive stiffness [53]. During dynamic loading, cartilage is stiff due to the interplay of the incompressible fluid phase, low permeability, and the deformation resisting collagen network [46]. In static loading, the interstitial fluid gradually flows out of the tissue, aiding in the distribution of load to a larger contact area. The flow of fluid allows the cartilage to deform until a mechanical equilibrium is reached. The load at that phase is predominantly supported by the interstitial fluid binding PGs

[9]. Upon removal of the static load, the interstitial fluid flows back into the matrix, and the cartilage swells back to its initial shape.

Apart from absorbing load, articular cartilage, in conjunction with synovial fluid in the knee joint cavity, provides nearly frictionless movement of the joint. This is achieved by two distinct mechanisms: the first mechanism is mediated by hyaluronic acid, lubricin, and surface-active phospholipids in the synovial fluid that lubricate the articular surface; the second mechanism involves the pressurized interstitial fluid that may be squeezed out from the cartilage surface forming a thin fluid film between contacting surfaces [54–56].

2.3 IDIOPATHIC AND POST-TRAUMATIC OSTEOARTHRITIS

Osteoarthritis (OA) is characterized by joint pain, reducing, or completely preventing the patient's mobility. As well as causing suffering in the patients, OA creates a high socio-economic burden on society [57]. In the United States, OA related healthcare costs accounted for 4.3% of the combined sum for all hospitalization [58]. OA is a joint condition resulting from the degeneration of cartilage and the underlying bone. The idiopathic OA is generally considered to result from the natural aging of the joint. It can take decades for the cartilage to deteriorate and develop into idiopathic OA (age-related OA). The second form of OA is post-traumatic osteoarthritis (PTOA) which is initiated after a fall, impact, or a sports accident [59]. Impact injuries and lesions in cartilage trigger a cascade of degeneration, leading to the development of PTOA. This period offers opportunities for pharmaceutical or surgical interventions to slow down the progression of the disease before the disease-modifying opportunities are restricted to joint replacement.

The structural changes occurring in osteoarthritic cartilage are progressive (Figure 2.3). Articular cartilage degeneration consists of damage to the collagen network, a decrease in PG content, and an increase in cartilage water content (swelling) [33,48,60,61]. In an attempt to repair the damage in the ECM, chondrocytes accelerate the production of the cartilaginous matrix. However, when the rate of cartilage degeneration exceeds the rate of repair, this leads to a disturbed tissue composition, structure, and function which causes the detachment of small cartilage fragments and ultimately the formation of cracks that reach into subchondral bone. In OA, there are failures in both the collagen network and the PG solid matrix [1]. The degeneration of the constituents leads to increased tissue permeability and decreased stiffness of the tissue, allowing harmful strains and stresses in articular cartilage to take place during daily loading. The detection of the early changes in cartilage morphology and composition post-trauma is challenging with the existing

diagnostic techniques; in fact, a deterioration is often only noticed after significant degradation of the cartilage has occurred. Early detection of cartilage injuries is necessary to enable timely non-surgical interventions and disease management, and to decelerate the progression of the disease. Various non-surgical and pain management options such as pharmacological (acetaminophen, tramadol), non-pharmacological (exercise, physiotherapy), dietary supplements, and intra-articular injections (corticosteroids, hyaluronic acid) are available. These non-surgical treatment options may not be an ideal solution for OA management; however, they offer an option to mitigate the condition and a possibility to avert or delay surgical procedures.

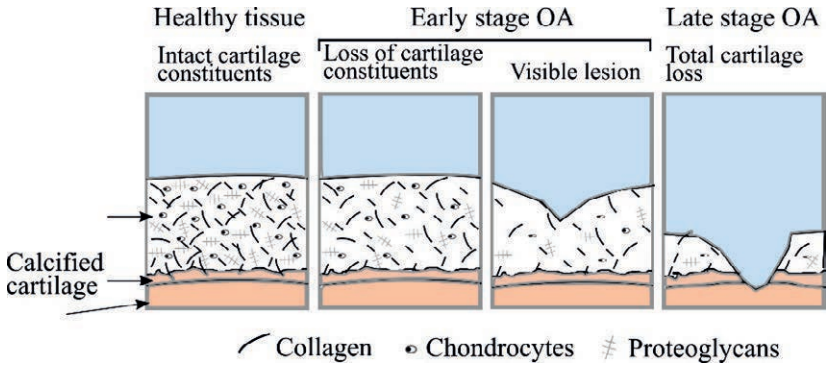

Figure 2.3: Different phases of osteoarthritis related cartilage degeneration.

2.4 DIAGNOSTIC IMAGING AND EVALUATION OF CARTILAGE INJURIES

The clinical examination of the condition of the joint is based on the patient's symptoms. Generally, joint diagnostics is carried out first with a physical examination followed by native X-ray imaging. As cartilage and synovial fluid provide low and comparable X-ray attenuation, it is difficult to distinguish between these two components. With native X-ray imaging, the diagnosis of OA progression and the severity of the disease can be assessed based on the narrowing of joint space between the bones and the calcification of subchondral bone. However, these changes are only detectable in a later stage of the disease progression. In trauma and sports accident associated cartilage damage, the lesions are local, and they cannot be detected by native X-ray imaging.

Lesions can be diagnosed and evaluated using arthroscopy. Arthroscopy is an invasive technique where an optical probe is inserted into the joint cavity via an

incision. Surgeons visually evaluate the cartilage surface for signs of fibrillation, lesions, or minor damage. It is not a totally effective diagnostic technique as it is user-dependent and there is extensive inter-user variability [62]. Further, during arthroscopy, the surgeon has a limited time to perform the assessment, and it is easy to overlook some sites in a joint with multiple lesions.

Magnetic Resonance Imaging (MRI) has an excellent soft-tissue contrast allowing small OA related changes in cartilage structure to be detected [63–65]. Cartilage is mostly composed of water; hence it is an ideal tissue for the evaluation with MRI. The evaluation of cartilage lesions based on the severity of damage is done using the International Cartilage Repair Society (ICRS) grading. High-resolution imaging using MRI is challenging as it requires scanners of high field strength and appropriate receiver coils to maximize spatial resolution and provide adequate contrast [63]. High strength MRI is expensive, not readily available, and is often plagued by long queuing time.

Computed tomography scanners are X-ray based diagnostic imaging devices. Clinical CT scanners can provide high-resolution 3D images. CT imaging is more widely available than MRI, provides fast image acquisition, and is less expensive [66]. The introduction of dual-energy source and multi-detector technology has further advanced CT by enabling material characterization and reducing the image acquisition time. However, since it is an X-ray based device, soft tissues cannot be distinguished properly with CT alone. Hence, the rapid assessment of cartilage morphology and composition is possible only via contrast-enhanced CT.

3 CONTRAST ENHANCED COMPUTED TOMOGRAPHY

3.1 BASICS OF RADIOGRAPHY

In 1895, Wilhelm Roentgen discovered X-rays; these are a form of electromagnetic radiation (λ = 0.01-100 nm) utilized in X-ray imaging. X-ray attenuation varies between materials and this variation in attenuation forms the basis for image formation. The attenuation of photonic radiation is expressed as,

$$I_E(x) = I_{oE} e^{-\mu_E(x)}$$

where, I_{oE} and I_E are the intensities of the incident and transmitted X-ray (having energy E) beams, respectively, through a material with an attenuation coefficient μ_E and a thickness x. In X-ray imaging, the photons that pass through the material reach the detector and a projection is formed.

Interactions such as photoelectric absorption, Compton scattering, and elastic scattering can take place between incident X-rays (photons) and the material, reducing the intensity of the X-ray beam. If the energy of an incoming photon is above the binding energy of an electron, the electron may be displaced from its orbit, creating photoelectric absorption. The photon is completely absorbed, and the excess energy is transferred to the ejected electron (photoelectron) in the form of kinetic energy. The most tightly bound electrons in the K-shell create the K-absorption edge of an atom. In a Compton interaction, photons transfer some energy to an outer shell electron while scattering in a new direction. In general, Compton scattering is responsible for image noise whereas photoelectric absorption contributes to image contrast [67,68].

CT is an X-ray based diagnostic imaging device, invented by Sir Godfrey Hounsfield. The first clinical CT-scans were conducted in 1972. CT uses X-rays to create cross-sectional images also known as slices of an object. When compared to 2D plain radiography, CT creates a 3D visual representation of a structure. The primary components of a CT scanner are the X-ray generator tube, detector, and computer. X-rays produced by the X-ray tube pass through an object, become attenuated, and hit the detector. The X-ray fan beam and the arc of detectors rotate allowing topographical reconstruction of cross-sectional planes to create 3D images. The beam along the axis is collimated so that information acquired for a slice in the single rotation is limited to a small area of an object. With modern CT scanners, up to many

hundreds of slices can be acquired in a single rotation, considerably shortening the image acquisition time.

3.1.1 Spiral CT

Currently, spiral CT is the most widely used CT technology in clinical practice. It uses a point X-ray source and rows of detectors. The X-ray beam is collimated to fit into a row of detectors (curved or plane). The main feature of this CT is the rotating source and detector, and the continuous movement of the patient support table through the gantry, throughout the scan (Figure 3.1). The rate of table movement and the rotation of source and detector can be adjusted to vary the scan time. The introduction of slip-ring technology-facilitated continuous gantry movement allowing an uninterrupted transfer of power to the tube and collimator and retrieving the signal from the detector. This technology considerably shortens the image acquisition time in spiral CT.

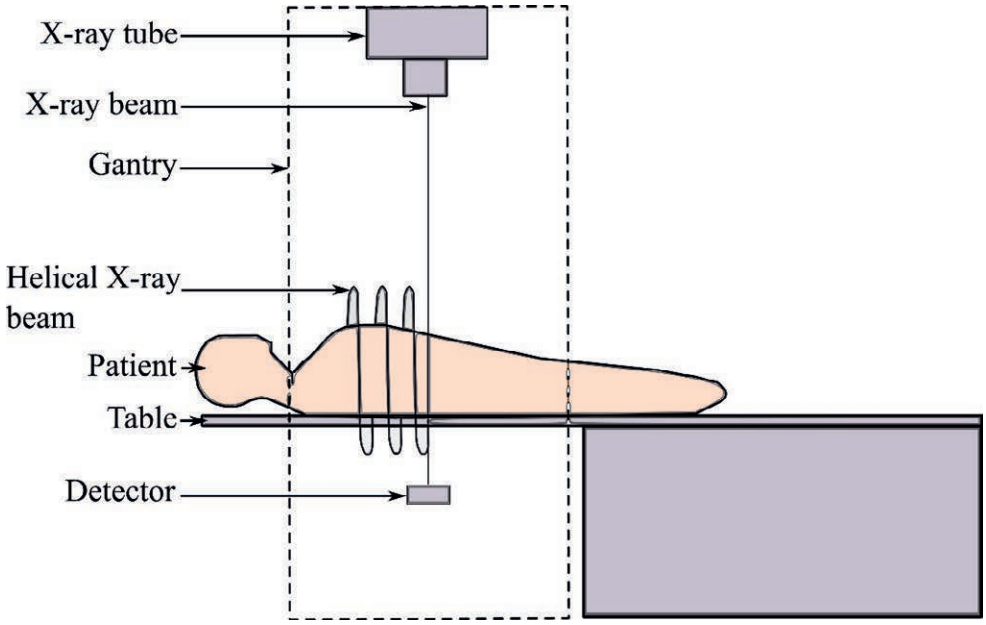

Figure 3.1: Diagrammatic illustration of a spiral computed tomography system.

3.1.2 Dual-energy CT

Conventional CT acquires images with a single X-ray tube voltage (i.e., single X-ray energy spectrum). However, dual-energy CT images are acquired by utilizing two X-ray energies and predominantly applied in material characterization (Figure 3.2). X-ray attenuation of a material varies with the energy of the incident X-ray photon. Based on this difference, materials/structures are differentiated/delineated. Dual-energy CT can be realized by tube kilovoltage (kV) switching (fast and slow) with a

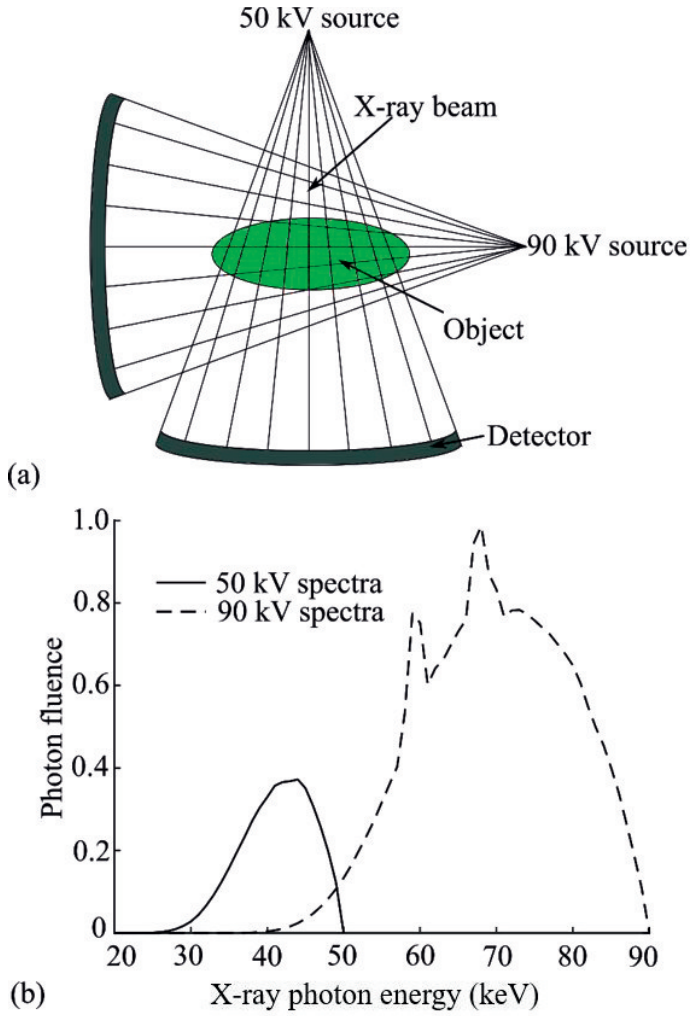

Figure 3.2: (a) Schematic of a dual-energy CT, (b) Normalized X-ray energy spectra at tube voltages of 50 and 90 kV.

single source CT or with a dual-source CT. With fast kilovoltage switching, the high energy spectra cannot be filtered, leading to a large overlap in the low and high energy source spectra. In slow kilovoltage switching, the source spectra can be filtered, but image registration is a challenge as patients may not remain immobile in the same place between the scans.

3.1.3 Spectral CT

Spectral CT is an emerging X-ray based molecular imaging technique capable of providing quantitative information of the scanned object. With conventional CT, the detector measures total attenuation, and this can result in some materials having the same integrated Hounsfield values [69]. The spectral CT system overcomes this limitation by utilizing a photon-counting detector. With this type of detector, a varying range of energy spectrum can be selected for sampling [70]. Material characterization is possible with both spectral and dual-energy CT systems.

3.1.4 X-ray microtomography

X-ray microtomography is generally employed in laboratory-based studies to achieve high-resolution images [71]. Generally in a microtomography system, the sample stage rotates with the source whereas the detector assembly remains fixed. The distance between the detector and object stage is adjusted to achieve the desired pixel size (Figure 3.3). In many systems, the source and detector assembly are fixed, and the object is placed on a rotating stage. The magnification (M) of an object in an image depends on the distance between Source-Object (DSO) and Object-Detector (DOD), and can be expressed as,

$$M = \frac{Oi}{O} = \frac{DSO+DOD}{DSO} \tag{2}$$

where M is the magnification, O is the object size and Oi is the size of the object in the detector.

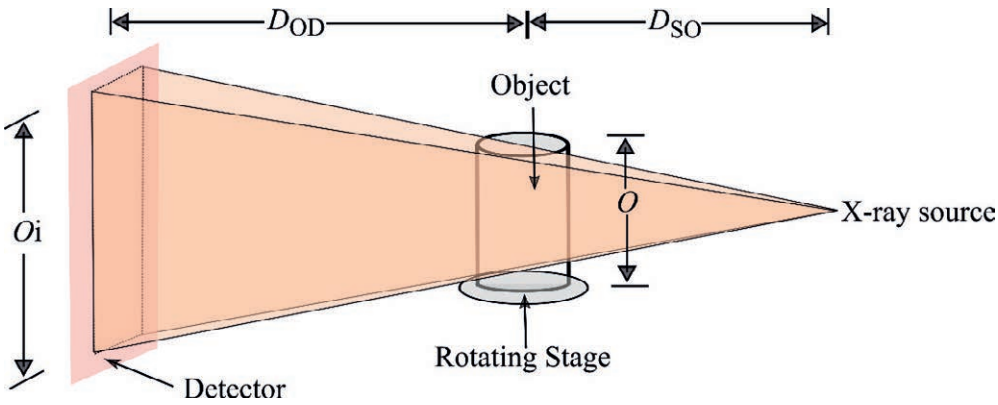

Figure 3.3: Schematic picture of an X-ray microtomography imaging system.

3.2 CONTRAST ENHANCEMENT

X-rays provide good contrast in imaging of hard and dense tissues and they are widely used in bone imaging. However, X-ray attenuation in soft tissues is low and highly constant; this obscures the clarity of interfaces between adjacent tissue structures in the radiographic image. A good example is the articular cartilage, which is a soft tissue that has a very similar density as the surrounding synovial fluid. The presence of contrast agents create a greater difference in CT attenuation between the structures, improving image contrast (i.e. the signal to noise ratio). The addition of an external contrast to the tissue or the surrounding region improves their differentiation during radiographic imaging. In knee joint imaging, an agent is injected into the intra-articular space, where it enables visualization of cartilage tissue contour and shape, synovial space, and the surrounding bone. This provides a good contrast to assess the cartilage morphology as both bone and contrast agents in the joint space are highly X-ray attenuating.

3.2.1 CT contrast agents

CT-based contrast agents must fulfill specific functional requirements for clinical use, such as

1. contrast agent should be non-toxic,
2. contrast agent should localize and increase absolute CT attenuation of the region of interest or its surroundings (not both),

3. the amount and concentration of an agent should be optimal so that retention in the body is long enough to provide a good SNR (signal to noise ratio) during image acquisition, after which the agent should be cleared out from the body within a short time (e.g. a few hours).

Contrast agents based on iodine (I), lanthanides [Gadolinium (Gd), dysprosium (Dy), ytterbium (Yb)], bismuth (Bi), tantalum (Ta), and gold (Au) are used in various imaging applications [66]. I and Gd-based contrast agents have been in routine clinical use for contrast-enhanced imaging with CT and MRI, respectively [72]. The agents offer increased absorption of X-rays as the energy of X-ray source (80-150 kV) in use in clinics matches the K-absorption edges of both I and Gd [66]. The K-absorption edge is utilized in contrast-enhanced imaging to obtain the maximum attenuation of the incident X-rays, resulting in improved contrast of tissue relative to its surroundings.

The CT-based contrast agents used for articular cartilage imaging fall into three broad categories based on their molecular charge (i.e. anionic, non-ionic, and cationic). Anionic contrast agent molecules are negatively charged. PGs in cartilage ECM are also negatively charged and thus they oppose the diffusion of the anionic agents inside the tissue. Hence, the molar concentration of the anionic agent in cartilage is inversely proportional to the cartilage PG content. In degenerated cartilage, which has a low PG content and high-water content, the negatively charged particles diffuse more easily as compared to healthy cartilage that is rich in PGs. By following the variations in the diffusion of the contrast agent using arthrography (CT, MRI), information on cartilage health may be collected. Commercially available anionic agents such as ioxaglate and iothalamate have demonstrated a high correlation with the cartilage GAG content *ex vivo* [2–6] *and* ICRS grade *in vivo* [7].

Cationic agents (positively charged) were developed to utilize the negative charge of the PGs to improve the diffusion and partition of the agent into the tissue (Figure 3.4). The favorable electrostatic interactions promote contrast agent retention in tissue, enable improved SNR as compared to anionic agents, which are repelled from cartilage tissue. For this reason, cationic agents are more sensitive in detecting cartilage injuries as compared to anionic agents [73]. The uptake of cationic agents is higher than the anionic agents, providing a stronger signal as well as enabling an evaluation of the depth-dependent assessment of the cartilage's condition due to enhanced penetration into the deeper layers of cartilage [23,26]. X-ray attenuation induced by a cationic agent is directly proportional to the amount of PGs and strongly correlates with the mechanical properties and composition of the tissue [26,74]. Cationic contrast agents may thus allow for better clinical diagnostics of joint injuries

and disease. The high osmolality of ionic agents has often been associated with adverse health effects in patients [8]. Fortunately, the cationic contrast agent can be administered in lower concentrations as compared to anionic agent [11]. This helps to potentially reduce adverse side-effects in the body that might result from the administration of contrast agents [8]. Iodine-based cationic contrast agents CA2+, CA4+ have been recently developed and used for contrast-enhanced imaging in preclinical studies [6,9,12].

Non-ionic agents (neutral charge) have no electric affinity towards the fixed negative charge carried by the PGs in cartilage ECM. Thus, the diffusion of these agents is dependent on the cartilage permeability, water content, and the concentration gradient between tissue and the agent. In cartilage, as compared to anionic agents, the non-ionic agent shows a higher partition, i.e., the ratio of the contrast agent concentration in cartilage relative to the concentration of the agent in the bath at diffusion equilibrium [20]. Gadolinium-based contrast agents gadopentetate dimeglumine, gadodiamide, gadobutrol, and gadoteridol have been approved and used for routine clinical MR imaging. Due to the high atomic number of gadolinium, the use of a gadolinium-based contrast agent has also been explored in CT imaging [2].

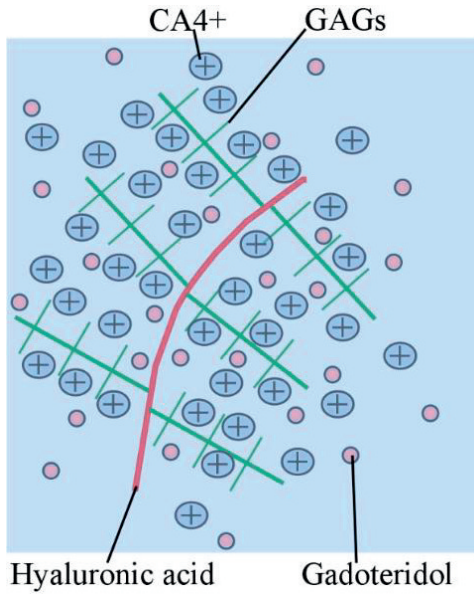

Figure 3.4: CA4+ molecules attracted to GAGs (PGs) inside cartilage extracellular matrix (ECM), while gadoteridol diffuses in freely.

3.2.2 Diffusion of contrast agents in cartilage

Cartilage is an avascular tissue, and the nutrients for the metabolic function are transported via diffusion. The structural properties of cartilage ECM (extracellular matrix) influence the transport of solutes. The movement of molecules suspended in a fluid is random and follows Brownian motion [29,77]. Solutes move randomly and travel from areas of higher concentration to areas of lower concentration until an equilibrium is reached. Solute flux (J) across the surface of cartilage can be expressed using Fick's second law as,

$$J = -h\frac{\partial C}{\partial t}, \tag{3}$$

where h is the cartilage thickness and C is the bulk concentration of contrast agents in cartilage.

Cartilage consists of negatively charged glycosaminoglycan fixed to the ECM. When cartilage is immersed in an electrolytic solution, the inherent negative charge in cartilage creates a Donnan potential between the tissue and the solution. The mobile ions in the tissue and electrolytic solution follow the equilibrium proposed by Donnan and can be expressed as [78]:

$$\left(\frac{[\text{cation}]_{\text{bath}}}{[\text{cation}]_{\text{cartilage}}}\right)^{Z_{\text{cation}}} = \left(\frac{[\text{anion}]_{\text{cartilage}}}{[\text{anion}]_{\text{bath}}}\right)^{Z_{\text{anion}}}, \tag{4}$$

where $[cation]_{bath}$ and $[anion]_{bath}$ are the positive and negative charges in the bath, respectively. Similarly, $[cation]_{cartilage}$ and $[anion]_{cartilage}$ are the positive and negative charges in cartilage, respectively, and Z is the valence of the molecule. When there is electroneutrality condition, the following must hold:

$$Z_{\text{cation}}\, C_{\text{cation}} = Z_{\text{anion}}\, C_{\text{anion}} + \text{FCD}, \tag{5}$$

where FCD is the net negative charge induced by the immobile chondroitin and keratin sulfate in cartilage. The molar concentration (C) of the diffused cationic agent in the tissue is directly proportional to the amount of FCD in cartilage.

3.3 DELAYED CONTRAST-ENHANCED COMPUTED TOMOGRAPHY

CT imaging of knee joint can be performed immediately after the intra-articular injection of contrast agents. This makes possible an examination of cartilage structure and identification of major cracks in the cartilage surface. The use of contrast agents is not limited to examining cartilage morphology, and can also be used to determine

tissue composition (i.e., PG and water contents) if the imaging is performed between 45 min and 1 h after administration of the contrast agent (Delayed contrast-enhanced computed tomography, delayed-CECT) [20,30,73,79] i.e. this allows early identification of areas undergoing macroscopic deterioration [28,80,81]. Delayed-CECT is an analogous technique to the clinically established delayed gadolinium-enhanced magnetic resonance imaging of cartilage (dGEMRIC) [15,82].

In articular cartilage, the uptake of cationic agents is proportional to the PG content in the tissue [83,84]. However, the diffusion is restrained by the tissue porosity/permeability. Hence, it is challenging to make a sensitive differentiation between an intact (high PG content, low permeability) and mechanically damaged (decreased PG content, high permeability) cartilage based on only diffusion of the contrast agent. Especially in early OA, the simultaneous increase in cartilage water content, the decrease in PG content, fibrillation, and disruption of the collagen network have opposite effects on the diffusion of the cationic agents. The effect of these degenerative changes on the diffusion of the cationic agent and the diagnostic potential of this phenomenon are still unknown.

4 AIMS OF THE PRESENT STUDY

The thesis is focused on the determination of the structural integrity and composition of cartilage based on the simultaneous diffusion of two contrast agents, by introducing and developing a dual-energy CT technique suitable for cartilage.

The specific aims of the study were:

1. to develop and validate a quantitative technique for the simultaneous determination of I and Gd-based contrast agents in the cartilage at near diffusion equilibrium
2. to evaluate the diagnostic potential of the dual-contrast technique to assess changes in cartilage's biomechanical and histopathological state as a function of the diffusion time of the contrast agent (10 min to 72 h)
3. to examine the effect of the concentrations of the solid constituents of cartilage (i.e. PG and collagen) and interstitial water content on the diffusion of a cationic and non-ionic agent in a time- and depth-dependent manner.

5 MATERIAL AND METHODS

This thesis comprises three independent studies. The materials used and the methodology applied in the studies are presented briefly in this chapter. More comprehensive details of the materials and methodology are provided in the original publications (attached to the thesis as appendices).

5.1 SAMPLE PREPARATION

In study **I**, osteochondral samples (n = 57, d = 8 mm) were drilled out from human cadaver (n = 2) distal femur (n = 4) and proximal tibia (n = 4). The samples were stored frozen in phosphate-buffered saline (PBS) (-22 °C). Before the diffusion experiment, the samples were cut into two halves, thawed, and the edges were sealed with cyanoacrylate to allow contrast agent diffusion only through the articular surface (Figure 5.1).

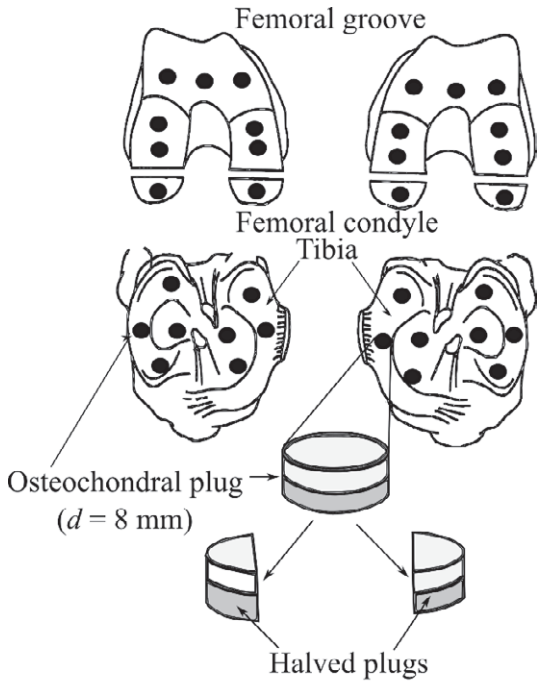

Figure 5.1: Osteochondral plugs (d = 8 mm) were extracted (locations marked as black dots) from human cadaver lateral and medial tibial plateaus and femoral condyles of the left and right knee joints. The samples were halved for diffusion experiments and reference measurements.

In studies **II** and **III**, the sample preparation technique was identical to that used in study **I**. Human osteochondral plugs (n = 33 in study **II**, n = 15 in study **III**) were extracted from lateral and medial tibial plateaus and femoral condyles of the left and right knee joints of human cadavers (n = 4, Mean Age = 71.25 ± 5.18 years). The Research Committee of the Northern Savo Hospital District granted a favorable opinion on collecting the human tissue (Kuopio University Hospital, Kuopio, Finland, Decision numbers: 134/2015 and 58/2013).

5.2 X-RAY MICROTOMOGRAPHY

The delayed-CECT technique uses a single contrast agent to examine cartilage health. In the dual-contrast method, two contrast agents are used simultaneously. The molar concentration and the depth-wise distribution of the contrast agents in cartilage was quantified by using a dual-energy X-ray (i.e., imaging with two X-ray tube voltages). In this approach, the contrast agents must have well-separated k-absorption edges (Figure 5.2).

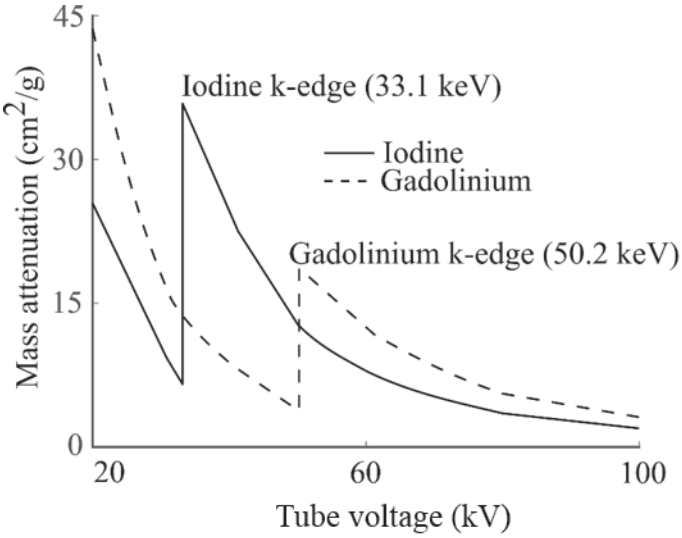

Figure 5.2: Mass attenuation curves for iodine and gadolinium.

Study **I** was carried out using a microtomography scanner (Skyscan 1172, Skyscan, Kontich, Belgium), the isotropic voxel size was 25 µm × 25 µm × 25 µm and the utilized tube voltages: 100 kVp and 50 kVp. In study **I**, the dual-energy technique was first calibrated with measurements of contrast agent mixtures of known I (CA4+) and Gd (gadoteridol) concentrations, ratios of 4.8/43.2, 9.6/38.4, 14.4/33.6, 19.2/28.8,

24.0/24.0, 28.8/19.2, 33.6/14.4, 38.4/9.6, and 43.2/4.8 (mg/ml). The human osteochondral plugs were imaged before and after 72 h immersion in a mixture of contrast agents CA4+ (5,5'-(malonylbis(azanediyl))bis(N^1,N^3-bis(2-aminoethyl)-2,4,6-triiodoisophthalamide, q = +4, M = 1355 g/mol, 24 mgI/ml) and gadoteridol (Prohance, Bracco International B. V., Amsterdam, Netherlands, q = 0, M = 559 g/mol, 24 mgGd/ml).

In studies **II** and **III,** the microtomography scanner was a Quantum FX (Perkin Elmer, Waltham, MA, USA). In studies **II** and **III,** dual-energy scans were conducted using tube voltages of 90 kVp and 50 kVp, with a 20 mm × 20 mm field of view (FOV) and an isotropic voxel size 40 μm × 40 μm × 40 μm (Figure 5.3).

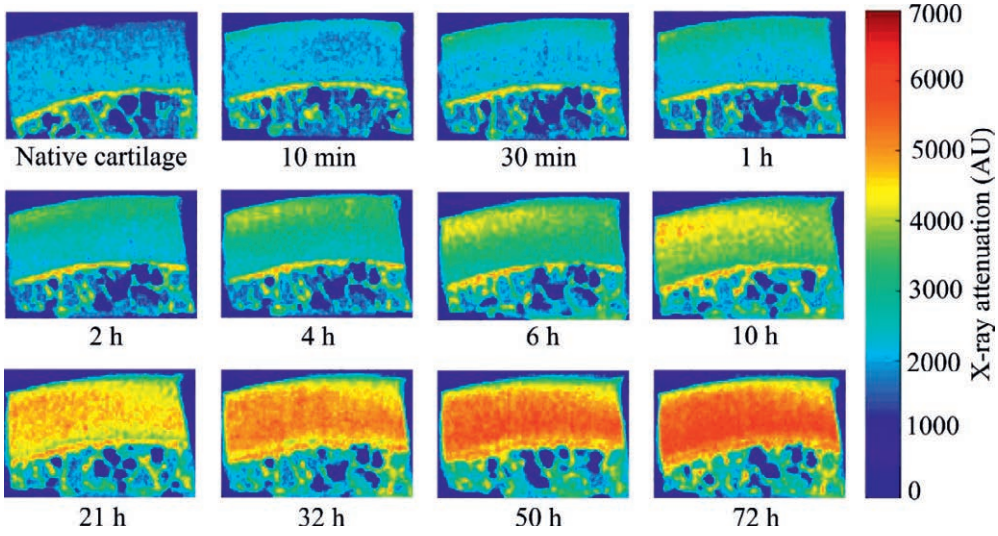

Figure 5.3: Human osteochondral plug (frontal plane) imaged with a high-resolution microcomputed tomography scanner (tube voltage = 50 kVp) before and after immersion in a contrast agent bath (a mixture of CA4+ and gadoteridol) for 10 min, 30 min, 1, 2, 4, 6, 10, 21, 32, 50, and 72 h. The higher X-ray attenuation in the cartilage results from the increase in immersion time.

Before conducting the contrast agent diffusion experiment in cartilage, the dual-energy microtomography was calibrated with measurements of different compositions of the contrast agent mixture consisting of gadolinium (8, 12, and 20 mgGd/ml) and iodine (0, 10, 20, 30 ,40, 50, 60, and 70 mgI/ml). The I/Gd concentration (mg/ml) ratios (0/20, 10/20, 20/20, 30/20, 40/20, 50/20, 60/20, 70/20, 20/12, 30/12, 40/12, 50/12, 60/12, 70/12, 10/8, 20/8, 40/8, 50/8 and 60/8) were measured. After calibration, the osteochondral plugs were immersed in a mixture of CA4+ (10 mgI/ml) and gadoteridol (20 mgGd/ml) and imaged in air after 10 min, 30 min, 1, 2, 4, 6, 10, 21, 32, 50, and 72 h. Throughout the studies, image segmentation and data analyses were

carried out using Seg3D software (vs. 2.4.0, University of Utah, Salt Lake City, UT, USA) and Matlab (R2016b, The Mathworks Inc., Natick, MA, USA), respectively.

5.3 IMAGE ANALYSIS

The concentration of contrast agents (i.e., I and Gd) can be determined from a dual-energy X-ray scan using Beer-Lambert law (Eq. 1) and Braggs additivity rule [85],

$$\alpha_E = \mu_{\mathrm{I}_E} C_{\mathrm{I}} + \mu_{\mathrm{Gd}_E} C_{\mathrm{Gd}}\,, \tag{7}$$

where C_{I} and C_{Gd} are the concentrations of I and Gd in the contrast agents, respectively, $\mu_{I_E}$and $\mu_{Gd_E}$are the mass attenuation coefficients of I and Gd, respectively, and α_E is the X-ray attenuation at X-ray tube voltage *E*. When CT scan is made using high [$E(High)$] and low [$E(Low)$] X-ray tube voltages, the concentrations can be solved from equation 7 as follows,

$$C_{\mathrm{I}} = \frac{\alpha_{E(High)}\mu_{\mathrm{Gd}_{E(Low)}} - \alpha_{E(Low)}\mu_{\mathrm{Gd}_{E(High)}}}{\mu_{\mathrm{I}_{E(High)}}\mu_{\mathrm{Gd}_{E(Low)}} - \mu_{\mathrm{I}_{E(Low)}}\mu_{\mathrm{Gd}_{E(High)}}}\,, \tag{8}$$

$$C_{\mathrm{Gd}} = \frac{\alpha_{E(High)}\mu_{\mathrm{I}_{E(Low)}} - \alpha_{E(Low)}\mu_{\mathrm{I}_{E(High)}}}{\mu_{\mathrm{Gd}_{E(High)}}\mu_{\mathrm{I}_{E(Low)}} - \mu_{\mathrm{Gd}_{E(Low)}}\mu_{\mathrm{I}_{E(High)}}}\,. \tag{9}$$

Using Eq. 8 and 9, the depth-wise concentration of I and Gd-based agents in cartilage can be determined. The depth-wise concentrations of the agent can be used to estimate the cartilage PG and water content.

5.4 BIOMECHANICS

In studies **I** and **II**, a custom-built material testing device [(resolution: 0.1 μm, 0.005 N) (PM500-1 A, Newport, Irvine, CA, USA)] was employed for biomechanical testing in indentation geometry. First, a flat-ended metallic indenter (d = 728 μm or d = 667 μm) was driven to make a perpendicular contact with the articular surface (pre-stress of 12.5 kPa) [86]. Then, a stress relaxation protocol, consisting of four compressive steps (each representing 5% of cartilage thickness, 100%/s ramp rate), was implemented with a 900 s relaxation after each step [87,88]. The solution proposed by Hayes et al. was used in the calculation of the moduli [89–91]. For that, Poisson's ratios were set to ν = [0.3 (Tibia), 0.2 (Femur)] and ν = 0.5, when calculating equilibrium ($E_{equilibrium}$) and instantaneous ($E_{instantaneous}$) modulus, respectively. In study **I**, the dynamic modulus ($E_{dynamic}$) was determined from sinusoidal loading (f = 1 Hz, *strain amplitude* = 2 % of cartilage thickness) which was performed after the stress-relaxation test at 20% strain.

5.5 HISTOLOGY, SPECTROSCOPY AND WATER CONTENT MEASUREMENT

In studies **II** and **III**, PG distribution in cartilage was determined with digital densitometry (DD), by measuring the optical density (OD). The samples were prepared by fixing them in 10% formalin, decalcified in EDTA, processed in graded alcohol solutions, embedded in paraffin, and cut into 3 μm thick sections. The paraffin was dissolved, and the cut sections stained with Safranin-O (cationic dye) [92]. This dye binds to the fixed negative charge and thus indicates the PG distribution in a sample [92].

In study **III**, the cartilage collagen content (n = 15) was analyzed from the spectral data obtained with Agilent Cary 600 spectrometer coupled with Cary 610 Fourier transform infrared (FTIR) microscope (Agilent Technologies, Santa Clara, CA, USA). The infrared light absorption spectrum (3800 cm^{-1} to 750 cm^{-1}) was collected pixel-by-pixel (Figure 5.4). To optimize SNR, 8 scans per-pixel and three slices per sample were measured in full-thickness. The spatial pixel size was 5.5×5.5 μm, and the spectral resolution was set to 4 cm^{-1}. Applying a constant baseline correction (2000 cm^{-1} to 900 cm^{-1}), the amide I region (1720cm^{-1} to 1595cm^{-1}) of the infrared spectra was analyzed to determine the collagen content [93].

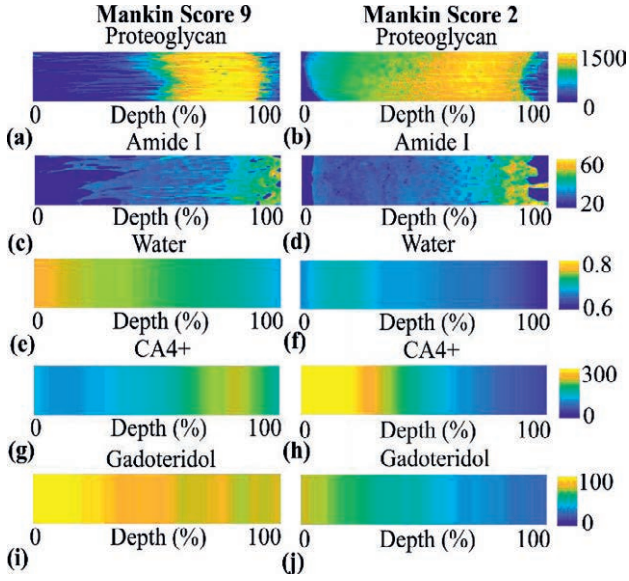

Figure 5.4: In a degenerated (Mankin score: 9) and healthy human cartilage (Mankin score: 2) samples depth-dependent proteoglycan (a, b), collagen (c, d), and water (e, f) distributions along with CA4+ (g, h) and gadoteridol (i, j) partitions after 10 h of contrast agent diffusion (equilibrium not reached yet).

In study **III**, the depth-dependent cartilage water content was determined by freeze-drying cartilage sections in a lyophilizer (Christ, Alpha 1-2, B. Braun Biotech International, 37520 Osterode, Germany, p = 4.58 mmHg). In the water content measurement, the samples initially used in contrast agent diffusion experiments were reutilized. Contrast agents from the samples were first washed out by immersing the plugs in PBS for 5 days. During immersion, the bath was maintained at 4° C, constantly stirred, and the PBS changed every 24 hours. After removing the contrast agent, the plugs (n = 15) were then attached (LAMB-OCT, ThermoFisher SCIENTIFIC, Waltham, MA, USA) to a metallic sample holder, and placed inside the cryomicrotome (Leica CM3050 S, Leica Biosystems, Weltzar, Germany) chamber maintained at -21°C. 200 μm thick cartilage sections were cut along the transverse plane, and freeze-dried inside a lyophilizer chamber for 48 h. The slices were weighed three times, lyophilized and weighed again. The water content was then determined by subtracting the average dry and wet weights.

5.6 ICRS GRADING AND MANKIN SCORING

In study **I**, prior to the extraction of the osteochondral plugs, the sample locations were graded by an experienced surgeon using the ICRS (International Cartilage Repair Society) grading (scale 0 to 4) [94]. For the samples used in studies **II** and **III**, the severity of OA was evaluated using the Mankin grading system. Four independent observers assessed and assigned scores based on the severity of OA using the Safranin-O stained sections [95]. Three sections per sample were scored and averaged. The scores were based on staining (0 to 4), tidemark integrity (0 to 1), abnormality in structure (0 to 6), and cellularity (0 to 3) (Table 1). Finally, the Mankin score was determined as an average of the scores assigned by the four observers.

5.7 STATISTICAL ANALYSIS

In studies **I** and **II**, the relationship between the true and dual-energy CT determined I and Gd concentrations in contrast agent mixtures (CA4+ and gadoteridol) was analyzed using Pearson's correlation. In study **I**, the relationship between cartilage contrast agent partitions and the tissue biomechanical moduli was analyzed using Spearman's rho (ρ). In study **II**, the correlations of contrast agent partitions with the histopathological and biomechanical reference parameters were evaluated using Pearson's correlation analysis. In study **III,** Pearson's correlation analysis was used to examine the depth-wise relationship between contrast agents partition in cartilage with its PG, water, and collagen contents. The statistical analyses were conducted

using SPSS (v. 23.0 SPSS Inc., IBM Company, Armonk, NY, USA) statistical software. In all of the statistical tests, $p < 0.05$ was set as the limit of statistical significance.

Table 1: Histological and histochemical grading of Safranin-O stained samples using Mankin scoring system [95].

I	Structure	Grade	II	Cells	Grade
a	Normal	0	a	Normal	0
b	Surface irregularities	1	b	Diffuse hypercellularity	1
c	Pannus and surface irregularities	2	c	Cloning	2
d	Clefts in the transitional zone	3	d	Hypocellularity	3
e	Clefts in the radial zone	4	**IV**	**Safranin-O staining**	
f	Clefts in the calcified zone	5	a	Normal	0
g	Complete disorganization	6	b	Slight reduction	1
III	**Tidemark integrity**		c	Moderate reduction	2
a	Intact	0	d	Severe reduction	3
b	Crossed by a blood vessel	1	e	No dye noted	4

6 RESULTS

The most important results from the studies are summarized in this chapter. Complete results can be found in the original publications attached as appendices to this thesis.

6.1 DUAL-CONTRAST TOMOGRAPHY OF HUMAN ARTICULAR CARTILAGE

In studies **I-III**, the dual energy technique was first calibrated with measurements of contrast agent mixture of known I (CA4+) and Gd (gadoteridol) concentrations. In study **I**, true and the measured I/Gd concentrations were found to be linearly correlated (R^2 = 0.99). In studies **II and III**, the true and measured contrast agent mixture compositions consisting of gadolinium (8, 12, and 20 mgGd/ml) and iodine (0, 10, 20, 30, 40, 50, 60, and 70 mgI/ml) were found to correlate linearly (R^2 > 0.97).

After validation, the technique was employed to determine CA4+ and gadoteridol partitions in human osteochondral samples. In study **I**, the resulting partitions (mean ± SD) of CA4+ and gadoteridol in cartilage after 72 h were found to be 197.6 ± 28.4% and 66.0 ± 9.2%, respectively. In study **II**, the CA4+ and gadoteridol partitions in cartilage increased from 14.4 ± 8.8% and 10.2 ± 5.6% at 10 min to 344.0 ± 77.9% and 91.4 ± 9.7% at 72 h, respectively (Figure 6.1).

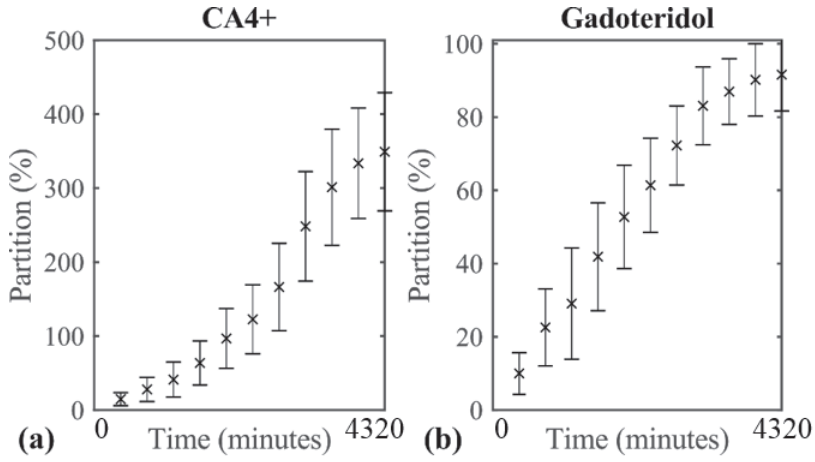

Figure 6.1: Mean a) CA4+ and b) gadoteridol partitions in cartilage as a function of diffusion time.

The cationic agent's uptake in the deep cartilage zone was 2.5 times greater than in the cartilage surface zone. The depth-dependent CA4+ and gadoteridol partitions showed increasing and decreasing trends, respectively.

In study **II**, the average CA4+ and gadoteridol concentration maxima were 35 and 17 mg/ml, respectively. The time required for the CA4+ to reach 63.2% of the maximum concentration was 1032 min. After 10-min of contrast agent diffusion, a delay of 2 min between image acquisitions at two energies induced an error of 74.4% for CA4+ and 23.5% for gadoteridol partitions. After 100-min of contrast agent diffusion, the error had become reduced to 6.2% for CA4+ and 2.2% for gadoteridol.

6.2 CAPABILITY OF THE TECHNIQUE TO REVEAL CARTILAGE FUNCTIONAL AND STRUCTURAL PROPERTIES

In study **I**, the CA4+ partitions in the cartilage were found to correlate significantly ($\rho = 0.492$, $P < 0.05$) with the equilibrium modulus. After normalization of the CA4+ partition with the gadoteridol partition, the correlation with the equilibrium modulus decreased ($\rho = 0.364$, $P < 0.05$). Upon inspecting the superficial cartilage (500 μm thick), CA4+ partition after normalization with the gadoteridol partition, a higher correlation was revealed (from $\rho = 701$ *to* $\rho = 795$, $P < 0.05$) with the equilibrium modulus. However, the change in correlation after the normalization of CA4+ partition with the gadoteridol partition in the superficial and bulk cartilage was not statistically significant. In study **II**, the equilibrium modulus correlated significantly with the CA4+ partition, when normalized by the gadoteridol partition ($P < 0.01$) earlier (at 21 h) as compared to non-normalized CA4+ partition ($P < 0.004$, at 32 h). The correlation coefficient between the optical density (i.e., proteoglycan content) and the CA4+ partition in bulk cartilage showed an increasing trend as a function of the contrast agent's diffusion time (from $R = 0.17$ at 1 h to $R = 0.70$ at 72 h). In the superficial 10% of cartilage thickness, the correlation between CA4+ partition and OD value (PG content) was found to be significant during the first hour of diffusion. Upon inspecting the bulk cartilage, it was evident that the gadoteridol partition, normalized CA4+ partition, correlated significantly with OD 4 h earlier (i.e., 6 h after immersion) as compared to non-normalized CA4+.

In study **I**, normalization of CA4+ partition with the gadoteridol partition strengthened the correlation between the CA4+ partition and ICRS grade in full-thickness cartilage from $\rho = -0.385$ to $\rho = -0.458$. In study **II**, the correlation between CA4+ partition in full-thickness cartilage and the Mankin score was improved after

normalization throughout the diffusion (Figure 6.2). Furthermore, the gadoteridol partition was found to correlate significantly with the Mankin score until 10 h after immersion.

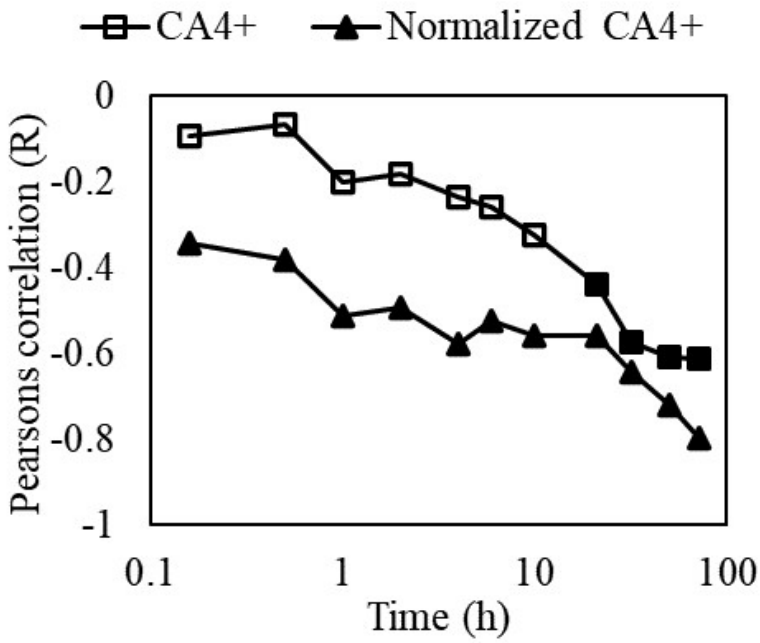

Figure 6.2: Pearson's correlation coefficient (R) between the gadoteridol partition normalized CA4+ partition and the non-normalized CA4+ partition with histopathological and histochemical grading (Mankin score) of osteochondral samples (n = 33).

6.3 EFFECT OF CARTILAGE CONSTITUENTS AND CONTRAST AGENT DIFFUSION

In study **III**, after 72 h of immersion, the CA4+ concentration maximum ($C_{CA4+\,max}$) correlated significantly ($R < -0.521$, $p < 0.04$) with the water content in the superficial and mid cartilage zones (up to 60% of cartilage depth) (Figure 6.3). At the same diffusion time, $C_{CA4+\,max}$ correlated significantly with the PG concentration ($R > 0.671$, $p < 0.006$) in the mid and deep cartilage regions (40-100% of cartilage depth). In bulk cartilage, the gadoteridol concentration maximum ($C_{Gd\,max}$) correlated inversely with the collagen content ($R < -0.514$, $p < 0.05$), at the 21 h diffusion time-point. However,

the correlation with the water content was not statistically significant. At the later time-point (72 h), $C_{Gd\ max}$ correlated inversely with the collagen content ($R < -0.705$, $p < 0.003$) in the superficial 40% of cartilage depth, and correlated positively ($R > 0.567$, $p < 0.002$) with the PG content from 40% depth until the cartilage-bone interface.

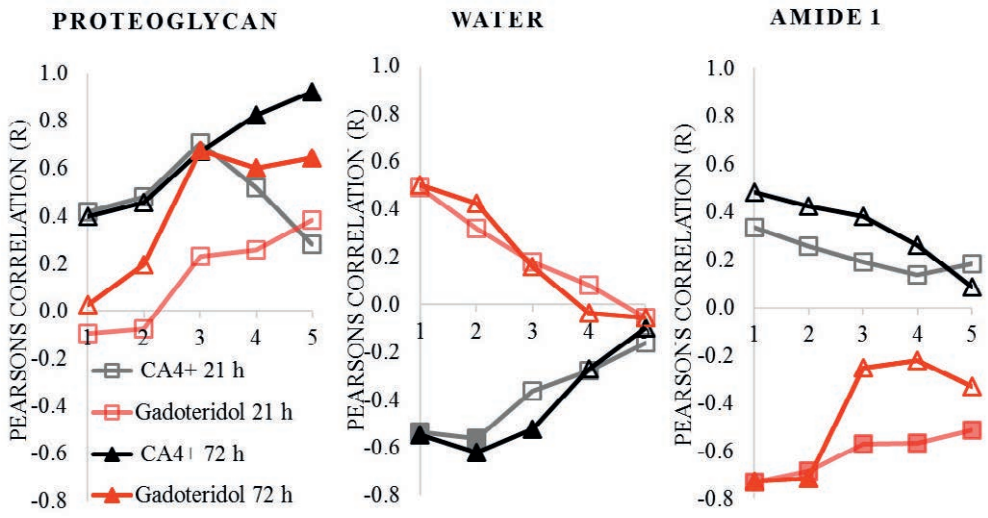

Figure 6.3: Pearson's correlation coefficient between the mean contrast agent partitions and **(a)** the proteoglycan concentration, **(b)** the water content, and **(c)** the collagen (amide I) concentration in 20% thick cartilage layers (1 indicates cartilage surface and 5 indicates deep cartilage).

The diffusion time for CA4+ and gadoteridol to reach 40% of the cartilage depth was comparable. Gadoteridol reached the cartilage-bone interface in 141 ± 83 min, and CA4+ in 216 ± 165 min (Figure 6.4). In more degenerated samples (Mankin score > 5), gadoteridol reached the cartilage-bone interface more rapidly ($p = 0.01$) than CA4+ (111 ± 63 min vs 248 ± 171 min). In less degenerated samples (Mankin Score <= 5), the diffusion times were comparable being 179 ± 163 min and 175 ± 95 min.

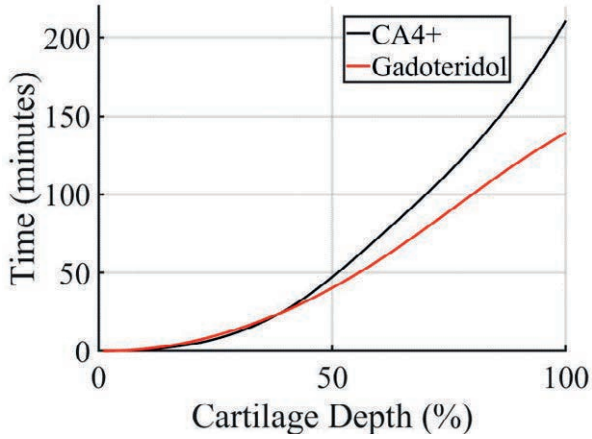

Figure 6.4: Diffusion times for CA4+ and gadoteridol to reach the cartilage bone interface in human osteochondral plugs (n = 15).

7 DISCUSSION

In this thesis, a quantitative dual-energy CT (QDECT) technique was developed to simultaneously quantify the PG and water contents in articular cartilage. The technique is based on the simultaneous diffusion of a cationic and a non-ionic CT contrast agent in human articular cartilage. In study I, the technique was developed and tested to evaluate the functional properties of human articular cartilage after immersion in a contrast agent bath for 72 h. In addition, the sensitivity of the cationic agent at near diffusion equilibrium to detect changes in cartilage structural integrity was examined when simultaneously used with a non-ionic agent. However, cartilage diagnosis in diffusion equilibrium is not possible in clinic as contrast agents undergo rapid clearance from the joint capsule after intra-articular administration. Hence, in study II, the potential of the technique to probe cartilage composition and structural integrity was examined longitudinally throughout diffusion (from 10 min to 72 h). In study III, the effect of the cartilage constituents on the simultaneous diffusion of cationic and non-ionic contrast agent was examined.

7.1 QUANTITATIVE DUAL ENERGY CT

The contrast agent diffusion experiment was conducted on human articular cartilage samples after their immersion in the bath mixture of CA4+ and gadoteridol. In study **I**, the partitions of the cationic (CA4+) and the non-ionic agent (gadoteridol) in the samples were quantified near to diffusion equilibrium (72 h). In study **II**, the partitions of CA4+ and gadoteridol in human articular cartilage plugs were determined throughout the diffusion process (from 10 min to 72 h, 11 time-points), and more importantly, at clinically relevant diffusion time-points (< 1 h). The precise determination of the contrast agents' partitions at early time-points was possible due to the short image acquisition times. Based on the results from study I and a dual-contrast study [1] that had used a clinical CT, the technique was improved by lowering the concentration of the contrast agents in study II, while other experimental conditions were kept constant. In studies **II** and **III**, the dual-energy imaging was performed using a microtomography scanner Quantum FX. The image acquisition was faster than was possible with the scanner used in study **I** (Skyscan). With each tube voltage, i.e., 90 kV and 50kV, the image acquisition time was 2 min. In QDECT, it is desirable to acquire images at two different energies swiftly and simultaneously.

7.2 QDECT TO ASSESS CARTILAGE COMPOSITION AND MECHANICAL PROPERTIES

As expected and reported in previous studies, the partitioning of the cationic agent was high in the middle and deep cartilage zones, which are rich in PGs [18,96]. Conversely, the partitioning of the non-ionic gadoteridol in cartilage reflected the depth-dependent decrease in the tissue water content [34,97]. The diffusion of electrically neutral agents across articular cartilage is slowed down with increasing cartilage tissue depth. This is because there is a gradual increase in the steric hindrance as cartilage depth increases due to the denser collagen network along with it higher PG concentration [98–100]. As a result of the steric hindrance, the diffusion of the non-ionic agent towards the deep cartilage is gradually curbed. Hence, the quantification of the non-ionic agent's partition and the rate of diffusion through the tissue provides insights into both the water content and diffusion attributes (permeability) of the extracellular matrix surrounding the cartilage, respectively.

In study **I**, in line with our hypothesis, normalization of the CA4+ partition with gadoteridol partition in cartilage (surface to 500 μm depth) improved the correlation with the cartilage equilibrium modulus ($E_{equilibrium}$). $E_{equilibrium}$ correlated significantly with both CA4+ and gadoteridol partitions, when normalized according to the CA4+ partition. Hence, the partition of cationic agents can provide information on the mechanical properties of cartilage. However, CA4+ partition, normalized according to the gadoteridol partition, did not reveal a higher correlation with the equilibrium modulus in the bulk cartilage, as seen in the surface layer. This could be due to the superficial layer controlling the cartilage indentation response [86,101]. In study **II**, normalized and non-normalized CA4+ correlated significantly with the equilibrium modulus after 21 and 32 h, respectively. Gadoteridol partition normalized CA4+ partition correlated with the instantaneous modulus at a later time-point (32 h).

In study **II**, CA4+ partition correlated significantly with the PG content in the superficial cartilage (10% of thickness) in the first hour of diffusion. With respect to the superficial 20% of the cartilage thickness, the correlation was observed only after 6 h. When inspecting the bulk cartilage, the correlation with PG content was relatively weak at early time-points. This weak correlation is a result of the absence of the contrast agents in deep cartilage at early diffusion time-points. In study **III**, we calculated the times required for the agents to reach 20% of the bath concentration in the cartilage-bone interface; they were 141 ± 83 min for gadoteridol and 216 ± 165 min for CA4+, respectively. In study **II**, after 10 h of CA4+ diffusion, the correlation with PG content was stronger and statistically significant in the bulk cartilage. More importantly, the gadoteridol partition, normalized according to the CA4+ partition,

revealed a significant correlation with cartilage PG content at the 4 h diffusion time point, 6 h earlier as compared to the non-normalized CA4+. Hence, the sensitivity of CA4+ partition to detect PG content had been improved after normalization with the gadoteridol partition. Theoretically, the improvement due to normalization is greatest during the early hours of diffusion when the agent fluxes are at their highest.

Diffusion of non-ionic agent is governed by the interstitial water content and permeability of cartilage [20,29]. Hence, at diffusion equilibrium, the depth-dependent partition profile of the non-ionic agent should be similar to the depth-dependent water content in cartilage. In study **I**, the partition of the non-ionic gadoteridol decreased gradually from the articular surface towards the cartilage-bone interface [1]. Lyophilization in study **III** revealed that the cartilage water content decreased similarly, a finding which has also been reported in previous studies [46,102]. In study **II,** although it was predicted that the gadoteridol partition would follow the depth-dependent trend of cartilage water content, it was surprising to detect rather high partitions in the deeper zones at later (> 21 h) diffusion time-points. This may be a result from a high uptake of the cationic agent into deep cartilage at later diffusion time-points (>21 h) potentially causing X-ray beam hardening which would affect the accuracy of the QDECT technique. This limitation is discussed in more detail in section 7.4.

In study **I**, normalization with the gadoteridol partition demonstrated a higher correlation between the CA4+ partition and the structural integrity of the cartilage (ICRS grade). Similarly, in study **II**, the correlation of CA4+ partition with the histopathological-histochemical grade, i.e., the Mankin score was higher throughout diffusion, after normalization with the gadoteridol partition. Mankin grading provides a comprehensive and detailed estimate of cartilage integrity based on its histological structure, Safranin O-staining, cellularity, and tidemark integrity. In contrast, ICRS grades are assigned only based on the intactness of the cartilage structure, more specifically on the depth of the localized lesion. For instance, the assessment of PG content is beyond the scope of ICRS grading. Nonetheless, with both standard grading systems, the normalization with gadoteridol partition revealed a higher correlation between the cationic agent partition and the changes in health condition of the studied cartilage.

7.3 EFFECT OF CARTILAGE CONSTITUENTS ON DIFFUSION OF CONTRAST AGENTS

We systematically evaluated the effect of the major solid constituents of cartilage, i.e., PG and collagen concentrations as well as the interstitial water content on the

diffusion of the cationic and non-ionic agents. Based on earlier findings, CA4+ diffusion was considered to be governed mostly by cartilage PG content [23,84]. However, when correlating the depth-wise PG concentration with the CA4+ partition in cartilage, we observed that CA4+ partition in the superficial and middle zone (surface - 40% cartilage depth) seemed to be controlled not only by the PG concentration but to an even greater extent by the tissue water content. In the middle and deep cartilage, i.e., 40% depth to the calcified cartilage layer, the CA4+ partition correlated significantly with the PG concentration. The samples showed signs of degeneration, as indicated by the Mankin score that ranged from 2 to 9 (n = 15, *Mean Mankin score* = 5.6). Cartilage degeneration generally begins from the surface and involves both decreased PG concentrations and an increased water content. These degeneration related changes in PG and water contents affect CA4+ diffusion. However, there was no correlation between the collagen concentration and CA4+ partition indicating that they exerted no direct effect on the diffusion of the cationic agent.

The depth-wise gadoteridol partition profiles resembled the water content distribution [20,29]. However, the depth-dependent relationship between the cartilage water content and gadoteridol partition did not reach statistical significance. At the 21 h diffusion time-point, gadoteridol partition correlated significantly and inversely with the concentration of the major solid constituent of cartilage i.e., collagen. The collagen and proteoglycan network interacts in cartilage to form a fiber-reinforced composite [103]. This interaction provides compressive stiffness, Donnan osmotic pressure, and regulates cartilage pore size and hydraulic permeability [1]. Any fibrillation of the collagen structure alters the permeability of cartilage and offers less resistance to the diffusion of non-ionic agents inside cartilage.

The present results demonstrate that the OA related degradation of cartilage and the associated compositional variations not only affect the contrast agents' partitions but also influences their diffusion rates. The diffusion of the agents in cartilage is non-uniform throughout, and the time for CA4+ to reach 20% partition in the deep cartilage was longer compared to that of gadoteridol. We infer this might be due to the summation of multiple factors such as the larger molecular size, multivalent electrostatic interactions between CA4+ and PGs as a function of tissue depth, and the reduced PG concentration in the superficial zone offering less electrostatic attraction. The time for CA4+ partition to reach 20% of the bath concentration in cartilage-bone interface was double the time required by gadoteridol in more degenerated cartilage (Mankin score > 5). However, in relatively intact samples (Mankin score ≤ 5), the diffusion times of both the agents were comparable.

In study **I,** the bath concentration of CA4+ was ~2.5 times the concentration used in study **II**. In studies **I** and **II**, after 72 h of immersion, the cationic agents (CA4+) partition was nearly three and five times that of the non-ionic agent, gadoteridol, respectively. It is known that as the concentration of the bath agent increases, the partition of a cationic agent in cartilage decreases in a non-linear manner [27,30,80]. Hence, the partition of cationic agents in cartilage is inversely proportional to the agent's concentration in the bath. A dual-contrast study requires that image acquisition is conducted with two X-ray energies (i.e., two tube voltages). In study **I**, the total image acquisition time with the microtomography scanner (Skyscan 1172, Skyscan, Kontich, Belgium) was 28 min. This lengthy image acquisition time of the system limited the ability of the technique to precisely quantify I (CA4+) and Gd (gadoteridol) in cartilage before the diffusion equilibrium [80]. This is due to the dynamic change in the depth-wise distribution and partition of contrast agent in cartilage until diffusion equilibrium. Thus, in study **I**, the QDECT technique was applied to evaluate the partition of both a cationic and a non–ionic agent in cartilage near to the diffusion equilibrium, i.e., after 72 h of immersion in the contrast agent bath [31,80]. The summary of the main findings and conclusions of the studies are presented in (Figure 7.1).

At clinically relevant diffusion time-points, contrast agent fluxes in cartilage are high, and even a difference of 2 min between the scans results in inaccuracies in the depth-wise quantification of the agent partitions. The error in contrast agent quantification due to the delay in imaging between two X-ray tube voltages was evaluated using numerical simulations. These simulations revealed that an increase in time between the acquisitions resulted in a higher error of the determined contrast agent partition values. The relative error was higher at the early diffusion time-points, and more for CA4+ than encountered with gadoteridol throughout diffusion. This was expected as the diffusion flux of CA4+ is higher [7,20,75]. Hence, image acquisition time is an important factor to be considered while planning a dual-contrast study.

Study I

The dual-contrast technique is applicable for the diagnosis of cartilage conditions at diffusion equilibrium.

- QDECT enabled the simultaneous determination of the distribution of I- and Gd-based contrast agents in cartilage.
- The sensitivity of the cationic contrast agent to detect changes in cartilage biomechanical properties was improved by simultaneously using it with a non-ionic agent.

Study II

The technique allows the diagnosis of cartilage conditions at clinically relevant time points.

- QDECT was applicable in all phases of contrast agent diffusion, and most importantly, in clinically relevant imaging time points.
- The technique improved the sensitivity of the cationic agent to detect changes in cartilage histopathological status throughout diffusion, allowing swifter determination of cartilage integrity.

Study III

- In superficial-mid cartilage, cationic agents' partition correlated with the tissue water content, whereas in the deep cartilage, it correlated with the PG concentration.
- Throughout cartilage, the non-ionic agents' partition correlated inversely with the tissue collagen concentration.
- Cartilage degeneration substantially decreased the time for the non-ionic agent to reach the cartilage-bone interface, while the opposite was the case with the cationic contrast agent.

Figure 7.1: Summary of the main findings and conclusions.

7.4 LIMITATIONS

The studies in this thesis are affected by certain limitations that need to be addressed; first, they were designed based on the availability of the human articular cartilage

samples. The samples were extracted from femur and tibia from a limited number of available cadavers (study **I**: $N = 2$, $n = 57$, study **II**: $N = 4$, $n = 33$, study **III**: $N = 4$, $n = 15$), with varying degrees of degeneration. Acquiring osteochondral samples from a higher number of cadavers would have improved the reliability of the conclusions. The plugs ($d = 8$ mm) were cut into two halves to make it possible to conduct the diffusion experiment and the reference measurements separately. This might have introduced an error when comparing the contrast agent partition in cartilage to the histological and spectroscopic measurements in the separate halves. However, we consider this source of error to be minimal, as the regions are adjoining, and the samples appeared visually homogeneous in both halved plugs.

In all of the studies, the samples were immersed in a contrast agent bath maintained at 4° C. The temperature was chosen to limit the degeneration of the samples and to inhibit bacterial and fungal growth during the long immersion hours. However, if one considers the clinical application of the agents inside the human body, then diffusion takes place at a higher temperature (i.e., 37° C). In study **II,** the diffusion time constant of the cationic agent CA4+ in human cartilage samples was $\tau = 1032$ min. Studies conducted at room temperature on bovine knee and human metacarpal cartilage samples with CA4+ have reported enhanced diffusion time constants of $\tau = 104.4$ min (*equilibrium time* = 25 h) and $\tau = 130$ min (*equilibrium time* = 14 h), respectively [75,104]. The diffusion equilibrium times and τ reported in these studies were shorter than the equilibrium time reported in a separate study using a smaller cationic agent CA2+ (686 g/mol, *equilibrium time* = 35.8 ± 6.5 h)[84]. Other influencing factors include,

(a) the difference in thicknesses and age of bovine (*Age* = 1-2 years) and human cartilage (*Mean age* = 71.25 ± 5.18,), and

(b) thinner human metacarpal cartilage (*Thickness* = 0.6-0.9 mm) compared to knee joint cartilage (*Thickness* = 2.56 mm) [104,105].

(c) the cyanoacrylate sealing of the edges allowed diffusion to take place only through the surface of the samples in study **II**, as in physiological conditions in contrast to the published study [75].

Hence, higher temperatures would promote faster contrast agent diffusion and are therefore expected to expedite the assessment of cartilage integrity [29]. Further, the results from the current studies show the uptake of the cationic agent in cartilage would continue beyond 72 h time-point. When designing the experiment, the immersion time of 72h was deemed sufficient for CA4+ to reach diffusion equilibrium based on a previous work [11]. However, CA4+ did not reach diffusion equilibrium. This is

acknowledged as a limitation of the study. However, longer immersion times could have jeopardized the integrity of the tissue due to possible proteolytic degeneration.

In studies **II** and **III**, gadoteridol partition in cartilage reached equilibrium before the 21 h diffusion time-point. After 21 h, unrealistic gadoteridol partition profiles were observed in the deep cartilage. At the 72 h time-point, gadoteridol correlated with the PG concentration, which was not observed at 21 h diffusion time-points. Furthermore, at 72 h the correlation observed earlier (at 21 h) with the collagen concentration was lost in the deeper cartilage layers. At the 21 h imaging time point, the partition of gadoteridol showed an unexpected increase from the surface towards the cartilage-bone interface. Conversely, gadoteridol should diffuse into cartilage according to the tissue water content, i.e., gradually decreasing from the surface to the cartilage bone interface [1,20]. The unexpected partitioning of gadoteridol in the mid- and deep-cartilage zones might have resulted from the high diffusion flux of the cationic agent (CA4+) [106–108]. Another possibility was that the high gadoteridol partition resulted from the X-ray beam hardening. The high gadoteridol partition was seen only at later diffusion time-points (> 21 h) in the mid- and deep cartilage zones with a high concentration of CA4+. However, when examining the contrast agent phantoms with concentrations similar to the concentrations measured in cartilage at 72 h diffusion time-point, there were no visible signs of X-ray beam hardening. The findings of these high gadoteridol partitions observed only at later diffusion time-points will require further investigation and should be considered when planning future dual-contrast experiments involving imaging at diffusion equilibrium.

7.5 CLINICAL APPLICATION OF QDECT AND FUTURE RESEARCH DIRECTIONS

Diffusion is a dynamic process, and the depth-wise concentration of the agents in cartilage changes continuously until equilibrium. The change is most profound during the early hours of diffusion when the concentration gradient is high between the contrast agent bath and cartilage. Scan time does not pose a problem in diffusion equilibrium when there is no longer any change in the depth-dependent concentration of the agents. However, imaging at diffusion equilibrium is not clinically feasible. Physiological excretory mechanisms will be active in removing the agent from the body. Hence, the clinical application of the dual-contrast technique would require that imaging should be performed simultaneously and instantaneously, e.g. during the first hour after contrast agent administration [24].

In this study, prior to the determination of contrast agent partitions, the X-ray attenuation of the native cartilage was subtracted from the attenuation of the contrast-enhanced cartilage. This requires the performance of two dual-energy CT scans, and this could be a problem for clinical application as the patient would be exposed to more ionizing radiation. Further, image co-registration and subtraction is required. Hence, if one wishes to avoid image subtraction and to minimize patient dose, the technique should be tailored to function with a single dual-energy CT scan. The technique requires the simultaneous administration of two contrast agents. Gadoteridol is widely used in clinics, and the incidence of acute adverse reactions has been reported to be low [109]. A preliminary study on the safety of CA4+ has been conducted *in vivo* [75,96]. However, the safety implications when the agents are combined should be addressed.

The technique requires further research before its adaptation to the clinic can be realized. The next step forward is to employ the technique on animal/cadaver joints ex *vivo* using a clinical CT protocol. Application of the technique i*n vivo* would require optimizing and establishing imaging protocols, such as the concentration of the agents to be used, joint movement, and acquisition time point after administering the agents. *In vivo* imaging requires intraarticular administration of contrast agents, and owing to their small molecular size, the agents undergo rapid clearance from the joint capsule. Fortunately, delayed-CECT imaging *in vivo* is possible when performed within the first hour after contrast agent administration [24]. Hence, the image acquisition time point after administering the contrast agents is key for accurate joint diagnostics while minimizing the amount and concentration of used agents. The presented topics need to be addressed in future dual-contrast imaging *in vivo*.

8 SUMMARY AND CONCLUSIONS

The main findings of the study are summarized as follows:

1. The QDECT technique is applicable in articular cartilage and enables the simultaneous determination of the partitions of iodine and gadolinium-based contrast agents.
2. The technique provides, for the first time, simultaneous information on depth-dependent cartilage PG and water contents.
3. The technique improves the diagnostic sensitivity of a cationic contrast agent when probing changes in cartilage histopathological and biomechanical status.
4. In degenerated cartilage, the diffusion of a cationic contrast agent in the superficial and middle cartilage zones is dependent not only on the PG content but to a greater extent also on the water content.
5. With degeneration, the diffusion rate of the cationic agent decreases, whereas the diffusion rate of the non-ionic agent increases.
6. The diffusion of the non-ionic contrast agent, gadoteridol, is significantly influenced by the cartilage collagen concentration.

9 BIBLIOGRAPHY

[1] Mow, V. C., Ratcliffe, A., and Poole, A. R., 1992, “Cartilage and Diarthrodial Joints as Paradigms for Hierarchical Materials and Structures.,” Biomaterials, **13**(2), pp. 67–97.

[2] Buckwalter, J. A., and Mankin, H. J., 1998, “Articular Cartilage: Degeneration and Osteoarthritis, Repair, Regeneration, and Transplantation.,” Instr. Course Lect., **47**, pp. 487–504.

[3] Ferry, T., Bergstrom, U., Hedstrom, E. M., Lorentzon, R., and Zeisig, E., 2014, “Epidemiology of Acute Knee Injuries Seen at the Emergency Department at Umea University Hospital, Sweden, during 15 Years.,” Knee Surg. Sports Traumatol. Arthrosc., **22**(5), pp. 1149–1155.

[4] Thomas, A. C., Hubbard-Turner, T., Wikstrom, E. A., and Palmieri-Smith, R. M., 2017, “Epidemiology of Posttraumatic Osteoarthritis.,” J. Athl. Train., **52**(6), pp. 491–496.

[5] Roemer, F. W., Eckstein, F., Hayashi, D., and Guermazi, A., 2014, “The Role of Imaging in Osteoarthritis.,” Best Pract. Res. Clin. Rheumatol., **28**(1), pp. 31–60.

[6] Hayashi, D., Roemer, F. W., and Guermazi, A., 2016, “Imaging for Osteoarthritis.,” Ann. Phys. Rehabil. Med., **59**(3), pp. 161–169.

[7] Lakin, B. A., Snyder, B. D., and Grinstaff, M. W., 2017, “Assessing Cartilage Biomechanical Properties: Techniques for Evaluating the Functional Performance of Cartilage in Health and Disease.,” Annu. Rev. Biomed. Eng., **19**, pp. 27–55.

[8] Viren, T., Saarakkala, S., Kaleva, E., Nieminen, H. J., Jurvelin, J. S., and Toyras, J., 2009, “Minimally Invasive Ultrasound Method for Intra-Articular Diagnostics of Cartilage Degeneration.,” Ultrasound Med. Biol., **35**(9), pp. 1546–1554.

[9] Laasanen, M. S., Toyras, J., Korhonen, R. K., Rieppo, J., Saarakkala, S., Nieminen, M. T., Hirvonen, J., and Jurvelin, J. S., 2003, “Biomechanical Properties of Knee Articular Cartilage.,” Biorheology, **40**(1–3), pp. 133–140.

[10] Viren, T., Saarakkala, S., Tiitu, V., Puhakka, J., Kiviranta, I., Jurvelin, J., and Toyras, J., 2011, “Ultrasound Evaluation of Mechanical Injury of Bovine Knee Articular Cartilage under Arthroscopic Control.,” IEEE Trans. Ultrason. Ferroelectr. Freq. Control, **58**(1), pp. 148–155.

[11] Brandt, K. D., Radin, E. L., Dieppe, P. A., and van de Putte, L., 2006, “Yet More Evidence That Osteoarthritis Is Not a Cartilage Disease.,” Ann. Rheum. Dis., **65**(10), pp. 1261–1264.

[12] Radin, E. L., 2005, “Who Gets Osteoarthritis and Why? An Update.,” J. Rheumatol., **32**(6), pp. 1136–1138.

[13] Anderson, D. D., Chubinskaya, S., Guilak, F., Martin, J. A., Oegema, T. R., Olson, S. A., and Buckwalter, J. A., 2011, “Post-Traumatic Osteoarthritis:

Improved Understanding and Opportunities for Early Intervention.," J. Orthop. Res., **29**(6), pp. 802–809.

[14] Bashir, A., Gray, M. L., Boutin, R. D., and Burstein, D., 1997, "Glycosaminoglycan in Articular Cartilage: In Vivo Assessment with Delayed Gd(DTPA)(2-)-Enhanced MR Imaging.," Radiology, **205**(2), pp. 551–558.

[15] Kallioniemi, A. S., Jurvelin, J. S., Nieminen, M. T., Lammi, M. J., and Töyräs, J., 2007, "Contrast Agent Enhanced PQCT of Articular Cartilage," Phys. Med. Biol., **52**(4), pp. 1209–1219.

[16] Kokkonen, H. T., Suomalainen, J.-S., Joukainen, A., Kröger, H., Sirola, J., Jurvelin, J. S., Salo, J., and Töyräs, J., 2014, "In Vivo Diagnostics of Human Knee Cartilage Lesions Using Delayed CBCT Arthrography.," J. Orthop. Res., **32**(3), pp. 403–412.

[17] Nieminen, M. T., Rieppo, J., Silvennoinen, J., Toyras, J., Hakumaki, J. M., Hyttinen, M. M., Helminen, H. J., and Jurvelin, J. S., 2002, "Spatial Assessment of Articular Cartilage Proteoglycans with Gd-DTPA-Enhanced T1 Imaging.," Magn. Reson. Med., **48**(4), pp. 640–648.

[18] Palmer, A. W., Guldberg, R. E., and Levenston, M. E., 2006, "Analysis of Cartilage Matrix Fixed Charge Density and Three-Dimensional Morphology via Contrast-Enhanced Microcomputed Tomography.," Proc. Natl. Acad. Sci. U. S. A., **103**(51), pp. 19255–19260.

[19] Kokkonen, H. T., Jurvelin, J. S., Tiitu, V., and Töyräs, J., 2011, "Detection of Mechanical Injury of Articular Cartilage Using Contrast Enhanced Computed Tomography.," Osteoarthr. Cartil., **19**(3), pp. 295–301.

[20] Silvast, T. S., Kokkonen, H. T., Jurvelin, J. S., Quinn, T. M., Nieminen, M. T., and Töyräs, J., 2009, "Diffusion and Near-Equilibrium Distribution of MRI and CT Contrast Agents in Articular Cartilage.," Phys. Med. Biol., **54**(22), pp. 6823–36.

[21] Kulmala, K. A. M., Karjalainen, H. M., Kokkonen, H. T., Tiitu, V., Kovanen, V., Lammi, M. J., Jurvelin, J. S., Korhonen, R. K., and Töyräs, J., 2013, "Diffusion of Ionic and Non-Ionic Contrast Agents in Articular Cartilage with Increased Cross-Linking—Contribution of Steric and Electrostatic Effects," Med. Eng. Phys., **35**(10), pp. 1415–1420.

[22] Evans, R. C., and Quinn, T. M., 2005, "Solute Diffusivity Correlates with Mechanical Properties and Matrix Density of Compressed Articular Cartilage.," Arch. Biochem. Biophys., **442**(1), pp. 1–10.

[23] Bansal, P. N., Joshi, N. S., Entezari, V., Malone, B. C., Stewart, R. C., Snyder, B. D., and Grinstaff, M. W., 2011, "Cationic Contrast Agents Improve Quantification of Glycosaminoglycan (GAG) Content by Contrast Enhanced CT Imaging of Cartilage.," J. Orthop. Res., **29**(5), pp. 704–709.

[24] Kokkonen, H. T., Aula, A. S., Kroger, H., Suomalainen, J.-S., Lammentausta, E., Mervaala, E., Jurvelin, J. S., and Toyras, J., 2012, "Delayed Computed Tomography Arthrography of Human Knee Cartilage In Vivo.," Cartilage, **3**(4), pp. 334–341.

[25] Kokkonen, H. T., Makela, J., Kulmala, K. A. M., Rieppo, L., Jurvelin, J. S., Tiitu, V., Karjalainen, H. M., Korhonen, R. K., Kovanen, V., and Töyräs, J.,

2011, “Computed Tomography Detects Changes in Contrast Agent Diffusion after Collagen Cross-Linking Typical to Natural Aging of Articular Cartilage.,” Osteoarthr. Cartil., **19**(10), pp. 1190–1198.

[26] Bansal, P. N., Stewart, R. C., Entezari, V., Snyder, B. D., and Grinstaff, M. W., 2011, “Contrast Agent Electrostatic Attraction Rather than Repulsion to Glycosaminoglycans Affords a Greater Contrast Uptake Ratio and Improved Quantitative CT Imaging in Cartilage.,” Osteoarthr. Cartil., **19**(8), pp. 970–976.

[27] Lakin, B. A., Grasso, D. J., Stewart, R. C., Freedman, J. D., Snyder, B. D., and Grinstaff, M. W., 2013, “Contrast Enhanced CT Attenuation Correlates with the GAG Content of Bovine Meniscus.,” J. Orthop. Res., **31**(11), pp. 1765–1771.

[28] Stewart, R. C., Honkanen, J. T. J., Kokkonen, H. T., Tiitu, V., Saarakkala, S., Joukainen, A., Snyder, B. D., Jurvelin, J. S., Grinstaff, M. W., and Töyräs, J., 2017, “Contrast-Enhanced Computed Tomography Enables Quantitative Evaluation of Tissue Properties at Intrajoint Regions in Cadaveric Knee Cartilage,” Cartilage, **8**(4), pp. 391–399.

[29] Albert Einstein, 1956, *Investigations on the Theory of, The Brownian Movement*, Dover Publications, Inc.

[30] Honkanen, M. K. M., Matikka, H., Honkanen, J. T. J., Bhattarai, A., Grinstaff, M. W., Joukainen, A., Kroger, H., Jurvelin, J. S., and Toyras, J., 2019, “Imaging of Proteoglycan and Water Contents in Human Articular Cartilage with Full-Body CT Using Dual Contrast Technique.,” J. Orthop. Res.

[31] Saukko, A. E. A., Turunen, M. J., Honkanen, M. K. M., Lovric, G., Tiitu, V., Honkanen, J. T. J., Grinstaff, M. W., Jurvelin, J. S., and Töyräs, J., 2019, “Simultaneous Quantitation of Cationic and Non-Ionic Contrast Agents in Articular Cartilage Using Synchrotron MicroCT Imaging.,” Sci. Rep., **9**(1), p. 7118.

[32] Abreu, E., 2005, “Mow VC, Huiskes R: Basic Orthopaedic Biomechanics and Mechano-Biology,” Biomed. Eng. Online, **4**(1), p. 28.

[33] Armstrong, C. G., and Mow, V. C., 1983, “The Mechanical Properties of Articular Cartilage.,” Bull. Hosp. Jt. Dis. Orthop. Inst., **43**(2), pp. 109–117.

[34] Brocklehurst, R., Bayliss, M. T., Maroudas, A., Coysh, H. L., Freeman, M. A., Revell, P. A., and Ali, S. Y., 1984, “The Composition of Normal and Osteoarthritic Articular Cartilage from Human Knee Joints. With Special Reference to Unicompartmental Replacement and Osteotomy of the Knee.,” J. Bone Joint Surg. Am., **66**(1), pp. 95–106.

[35] kuettner, K.E., Schleyerberg, R. , Hascall, V. C., 1986, *Articular Cartilage Biomchemistry*, Raven press, New York, USA.

[36] Buckwalter, J., and Mankin, H., 1997, “Articular Cartilage: Part II: Degeneration and Osteoarthritis, Repair, Regeneration, and Transplantation.,” J Bone Jt. Surg Am, **79**(4), pp. 612–632.

[37] Gilmore, R. S., and Palfrey, A. J., 1988, “Chondrocyte Distribution in the Articular Cartilage of Human Femoral Condyles.,” J. Anat., **157**, pp. 23–31.

[38] Sophia Fox, A. J., Bedi, A., and Rodeo, S. A., 2009, “The Basic Science of

Articular Cartilage: Structure, Composition, and Function.," Sports Health, **1**(6), pp. 461–468.

[39] van Kampen, G. P., Veldhuijzen, J. P., Kuijer, R., van de Stadt, R. J., and Schipper, C. A., 1985, "Cartilage Response to Mechanical Force in High-Density Chondrocyte Cultures.," Arthritis Rheum., **28**(4), pp. 419–424.

[40] Sah, R. L., Kim, Y. J., Doong, J. Y., Grodzinsky, A. J., Plaas, A. H., and Sandy, J. D., 1989, "Biosynthetic Response of Cartilage Explants to Dynamic Compression.," J. Orthop. Res., **7**(5), pp. 619–636.

[41] Freeman, P. M., Natarajan, R. N., Kimura, J. H., and Andriacchi, T. P., 1994, "Chondrocyte Cells Respond Mechanically to Compressive Loads.," J. Orthop. Res., **12**(3), pp. 311–320.

[42] Bader, D. L., and Kempson, G. E., 1994, "The Short-Term Compressive Properties of Adult Human Articular Cartilage.," Biomed. Mater. Eng., **4**(3), pp. 245–256.

[43] Eyre, D. R., Dickson, I. R., and Van Ness, K., 1988, "Collagen Cross-Linking in Human Bone and Articular Cartilage. Age-Related Changes in the Content of Mature Hydroxypyridinium Residues.," Biochem. J., **252**(2), pp. 495–500.

[44] Maroudas, A., Muir, H., and Wingham, J., 1969, "The Correlation of Fixed Negative Charge with Glycosaminoglycan Content of Human Articular Cartilage.," Biochim. Biophys. Acta, **177**(3), pp. 492–500.

[45] Huber, M., Trattnig, S., and Lintner, F., 2000, "Anatomy, Biochemistry, and Physiology of Articular Cartilage.," Invest. Radiol., **35**(10), pp. 573–580.

[46] Mow, V. C., Wang, C. C., and Hung, C. T., 1999, "The Extracellular Matrix, Interstitial Fluid and Ions as a Mechanical Signal Transducer in Articular Cartilage.," Osteoarthr. Cartil., **7**(1), pp. 41–58.

[47] Gu, W. Y., Lai, W. M., and Mow, V. C., 1998, "A Mixture Theory for Charged-Hydrated Soft Tissues Containing Multi-Electrolytes: Passive Transport and Swelling Behaviors.," J. Biomech. Eng., **120**(2), pp. 169–180.

[48] Bollet, A. J., and Nance, J. L., 1966, "Biochemical Findings in Normal and Osteoarthritic Articular Cartilage. II. Chondroitin Sulfate Concentration and Chain Length, Water, and Ash Content.," J. Clin. Invest., **45**(7), pp. 1170–1177.

[49] Eisenberg, S. R., and Grodzinsky, A. J., 1985, "Swelling of Articular Cartilage and Other Connective Tissues: Electromechanochemical Forces.," J. Orthop. Res., **3**(2), pp. 148–159.

[50] Kempson, G. E., Muir, H., Swanson, S. A., and Freeman, M. A., 1970, "Correlations between Stiffness and the Chemical Constituents of Cartilage on the Human Femoral Head.," Biochim. Biophys. Acta, **215**(1), pp. 70–77.

[51] Armstrong, C. G., and Mow, V. C., 1982, "Variations in the Intrinsic Mechanical Properties of Human Articular Cartilage with Age, Degeneration, and Water Content.," J. Bone Joint Surg. Am., **64**(1), pp. 88–94.

[52] Kempson, G. E., Muir, H., Pollard, C., and Tuke, M., 1973, "The Tensile Properties of the Cartilage of Human Femoral Condyles Related to the

Content of Collagen and Glycosaminoglycans.," Biochim. Biophys. Acta, **297**(2), pp. 456–472.

[53] Schinagl, R. M., Gurskis, D., Chen, A. C., and Sah, R. L., 1997, "Depth-Dependent Confined Compression Modulus of Full-Thickness Bovine Articular Cartilage.," J. Orthop. Res., **15**(4), pp. 499–506.

[54] Ateshian, G. A., 2009, "The Role of Interstitial Fluid Pressurization in Articular Cartilage Lubrication.," J. Biomech., **42**(9), pp. 1163–1176.

[55] Jay, G. D., Torres, J. R., Warman, M. L., Laderer, M. C., and Breuer, K. S., 2007, "The Role of Lubricin in the Mechanical Behavior of Synovial Fluid.," Proc. Natl. Acad. Sci. U. S. A., **104**(15), pp. 6194–6199.

[56] Schmidt, T. A., Gastelum, N. S., Nguyen, Q. T., Schumacher, B. L., and Sah, R. L., 2007, "Boundary Lubrication of Articular Cartilage: Role of Synovial Fluid Constituents.," Arthritis Rheum., **56**(3), pp. 882–891.

[57] Cross, M., Smith, E., Hoy, D., Nolte, S., Ackerman, I., Fransen, M., Bridgett, L., Williams, S., Guillemin, F., Hill, C. L., Laslett, L. L., Jones, G., Cicuttini, F., Osborne, R., Vos, T., Buchbinder, R., Woolf, A., and March, L., 2014, "The Global Burden of Hip and Knee Osteoarthritis: Estimates from the Global Burden of Disease 2010 Study.," Ann. Rheum. Dis., **73**(7), pp. 1323–1330.

[58] "HCUP."

[59] Barton, K. I., Shekarforoush, M., Heard, B. J., Sevick, J. L., Vakil, P., Atarod, M., Martin, R., Achari, Y., Hart, D. A., Frank, C. B., and Shrive, N. G., 2017, "Use of Pre-Clinical Surgically Induced Models to Understand Biomechanical and Biological Consequences of PTOA Development.," J. Orthop. Res., **35**(3), pp. 454–465.

[60] Mankin, H. J., and Thrasher, A. Z., 1975, "Water Content and Binding in Normal and Osteoarthritic Human Cartilage.," J. Bone Joint Surg. Am., **57**(1), pp. 76–80.

[61] Maroudas, A., and Venn, M., 1977, "Chemical Composition and Swelling of Normal and Osteoarthrotic Femoral Head Cartilage. II. Swelling.," Ann. Rheum. Dis., **36**(5), pp. 399–406.

[62] Spahn, G., Klinger, H. M., Baums, M., Pinkepank, U., and Hofmann, G. O., 2011, "Reliability in Arthroscopic Grading of Cartilage Lesions: Results of a Prospective Blinded Study for Evaluation of Inter-Observer Reliability.," Arch. Orthop. Trauma Surg., **131**(3), pp. 377–381.

[63] Link, T. M., Neumann, J., and Li, X., 2017, "Prestructural Cartilage Assessment Using MRI.," J. Magn. Reson. Imaging, **45**(4), pp. 949–965.

[64] Li, Q., Amano, K., Link, T. M., and Ma, C. B., 2016, "Advanced Imaging in Osteoarthritis.," Sports Health, **8**(5), pp. 418–428.

[65] Li, X., Pedoia, V., Kumar, D., Rivoire, J., Wyatt, C., Lansdown, D., Amano, K., Okazaki, N., Savic, D., Koff, M. F., Felmlee, J., Williams, S. L., and Majumdar, S., 2015, "Cartilage T1rho and T2 Relaxation Times: Longitudinal Reproducibility and Variations Using Different Coils, MR Systems and Sites.," Osteoarthr. Cartil., **23**(12), pp. 2214–2223.

[66] Lusic, H., and Grinstaff, M. W., 2013, “X-Ray-Computed Tomography Contrast Agents.,” Chem. Rev., **113**(3), pp. 1641–1666.

[67] Heaton, P. P. D. and B., 1999, *Physics for Diagnostic Radiology*, Institute of Physics Publishing, Brostol.

[68] Oppelt, A., 2005, *Imaging System for Medical Diagnostics*, Publicis Corporate Publishing, Erlangen.

[69] Anderson, N. G., and Butler, A. P., 2014, “Clinical Applications of Spectral Molecular Imaging: Potential and Challenges.,” Contrast Media Mol. Imaging, **9**(1), pp. 3–12.

[70] Rajendran, K., Lobker, C., Schon, B. S., Bateman, C. J., Younis, R. A., de Ruiter, N. J. A., Chernoglazov, A. I., Ramyar, M., Hooper, G. J., Butler, A. P. H., Woodfield, T. B. F., and Anderson, N. G., 2017, “Quantitative Imaging of Excised Osteoarthritic Cartilage Using Spectral CT.,” Eur. Radiol., **27**(1), pp. 384–392.

[71] Maret, D., Telmon, N., Peters, O. A., Lepage, B., Treil, J., Inglese, J. M., Peyre, A., Kahn, J. L., and Sixou, M., 2012, “Effect of Voxel Size on the Accuracy of 3D Reconstructions with Cone Beam CT.,” Dentomaxillofac. Radiol., **41**(8), pp. 649–655.

[72] Pasternak, J. J., and Williamson, E. E., 2012, “Clinical Pharmacology, Uses, and Adverse Reactions of Iodinated Contrast Agents: A Primer for the Non-Radiologist.,” Mayo Clin. Proc., **87**(4), pp. 390–402.

[73] Joshi, N. S., Bansal, P. N., Stewart, R. C., Snyder, B. D., and Grinstaff, M. W., 2009, “Effect of Contrast Agent Charge on Visualization of Articular Cartilage Using Computed Tomography: Exploiting Electrostatic Interactions for Improved Sensitivity.,” J. Am. Chem. Soc., **131**(37), pp. 13234–13235.

[74] Piscaer, T. M., van Osch, G. J. V. M., Verhaar, J. A. N., and Weinans, H., 2008, “Imaging of Experimental Osteoarthritis in Small Animal Models.,” Biorheology, **45**(3–4), pp. 355–364.

[75] Stewart, R. C., Bansal, P. N., Entezari, V., Lusic, H., Nazarian, R. M., Snyder, B. D., and Grinstaff, M. W., 2013, “Contrast-Enhanced CT with a High-Affinity Cationic Contrast Agent for Imaging Ex Vivo Bovine, Intact Ex Vivo Rabbit, and in Vivo Rabbit Cartilage.,” Radiology, **266**(1), pp. 141–150.

[76] McClennan, B. L., 1990, “Preston M. Hickey Memorial Lecture. Ionic and Nonionic Iodinated Contrast Media: Evolution and Strategies for Use.,” AJR. Am. J. Roentgenol., **155**(2), pp. 225–233.

[77] Millis, J., 1911, “BROWNIAN MOVEMENTS AND MOLECULAR REALITY.,” Science, **33**(846), pp. 426–427.

[78] Maroudas, A., 1968, “Physicochemical Properties of Cartilage in the Light of Ion Exchange Theory.,” Biophys. J., **8**(5), pp. 575–595.

[79] Kokkonen, H. T., Chin, H. C., Töyräs, J., Jurvelin, J. S., and Quinn, T. M., 2016, “Solute Transport of Negatively Charged Contrast Agents Across Articular Surface of Injured Cartilage.,” Ann. Biomed. Eng., **45**(4), pp. 973–981.

[80] Bhattarai, A., Honkanen, J. T. J., Myller, K. A. H., Prakash, M., Korhonen, M., Saukko, A. E. A., Viren, T., Joukainen, A., Patwa, A. N., Kroger, H., Grinstaff, M. W., Jurvelin, J. S., and Toyras, J., 2018, “Quantitative Dual Contrast CT Technique for Evaluation of Articular Cartilage Properties.,” Ann. Biomed. Eng., **46**(7), pp. 1038–1046.

[81] Saukko, A. E. A., Honkanen, J. T. J., Xu, W., Vaananen, S. P., Jurvelin, J. S., Lehto, V.-P., and Töyräs, J., 2017, “Dual Contrast CT Method Enables Diagnostics of Cartilage Injuries and Degeneration Using a Single CT Image.,” Ann. Biomed. Eng.

[82] Tiderius, C. J., Svensson, J., Leander, P., Ola, T., and Dahlberg, L., 2004, “DGEMRIC (Delayed Gadolinium-Enhanced MRI of Cartilage) Indicates Adaptive Capacity of Human Knee Cartilage.,” Magn. Reson. Med., **51**(2), pp. 286–290.

[83] Lakin, B. A., Ellis, D. J., Shelofsky, J. S., Freedman, J. D., Grinstaff, M. W., and Snyder, B. D., 2015, “Contrast-Enhanced CT Facilitates Rapid, Non-Destructive Assessment of Cartilage and Bone Properties of the Human Metacarpal.,” Osteoarthr. Cartil., **23**(12), pp. 2158–2166.

[84] Honkanen, J. T. J., Turunen, M. J., Freedman, J. D., Saarakkala, S., Grinstaff, M. W., Ylärinne, J. H., Jurvelin, J. S., and Töyräs, J., 2016, “Cationic Contrast Agent Diffusion Differs Between Cartilage and Meniscus.,” Ann. Biomed. Eng., **44**(10), pp. 2913–2921.

[85] Rangacharyulu, C., 2013, *Physics of Nuclear Radiations Concepts, Techniques and Applications*, Taylor and Francis.

[86] Korhonen, R. K., Laasanen, M. S., Töyräs, J., Lappalainen, R., Helminen, H. J., and Jurvelin, J. S., 2003, “Fibril Reinforced Poroelastic Model Predicts Specifically Mechanical Behavior of Normal, Proteoglycan Depleted and Collagen Degraded Articular Cartilage.,” J. Biomech., **36**(9), pp. 1373–1379.

[87] Korhonen, R. K., Laasanen, M. S., Toyras, J., Rieppo, J., Hirvonen, J., Helminen, H. J., and Jurvelin, J. S., 2002, “Comparison of the Equilibrium Response of Articular Cartilage in Unconfined Compression, Confined Compression and Indentation.,” J. Biomech., **35**(7), pp. 903–909.

[88] Julkunen, P., Wilson, W., Jurvelin, J. S., Rieppo, J., Qu, C.-J., Lammi, M. J., and Korhonen, R. K., 2008, “Stress-Relaxation of Human Patellar Articular Cartilage in Unconfined Compression: Prediction of Mechanical Response by Tissue Composition and Structure.,” J. Biomech., **41**(9), pp. 1978–1986.

[89] Hayes, W. C., Keer, L. M., Herrmann, G., and Mockros, L. F., 1972, “A Mathematical Analysis for Indentation Tests of Articular Cartilage.,” J. Biomech., **5**(5), pp. 541–551.

[90] Huttu, M. R. J., Puhakka, J., Makela, J. T. A., Takakubo, Y., Tiitu, V., Saarakkala, S., Konttinen, Y. T., Kiviranta, I., and Korhonen, R. K., 2014, “Cell-Tissue Interactions in Osteoarthritic Human Hip Joint Articular Cartilage.,” Connect. Tissue Res., **55**(4), pp. 282–291.

[91] Kiviranta, P., Rieppo, J., Korhonen, R. K., Julkunen, P., Toyras, J., and Jurvelin, J. S., 2006, “Collagen Network Primarily Controls Poisson’s Ratio of Bovine Articular Cartilage in Compression.,” J. Orthop. Res., **24**(4), pp. 690–

699.

[92] Kiviranta, I., Jurvelin, J., Tammi, M., Saamanen, A. M., and Helminen, H. J., 1985, “Microspectrophotometric Quantitation of Glycosaminoglycans in Articular Cartilage Sections Stained with Safranin O.,” Histochemistry, **82**(3), pp. 249–255.

[93] Saarakkala, S., and Julkunen, P., 2010, “Specificity of Fourier Transform Infrared (FTIR) Microspectroscopy to Estimate Depth-Wise Proteoglycan Content in Normal and Osteoarthritic Human Articular Cartilage,” Cartilage, **1**(4), pp. 262–269.

[94] Brittberg, M., and Winalski, C. S., 2003, “Evaluation of Cartilage Injuries and Repair.,” J. Bone Joint Surg. Am., **85-A Suppl**, pp. 58–69.

[95] Mankin, H. J., Dorfman, H., Lippiello, L., and Zarins, A., 1971, “Biochemical and Metabolic Abnormalities in Articular Cartilage from Osteo-Arthritic Human Hips. II. Correlation of Morphology with Biochemical and Metabolic Data.,” J. Bone Joint Surg. Am., **53**(3), pp. 523–537.

[96] Stewart, R. C., Patwa, A. N., Lusic, H., Freedman, J. D., Wathier, M., Snyder, B. D., Guermazi, A., and Grinstaff, M. W., 2017, “Synthesis and Preclinical Characterization of a Cationic Iodinated Imaging Contrast Agent (CA4+) and Its Use for Quantitative Computed Tomography of Ex Vivo Human Hip Cartilage.,” J. Med. Chem., **60**(13), pp. 5543–5555.

[97] Berberat, J. E., Nissi, M. J., Jurvelin, J. S., and Nieminen, M. T., 2009, “Assessment of Interstitial Water Content of Articular Cartilage with T1 Relaxation.,” Magn. Reson. Imaging, **27**(5), pp. 727–732.

[98] Muir, H., Bullough, P., and Maroudas, A., 1970, “The Distribution of Collagen in Human Articular Cartilage with Some of Its Physiological Implications.,” J. Bone Joint Surg. Br., **52**(3), pp. 554–563.

[99] Maroudas, A., 1975, “Biophysical Chemistry of Cartilaginous Tissues with Special Reference to Solute and Fluid Transport.,” Biorheology, **12**(3–4), pp. 233–248.

[100] Pouran, B., Arbabi, V., Zadpoor, A. A., and Weinans, H., 2016, “Isolated Effects of External Bath Osmolality, Solute Concentration, and Electrical Charge on Solute Transport across Articular Cartilage.,” Med. Eng. Phys., **38**(12), pp. 1399–1407.

[101] Julkunen, P., Korhonen, R. K., Herzog, W., and Jurvelin, J. S., 2008, “Uncertainties in Indentation Testing of Articular Cartilage: A Fibril-Reinforced Poroviscoelastic Study.,” Med. Eng. Phys., **30**(4), pp. 506–515.

[102] Buckwalter, J. A., Mankin, H. J., and Grodzinsky, A. J., 2005, “Articular Cartilage and Osteoarthritis.,” Instr. Course Lect., **54**, pp. 465–480.

[103] Makela, J. T. A., Huttu, M. R. J., and Korhonen, R. K., 2012, “Structure-Function Relationships in Osteoarthritic Human Hip Joint Articular Cartilage.,” Osteoarthr. Cartil., **20**(11), pp. 1268–1277.

[104] Freedman, J. D., Ellis, D. J., Lusic, H., Varma, G., Grant, A. K., Lakin, B. A., Snyder, B. D., and Grinstaff, M. W., 2020, “DGEMRIC and CECT Comparison of Cationic and Anionic Contrast Agents in Cadaveric Human Metacarpal

Cartilage.," J. Orthop. Res., **38**(4), pp. 719–725.

[105] Miese, F. R., Ostendorf, B., Wittsack, H.-J., Reichelt, D. C., Mamisch, T. C., Zilkens, C., Lanzman, R. S., Schneider, M., and Scherer, A., 2010, "Metacarpophalangeal Joints in Rheumatoid Arthritis: Delayed Gadolinium-Enhanced MR Imaging of Cartilage--a Feasibility Study.," Radiology, **257**(2), pp. 441–447.

[106] Honkanen, M. K. M., Saukko, A. E. A., Turunen, M. J., Shaikh, R., Prakash, M., Lovric, G., Joukainen, A., Kroger, H., Grinstaff, M. W., and Toyras, J., 2019, "Synchrotron MicroCT Reveals the Potential of the Dual Contrast Technique for Quantitative Assessment of Human Articular Cartilage Composition.," J. Orthop. Res.

[107] Bhattarai, A., Pouran, B., Mäkelä, J. T. A., Shaikh, R., Honkanen, M. K. M., Prakash, M., Kröger, H., Grinstaff, M. W., Weinans, H., Jurvelin, J. S., and Töyräs, J., 2020, "Dual Contrast in Computed Tomography Allows Earlier Characterization of Articular Cartilage over Single Contrast.," J. Orthop. Res. Off. Publ. Orthop. Res. Soc.

[108] Bhattarai, A., Mäkelä, J. T. A., Pouran, B., Kröger, H., Weinans, H., Grinstaff, M. W., Töyräs, J., and Turunen, M. J., 2020, "Effects of Human Articular Cartilage Constituents on Simultaneous Diffusion of Cationic and Non-Ionic Contrast Agents.," J. Orthop. Res. Off. Publ. Orthop. Res. Soc.

[109] *Www.Accessdata.Fda.Gov/Drugsatfda_docs/Label/2017/020131s027lbl.Pdf*.

Paper **II**

Bhattarai A, Pouran B, Mäkelä JTA, Shaikh R, Honkanen MKM, Prakash M, Kröger H, Grinstaff MW, Weinans H, Jurvelin JS, Töyräs J. "Dual Contrast in Computed Tomography Allows Earlier Characterization of Articular Cartilage over Single Contrast." *Journal of Orthopaedic Research,* 2020.**38**(10):2230-2238.

Received: 25 November 2019 | Accepted: 28 May 2020

DOI: 10.1002/jor.24774

RESEARCH ARTICLE

Journal of Orthopaedic Research®

Dual contrast in computed tomography allows earlier characterization of articular cartilage over single contrast

Abhisek Bhattarai[1,2] | Behdad Pouran[3] | Janne T. A. Mäkelä[1] | Rubina Shaikh[1] | Miitu K. M. Honkanen[1,2] | Mithilesh Prakash[1,2] | Heikki Kröger[4] | Mark W. Grinstaff[5] | Harrie Weinans[3,6,7] | Jukka S. Jurvelin[1] | Juha Töyräs[1,2,8]

[1]Department of Applied Physics, University of Eastern Finland, Kuopio, Finland

[2]Diagnostic Imaging Center, Kuopio University Hospital, Kuopio, Finland

[3]Department of Orthopaedic, University Medical Center Utrecht, Utrecht, The Netherlands

[4]Department of Orthopedics, Traumatology and Hand Surgery, Kuopio University Hospital, Kuopio, Finland

[5]Departments of Biomedical Engineering, Chemistry, and Medicine, Boston University, Boston, Massachusetts

[6]Department of Biomechanical Engineering, Faculty of Mechanical, Maritime, and Materials Engineering, Delft University of Technology (TU Delft), Delft, The Netherlands

[7]Department of Rheumatology, University Medical Center, Utrecht, The Netherlands

[8]School of Information Technology and Electrical Engineering, The University of Queensland, Brisbane, Australia

Correspondence
Abhisek Bhattarai, MSc (Tech.), Department of Applied Physics, University of Eastern Finland, Finland, PO Box 1627, 70211 Kuopio, Finland.
Email: abhisek.bhattarai@uef.fi

Funding information
Academy of Finland, Grant/Award Numbers: 269315, 307932; State Research Funding of the Kuopio University Hospital Catchment Area, Grant/Award Numbers: 5041746, 5041757, 5041769; Päivikki ja Sakari Sohlbergin Säätiö

Abstract

Cationic computed tomography contrast agents are more sensitive for detecting cartilage degeneration than anionic or non-ionic agents. However, osteoarthritis-related loss of proteoglycans and increase in water content contrarily affect the diffusion of cationic contrast agents, limiting their sensitivity. The quantitative dual-energy computed tomography technique allows the simultaneous determination of the partitions of iodine-based cationic (CA4+) and gadolinium-based non-ionic (gadoteridol) agents in cartilage at diffusion equilibrium. Normalizing the cationic agent partition at diffusion equilibrium with that of the non-ionic agent improves diagnostic sensitivity. We hypothesize that this sensitivity improvement is also prominent during early diffusion time points and that the technique is applicable during contrast agent diffusion. To investigate the validity of this hypothesis, osteochondral plugs (d = 8 mm, N = 33), extracted from human cadaver (n = 4) knee joints, were immersed in a contrast agent bath (a mixture of CA4+ and gadoteridol) and imaged using the technique at multiple time points until diffusion equilibrium. Biomechanical testing and histological analysis were conducted for reference. Quantitative dual-energy computed tomography technique enabled earlier determination of cartilage proteoglycan content over single contrast. The correlation coefficient between human articular cartilage proteoglycan content and CA4+ partition increased with the contrast agent diffusion time. Gadoteridol normalized CA4+ partition correlated significantly (P < .05) with Mankin score at all time points and with proteoglycan content after 4 hours. The technique is applicable during diffusion, and normalization with gadoteridol partition improves the sensitivity of the CA4+ contrast agent.

KEYWORDS

biomechanics, cartilage, cationic contrast agent, contrast-enhanced computed tomography, dual-energy CT

1 | INTRODUCTION

As a consequence of instantaneous impact (eg, related to sports accident), articular cartilage can become injured, leading to the development of post-traumatic osteoarthritis (PTOA).[1] Erosion of articular cartilage, bone remodeling, and joint inflammation are the major characteristic features of osteoarthritis (OA).[2] Often, only in advanced stages of the disease patients experience symptoms, such as pain and limited mobility. Therefore, PTOA is often diagnosed after irreversible damage to the cartilage has already occurred, limiting any possibility of early intervention. Early detection of cartilage damage could enable pharmaceutical or surgical interventions for preventing the progression of OA.[3,4] Early OA is characterized by loss of proteoglycans (PGs), leading to decreased cartilage fixed charge density, lower swelling pressure, and subsequently reduced matrix stiffness.[5] Fibrillation, due to collagen network disruption, also leads to decreased stiffness and increased tissue deformation under physiological loading predisposing the tissue to further degeneration.[6]

Today's medical imaging modalities provide multiple methods on how to quantify OA. However, they all suffer from limitations. Ultrasonography provides real-time image acquisition cost-effectively. However, the challenge in achieving perpendicularity between the ultrasound beam angle and the naturally curving cartilage surface limits accurate diagnosis.[7] Magnetic resonance imaging (MRI) is great for soft tissues (eg, cartilage), but it suffers from relatively long scan times and high costs.[8] Computed tomography (CT) imaging is substantially more accessible and affordable, and the image acquisition is swift, and the resolution superior to MRI. Further, significant advancement has been achieved with dose optimization techniques and imaging strategies in CT to reduce the radiation doses involved.[9,10] However, poor soft-tissue contrast prevents separating native cartilage tissue from the surrounding synovial fluid, and, thus, requires the use of contrast agents.[11,12]

Delayed contrast-enhanced CT (CECT) has been applied for imaging human articular cartilage *in vivo* to assess tissue morphology and composition.[13] The diagnosis is based on the evaluation of an anionic contrast agent distribution within cartilage after intra-articular administration. Recently, a cationic CT agent was introduced.[14-16] Cartilage fixed negative charge, created by PGs, provides strong electrostatic attraction to cationic agents. These distribute inside the cartilage in direct relation to the cartilage PG content.[17] For this reason, cationic agents offer a more sensitive technique for diagnosing the distribution of PGs in cartilage compared with conventional anionic agents.[15,18-20] Higher uptake of the cationic agents in cartilage provides higher X-ray attenuation and improves contrast allowing better visualization of PG distribution and its variation within cartilage. Thus, the detection of subtle changes in PG content is possible at different stages of cartilage degeneration.[16,17] Contrast agents diffusion in early time points is fast, especially in degenerated cartilage, due to increased permeability. The uptake of a cationic agent depends both on the electrostatic attraction between the positively charged molecule and the negative fixed charge in cartilage, and the passive diffusion controlled by cartilage water content and permeability.[21] Thus, in degenerated cartilage, the uptake of the cationic agent is simultaneously reduced due to the decrease of negatively charged PGs, and enhanced due to the increase in permeability and water content. These opposite effects limit the diagnostic effectiveness of the cationic agents, especially in the first hours of diffusion, which is vital for the clinical feasibility of the agent. After intra-articular administration, contrast agents diffuse into cartilage, while simultaneously, the body clears out the agent from the joint cavity, lowering the concentration as time progresses. The concentration of anionic ioxaglate in joint cavity has been reported to be adequate for delayed-CECT until 2 hours after the administration, while the agent concentration in patellar and femoral cartilage reached the maximum 30 and 60 minutes after the administration, respectively.[13] The molar concentration of cationic and non-ionic agents in cartilage increases faster compared with an anionic agent.[19,22] Thus, considering the diffusion in cartilage and the clearing out of the contrast agents from the joint cavity, the 30 to 60 minutes imaging time window could be clinically feasible for the application of both cationic and non-ionic agents.

Contrast agent partition in cartilage is quantified as a ratio of contrast agent-induced X-ray attenuation in the cartilage relative to the attenuation in the bath.[23] Normalization (division) of an iodine-based cationic agent (CA4+) partition with an electrically neutral gadolinium-based agent (gadoteridol) partition improved the sensitivity of CA4+ to probe cartilage PG content after 72 hours of diffusion.[24,25] Because water content and permeability of cartilage control the diffusion of the non-ionic gadoteridol the normalization minimizes the effect of these factors on the diffusion of the cationic agent.[25,26] In early diffusion time points, contrast agent diffusion flux is high.[15,22] Further, the agent fluxes are even higher in a degenerated cartilage due to loss of collagen network integrity and reduced PG, resulting in increased permeability.[12,25] Considering this, we hypothesize that the improvement in the sensitivity of the cationic agent after normalization is even more substantial in a degenerated cartilage at early time points. Here we study the diffusion of the agents at clinically relevant time points (<1 hour after contrast agent administration) and at later diffusion time points close to diffusion equilibrium. Further, we examine the validity of the hypothesis by evaluating the sensitivity of normalized CA4+ partition to reflect variation in histopathological and biomechanical properties of human articular cartilage samples. Improvement in the sensitivity of the cationic agent would enable early detection of minor injuries and lesions, allowing timely selection of treatment, thus reducing the risk for PTOA. This quantitative technique is based on the simultaneous diffusion of two contrast agents (iodine-based CA4+ and gadolinium-based gadoteridol) into cartilage. Accurate simultaneous quantification of concentrations of two contrast agents using single X-ray tube voltage is not possible, as X-ray attenuation of both agents contributes to the attenuation. Hence, as iodine and gadolinium have different x-ray attenuation properties as a function of energy imaging with two separate X-ray tube voltages allows quantitative determination of the concentration of the elements in the mix. Determining the concentration of CA4+ and gadoteridol in cartilage is possible by using the Beer-Lambert law and Bragg's additive rule for mixtures as described in literature[24-26] and also in the materials and methods chapter of this paper. As the contrast agents are constantly diffusing

in cartilage during a scan, CT acquisition at two different X-ray tube voltages must be nearly instantaneous for accurate determination of contrast agent tissue partition. In this study, we also quantify the error in the partition of the contrast agents arising from the ongoing diffusion in the cartilage when the imaging is performed separately with two X-ray tube voltages.

2 | MATERIALS AND METHODS

2.1 | Sample extraction and preparation

Human osteochondral plugs ($N = 33$, $d = 8$ mm) were extracted from the lateral and medial tibial plateaus and femoral condyles in left and right knee joints of human cadavers ($n = 4$, mean age = 71.25 ± 5.18 years).[27-29] The Research Committee of the Northern Savo Hospital District granted a favorable opinion on collecting the human tissue (Kuopio University Hospital, Kuopio, Finland, Decision numbers: 134/2015 and58/2013). The samples were stored frozen in phosphate-buffered saline (PBS; −22°C).

2.2 | Biomechanical measurements

Samples were thawed at room temperature. A custom-made, high precision material testing device (resolution: 0.1 µm, 0.005 N, PM500-1 A; Newport, Irvine, CA) was employed for biomechanical testing of the osteochondral plugs.[30] Measurement setup schematics are included in the supplementary material (Figure S6). During the test, the plugs were immersed in PBS containing inhibitors of proteolytic enzymes (5 mM EDTA, VWR International, and 5 mM benzamidine hydrochloride hydrate [Sigma-Aldrich Inc, St. Louis, MO]). A flat-ended metallic indenter ($d = 728$ µm [$n = 20$] or $d = 667$ µm [$n = 13$]) was driven in perpendicular contact with the articular surface. During the experiments, the tip of the indenter was accidentally damaged, and we had to continue the experiment with a spare indenter. The new indenter tip diameter was slightly different from the damaged indenter. However, the difference in the diameter is accounted for in the determination of the moduli values along Hayes et al.,[31] A pre-stress of 12.5 kPa defined the contact.[32] Based on literature, the Poisson ratios were set to ν = (0.3(Tibia), 0.2(Femur)) for $E_{equilibrium}$ and $\nu = 0.5$ for $E_{instantaneous}$.[33,34] The plugs were then again frozen, cut to two halves, and stored in a freezer (−22°C). One half was thawed for contrast-enhanced microCT imaging experiment, and the other half was prepared for reference histological analyses.

2.3 | MicroCT imaging

The dual-energy microCT set-up was tested and validated by quantifying iodine (I) and gadolinium (Gd) contents in phantoms with known contrast agent mixtures consisting of gadoteridol (20, 12, and 8 mgGd/mL) and CA4+ (0, 10, 20, 30, 40, 50, 60, and 70 mgL/mL). Calibration curves and the measurement setup are presented in the supplementary material (Figures S7, S8, and S9). The edges of the osteochondral samples were sealed using cyanoacrylate (Super glue Precision, Loctite, Düsseldorf, Germany) to allow the contrast agent diffusion only through the articulating surface. Before the immersion in contrast agent bath, the plugs were imaged with a high-resolution microCT scanner (Quantum FX, Perkin Elmer) with an isotropic voxel size of 40 × 40 × 40 µm and using a 20 × 20 mm field of view. Three samples were arranged in a sample holder and immersed in a contrast agent bath (15 ml) comprised of iodine-based CA4+ (5,5′-(malonylbis(azanediyl))bis(N^1,N^3-bis(2-aminoethyl)−2,4,6-triiodoisophthalamide, $q = +4$, $M = 1499.88$ g/mol) and gadolinium-based gadoteridol (Prohance; Bracco International B. V., Amsterdam, Netherlands, $q = 0$, $M = 559$ g/mol) diluted in PBS. The expected partitions of the contrast agents in cartilage were accounted for when designing the concentration to use for the bath, to achieve a similar relative contribution to X-ray attenuation at tube voltages of 50 and 90 kVp.[22,26,35] By doing so, the optimum signal to noise ratio was achieved while limiting excessive beam hardening and photon starvation artifacts. Based on these considerations 10 mgI/mL (CA4+) and 20 mgGd/mL (gadoteridol) were selected for the immersion bath. To prevent degradation of the samples, proteolytic inhibitors, 5 mM of ethylenediaminetetraacetic acid (EDTA, VWR International, France), 5 mM of benzamidine hydrochloride hydrate (Sigma-Aldrich Inc), and penicillin-streptomycin-amphotericin (Antibiotic Antimycotic solution, stabilized; Sigma-Aldrich Inc) were added to the bath. The samples were imaged using the Quantum FX microCT scanner at the following diffusion time points: 10 minutes, 30 minutes, 1, 2, 3, 4, 6, 10, 21, 32, 50, 72 hours. The osmolality of the contrast agent bath was 297 mOsm/kg measured using a commercial osmometer (Advanced Model 3320 micro-osmometer; Advanced Instruments, MA). The contrast agent bath was gently stirred throughout the immersion of the samples. The stirring assembly was placed inside a refrigerator (4°C) to preserve the cartilage and prevent bacterial and fungal growth. For microCT imaging, the samples were removed from the bath, gently blotted on the edges with blotting paper, and placed inside a humidified plastic tube. Scanning was performed using two X-ray energies (tube voltages of 90 and 50 kVp). Gd and I have well-separated K-absorption edges of 50.2 and 33.1 keV, respectively. When using a 50 kVp tube voltage, the maximum fraction of the spectrum was selected to be between the K-edges of I and Gd to maximize the ratio of X-ray absorption caused by I and Gd (μ_I/μ_{Gd}). Similarly, when using 90 kVp, the maximum fraction of the spectrum was selected to be above 50 kVp to maximize the μ_{Gd}/μ_I ratio (Figure S10). The tube current (0.2 mA) was set to the maximum value allowed by the manufacturer to improve the signal to noise ratio. Immediately after imaging, the samples were placed back into the contrast agent bath. The image acquisition time with each tube voltage was approximately 2 minute. Due to a human error, three samples were imaged twice using the same tube voltage at 1 hour diffusion time point. Thus, the partition results for those samples could not be calculated, and the 1 hour time point results of those samples have been excluded.

2.4 | Image analysis

The concentrations of iodine (C_I) and gadolinium-based (C_{Gd}) contrast agents in cartilage were resolved based on Beer-Lambert law and Bragg's additive rule of mixtures:

$$\alpha_E = \mu_{I(E)} C_I + \mu_{Gd(E)} C_{Gd}, \quad (1)$$

where α is X-ray attenuation in a medium at energy E (tube voltages of 90 and 50 kVp) as,

$$C_I = \frac{\alpha_{(90kV)}\mu_{Gd(50kV)} - \alpha_{(50kV)}\mu_{Gd(90kV)}}{\mu_{I(90kV)}\mu_{Gd(50kV)} - \mu_{I(50kV)}\mu_{Gd(90kV)}} \quad (2)$$

$$C_{Gd} = \frac{\alpha_{(90kV)}\mu_{I(50kV)} - \alpha_{(50kV)}\mu_{I(90kV)}}{\mu_{Gd(90kV)}\mu_{I(50kV)} - \mu_{Gd(50kV)}\mu_{I(90kV)}}. \quad (3)$$

The mass attenuation coefficients for CA4+ ($\mu_{I,E}$) and gadoteridol ($\mu_{Gd,E}$) were determined at both energies by imaging series of contrast agent solutions with known I and Gd concentrations in distilled water, respectively. Segmentation of the articulating surface and bone-cartilage interface was done using Seg3D software (vs. 2.4.0; The University of Utah, Salt Lake City, UT). The volume of interest was defined to be 2800 × 2000 μm × cartilage thickness. The X-ray attenuation profiles from the surface to deep cartilage were extracted using Matlab (R2016b; The Mathworks Inc, Natick, MA). To avoid partial volume effect arising from background and irregular and undulating surface, and cartilage-bone interface, 3% and 5% of cartilage thickness from the articular surface and cartilage-bone interface, respectively, was excluded from the attenuation profiles. X-ray attenuation profiles of the cartilage before immersion in contrast agent bath were subtracted from the contrast-enhanced cartilage profiles to obtain depth-wise attenuation profiles induced only by the contrast agents. Concentration profiles of I and Gd from the surface to the deep cartilage were calculated using Equations 2 and 3, respectively.

2.5 | Histological analysis and Mankin scoring

The osteochondral samples were decalcified in EDTA. Following dehydration, the EDTA decalcified samples were embedded in paraffin to be cut into 3 μm thick sections from the center of the plug along the coronal plane (from articulating surface to the cartilage-bone interface). After removing the paraffin, the cut sections were stained with Safranin-O.[36] Optical density (OD) of the staining in each section was determined by applying quantitative digital densitometry technique using a light microscope (Nikon Microphot-FXA, Nikon Co, Japan) equipped with a 12-bit CCD camera (ORCA-ER; Hamamatsu Photonics K.K., Japan). For each cartilage sample, three histological sections were measured. The depth-wise OD profiles of the sections were then normalized to the length of 100 points and averaged. Before the measurements, the system was calibrated using neutral density filters (Advanced Optics SCHOTT AG, Mainz, Germany) with OD range between 0 (low) and 3 (high).

Four independent observers (M. Honkanen, R. Shaikh, N. Hänninen, M. Prakash) assessed and assigned histopathological Mankin scoring based on the severity of OA using the Safranin-O stained sections.[37] Mankin score characterizes cartilage based on staining (0-4), tidemark integrity (0-1), abnormality in structure (0-6), and cellularity (0-3). Intact cartilage is assigned score 0, and a severely degenerated sample is scored 14. Mankin scores were calculated by averaging the scores of three sections per sample.

2.6 | Error simulation

Error in contrast agent concentrations arising from the progressing diffusion during the time between image acquisitions with two X-ray tube voltages (90 and 50 kVp) was studied using a numerical simulation. To describe the contrast agents diffusion in cartilage, equation $C = C_{max} \times [1 - \exp(-t/\tau)]$ was fitted to the experimental data (all the samples in the present study), where C represents I and Gd concentrations in mgI/ml and mgGd/ml, respectively, t is the diffusion time (minutes) and τ is the time required to reach 63.2% of the maximum concentration (C_{max}).[15] The error simulation was implemented in steps, as follows:

Step 1. Fitting was done for each sample individually, after which a mean of the parameters (C_{max} vs τ) for both contrast agents was calculated (Figure 1).

Step 2. Using equation 1, X-ray attenuation was simulated with both tube voltages, based on the contrast agent concentrations obtained from the fit (step 1). This was done with varying time (2, 5, 10, 15, 30, 45, and 60 minutes) between acquisitions with the 90 and 50 kVp tube voltages. This was done for all the diffusion time points until diffusion equilibrium (72 hours).

Step 3. Using the simulated data gathered in step 2, concentrations of the contrast agents were calculated (Equations 2 and 3).

Step 4. The simulated concentration values were then compared with the true concentration values (from the fit) to get the relative error, as illustrated in Figure 5.

2.7 | Statistical analysis

The statistical analyses were conducted using SPSS (v. 23.0 SPSS Inc; IBM Company, Armonk, NY) statistical software. The reliability in the Mankin scoring between the raters was evaluated by determining the Interclass Correlation coefficient. Shapiro-Wilk test showed the sample data to follow the normal distribution. Therefore, the correlations of contrast agent partitions with histopathological and biomechanical reference parameters were evaluated using a parametric test (Pearson's correlation analysis) within a selected cartilage region. For all statistical tests, $P < .05$ was set as the limit of statistical significance.

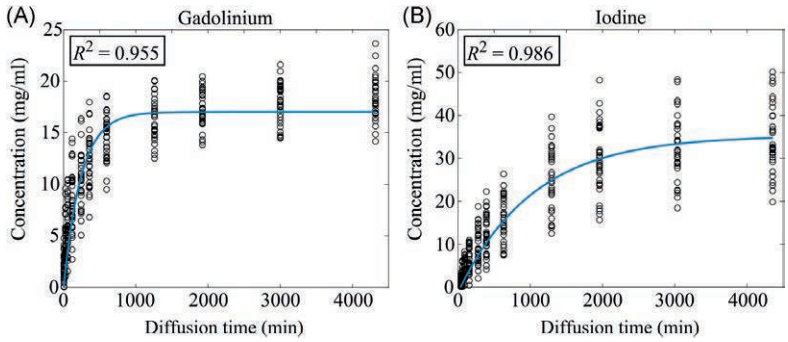

FIGURE 1 Full thickness cartilage concentration of (A) gadoteridol (gadolinium) and (B) CA4+ (iodine) presented as a function of diffusion time, C_{Gd} = 17 mg/mL (1-exp(-t/244 minute)) and C_I = 35 mg/mL (1-exp(-t/1032 minute)), respectively [Color figure can be viewed at wileyonlinelibrary.com]

3 | RESULTS

The CA4+ and gadoteridol partitions in cartilage increased from 14.4% ± 8.8% and 10.2% ± 5.6% at 10 minutes to 344.0% ± 77.9% and 91.4% ± 9.7% at 72 hours, respectively (Figures 1 and S11). The average C_{max} was 35 and 17 mg/mL, and τ was 1032 and 244 minutes, for the iodine (CA4+) and gadolinium (gadoteridol) in the cartilage, respectively. At 72 hours, the uptake of CA4+ was 2.5 times greater in deep cartilage compared with the superficial cartilage (Figure 2). The correlation coefficients between the Mankin score and CA+ partition of the full-thickness cartilage increased at all the diffusion time points after normalizing with the partition of the non-ionic gadoteridol (Figure 3). The Mankin score correlated significantly with gadoteridol partition from 10 minutes to 10 hours after the start of the immersion in contrast agent mix. The mean OD and thickness values of the cartilage samples were 1.07 ± 0.26 AU (min, 0.43; max, 1.47 AU), and 2.42 ± 0.68 mm (min, 1.01; max, 4.35 mm), respectively (Figure S12). The correlation coefficient between OD and CA4+ partition increased with the contrast agent diffusion time (Figure 4A). The correlation was significant in the earliest time points for the superficial 10% of cartilage ($P < .029$). The equilibrium modulus correlated significantly with the normalized CA4+ partition after 21 hours of diffusion ($P < .014$) and CA4+ partition after 32 hours of diffusion ($P < .004$) (Table 1). Based on the error simulation, a 2-minute delay between the acquisitions at the 10-minute diffusion time point would result in 74.4% and 23.5% relative error in determined CA4+ and gadoteridol partitions (Figure 5). At the 100-minute time point, the errors were 6.2% and 2.2% for CA4+ and gadoteridol, respectively. The mean Mankin score of all the samples was 6.27 ± 1.27 (min, 2; max, 9). The mean equilibrium modulus value for the samples was 0.26 ± 0.32 MPa (min, 0.01;

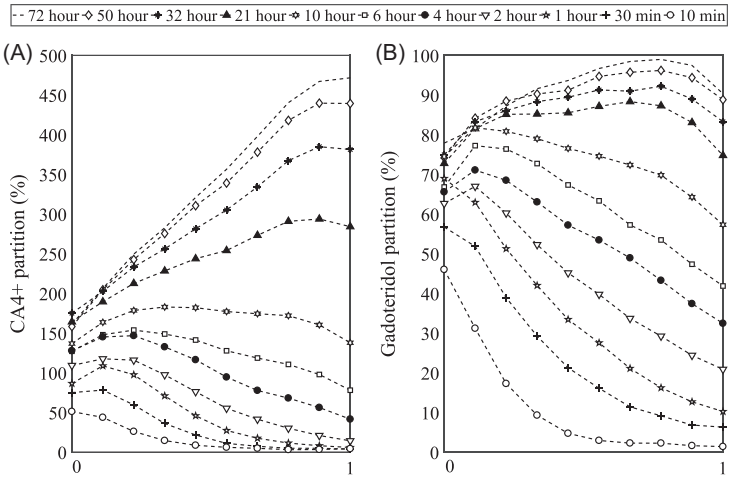

FIGURE 2 Mean contrast agent partition profiles in cartilage (N = 33, at 1 hour time point N = 30) in different diffusion time points; (A) Cationic iodine-based (CA4+) and (B) non-ionic gadolinium-based (gadoteridol) contrast agents. Cartilage (mean ± SD thickness 2.42 ± 0.68 mm) surface is denoted with 0 and cartilage-bone interface with 1

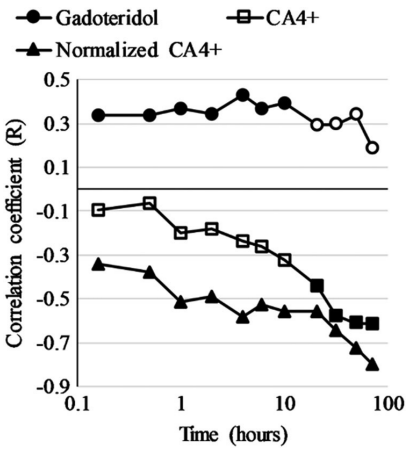

FIGURE 3 Correlation (Pearson's) coefficient between Mankin score and gadoteridol partition, CA4+ partition and CA4+ partition normalized with gadoteridol partition in the full thickness cartilage. Filled markers indicate statistically significant ($P < .05$) correlation

max, 1.49 MPa). The inter-rater reliability in the Mankin score was high (Inter-observer correlation = 0.93, $P < .01$). The Kruskal-Wallis test revealed no difference ($P > .79$) in the equilibrium modulus values 0.27 ± 0.36 and 0.25 ± 0.25 between the samples measured with indenters having tip diameters of 667 and 728 μm, respectively.

4 | DISCUSSION

In this ex vivo study, simultaneous diffusion of two contrast agents (CA4+ and gadoteridol) into cartilage was evaluated using a microCT scanner at multiple time points to probe cartilage composition and structural integrity. Normalization of the CA4+ partition with that of the gadoteridol improved the correlation with the Mankin score at all time points (Figure 3). Assessing cartilage structural integrity using only cationic agents at early time points is challenging as the uptake is comparably high in both intact and degenerated cartilage, due to high PG content, and increased permeability, respectively. This limits the sensitivity of cationic agents to quantify reduced PG content especially during the early points of contrast agent diffusion. Normalizing the CA4+ partition with that of gadoteridol improves its sensitivity to detect PG content. In this study, a similar effect is seen between CA4+ and PG content where the normalization with gadoteridol partition reveals a significant correlation six hours earlier, beginning at the 4-hour diffusion time point (Figure 4B).

During very early diffusion (<1 hour time points), the CA4+ significantly correlates with PG content (ie, OD, $P < .05$) in the superficial zone (10% of the cartilage thickness) (Figure 4A). Upon inspecting the first 20% of cartilage thickness, the correlation starts to be significant only after 6 hours of diffusion. In this zone, the normalization does not improve correlation with PG content

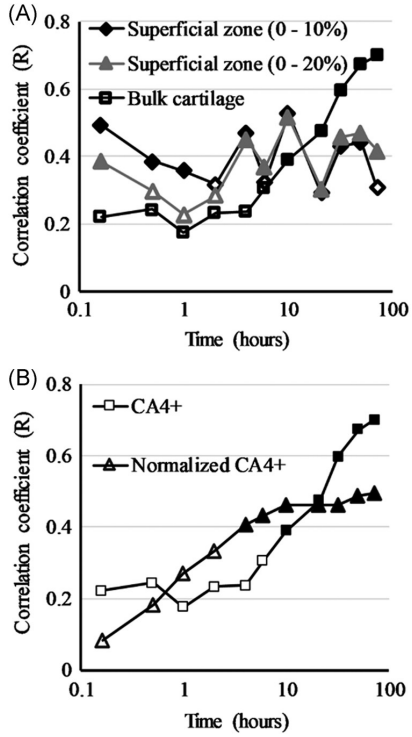

FIGURE 4 (A) The Pearson correlation coefficient between CA4+ partition and proteoglycan content (optical density) in the superficial (10% and 20%), and full thickness cartilage as a function of diffusion time. (B) Pearson correlation coefficient between the optical density and CA4+ partition (gadoteridol partition normalized and non-normalized) as a function of diffusion time. Filled markers indicate statistically significant ($P < .05$) correlation

(Table S1). This is likely due to the partial volume effect. In the full thickness cartilage, the correlation with PG content is relatively weak at early time points. However, with the diffusion of CA4+ into deep cartilage, the correlation becomes stronger and is significant ($P < .05$) after 10 hours of diffusion. The partition of CA4+ increases towards the deep cartilage at later diffusion time points (Figure 2). This is due to the increased electrostatic attraction, resulting from high PG content in the deep cartilage (Figure S13).[38,39] Concurrently, the water content in cartilage decreases towards the cartilage-bone interface.[5] Thus, expecting the gadoteridol partition to follow the trend of water content in cartilage, it is surprising to see the higher partitions in the deeper zones after the 21-hour diffusion time point. We suspect that this is a result of X-ray beam hardening, as very high uptake of the cationic agent is observed post 21-hour imaging time-point in the PG rich deep cartilage (Figure 2). Based on the present experiments and the results, we cannot determine whether the high CA4+ flux could have caused drag influencing the gadoteridol diffusion.[40] Additionally, the overall gadoteridol partition is not observed to rise after a 10-hour imaging time-point (Figure 1A).

TABLE 1 Pearson's correlation coefficients between contrast agent partitions ($N = 33$, at 1 h time point $N = 30$) and biomechanical moduli

	Time, min		Time, h								
	10	30	1	2	4	6	10	21	32	50	72
Equilibrium modulus, MPa											
CA4+	0.008	−0.129	0.156	0.071	0.162	0.186	0.209	0.311	**0.493****	**0.521****	**0.4 97** **
Normalized CA4+	0.212	−0.139	0.122	0.032	0.260	**0.330***	0.293	**0.422***	**0.654****	**0.730****	**0.648****
Gadoteridol	−0.218	−0.105	−0.192	−0.126	−0.246	−0.285	−0.246	−0.339	**−0.471***	**−0.453***	−0.282
Instantaneous modulus, MPa											
CA4+	−0.120	−0.048	0.223	0.131	0.172	0.182	0.131	0.169	0.216	0.209	0.176
Normalized CA4+	**0.534****	−0.064	0.177	0.043	0.170	0.248	0.178	0.213	**0.359***	**0.339***	**0.290***
Gadoteridol	−0.281	0.022	−0.124	0.035	−0.085	−0.140	−0.147	−0.176	**−0.441****	**−0.344***	−0.272

*Indicates that correlation is significant at the level $P < .05$ (two-tailed).

**Bold value Indicates that correlation is significant at the level $P < .01$ (two-tailed).

The correlation between the equilibrium modulus and CA4+ partition was significant and strengthened by the normalization after 21 hours until diffusion equilibrium. This was expected as the cationic agent's uptake is mostly due to the attraction to PG's, which controls cartilage biomechanical equilibrium response.[41] Therefore, it is natural that the CA4+ which is attracted by the PGs correlates strongly with equilibrium modulus.

Previously, we applied the QDECT technique to evaluate the cartilage PG and water contents at diffusion equilibrium (ie, after 72 hours of diffusion).[24,25] In the current study, we demonstrate the simultaneous determination of the solute concentration of two contrast agents in cartilage during diffusion at clinically relevant time points. The precise determination of the contrast agent partitions at early time points is possible with the use of short scan times (Figure 5).[15,24] In our previous study, reliable measurements during diffusion were impossible due to long imaging acquisition time (total of 28 minutes with two tube voltages) required by the applied microCT scanner (Skyscan 1172,;Skyscan, Kontich, Belgium).[24] With dual-contrast method, if the imaging is performed separately, an unavoidable error arises in the determination of partition of the contrast agent in cartilage. This is due to the ongoing diffusion during the imaging (in this study the time difference between acquisitions being ~2 minutes). In the present study, we evaluate this error using numerical simulations. An increase in time difference between the CT scans results in a higher error in the determined contrast agent partition values (Figure 5). The relative error is higher for CA4+ due to the higher diffusion flux of the cationic agent compared with that of the non-ionic gadoteridol. The short scan time enabled attenuation measurements of multiple contrast agents during diffusion, and more importantly, in the clinically relevant time points. With a modern dual-energy full-body CT scanner, the image acquisition at separate energies is simultaneous and practically instantaneous.[26] Hence, for the clinical application of the QDECT, this is not a source of significant error. However, the simulations will aid in the planning of the QDECT studies when imaging at two energies is performed separately.

The authors acknowledge limitations related to this study. The osteochondral plugs were extracted from a limited number of cadavers and from various locations: femur (lateral condyle = 4, medial condyle = 10), tibia (lateral plateau = 8, medial plateau = 7), and trochlea = 4. The availability of the cadaveric samples determined the sample size. As this was an exploratory study, and the effectiveness of the dual-contrast

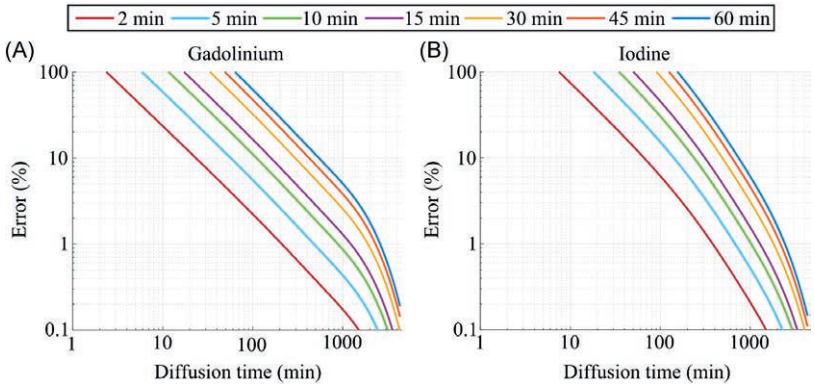

FIGURE 5 Simulation of error in (A) gadoteridol and (B) CA4+ partitions resulting from time (2 to 60 minutes) between acquisitions with the two X-ray tube voltages (90 and 50 kVp) [Color figure can be viewed at wileyonlinelibrary.com]

technique over the use of a single contrast agent in cartilage diagnostics was unknown, a power analysis was not conducted. Author's acknowledge that a higher number of samples would have enabled a more reliable evaluation of the diagnostic potential of the technique. The contrast agents' concentrations were selected to achieve the highest signal to noise ratio with the microCT scanner and toxicity issues were not taken into consideration. The development and introduction of a commercial clinical dual contrast application are not within the scope of this study, and the techniques may in the future rely on formulations differing from the ones applied here. The authors acknowledge the possibility of changes in cartilage properties arising from freeze-thaw cycles.[42] However, as all the samples were frozen and thawed following a uniform protocol, any changes in the mechanical/biological state between the samples should be similar.

The samples were immersed in the contrast agent bath maintained at 4°C. This temperature is lower than that during the intended clinical application of the agents in the human body (37°C). The time constant τ of CA4+ was 1032 minutes, being much higher than the value reported for diffusion in bovine cartilage at room temperature (τ =104.4 minutes, cartilage edges not sealed) (Figure 2).[15,43] With an increase in temperature, the diffusion rate of the contrast agent will also increase. Hence, at a warmer temperature, contrast agent diffusion will be faster, and reliable assessment of cartilage integrity may be conducted at earlier diffusion time point.

The challenges associated with the clinical application of the QDECT are yet to be explored. In the future, the QDECT should be tested on full knee joints using a clinical CT device, to obtain quantitative information on the capability of the technique to reveal cartilage matrix water and PG contents. In this study, we have demonstrated that QDECT allows the simultaneous determination of two different contrast agents in cartilage from early diffusion time-point (10 minutes) until diffusion equilibrium (72 hours). Normalization of the cationic contrast agent (CA4+) partition with that of the electrically neutral contrast agent (gadoteridol) enhances correlations with the histopathological and biomechanical characteristics allowing swifter determination of cartilage integrity. Thus, QDECT has the potential for diagnosis of cartilage degeneration at clinically relevant imaging time points.

ACKNOWLEDGMENTS

Antti Joukainen (MD), Tuomas Virén (PhD) and Juuso T.J. Honkanen (PhD) are acknowledged for assistance in sample extraction, and Amit N. Patwa (PhD) for preparing the CA4+ contrast agent. Sandra Sefa, (MSc) is acknowledged for assistance with the biomechanical measurements. Annina E.A. Saukko is acknowledged for assistance in sample holder preparation. Lassi Rieppo, Tarja Huhta, and Linda Rantamaa are acknowledged for the preparation of the histological section and Nina Hänninen for Mankin scoring of the cartilage sections. Academy of Finland (Projects 269315, 307932), State Research Funding of the Kuopio University Hospital Catchment Area (projects 5041746, 5041757, 5041769, PY210), and Päivikki and Sakari Sohlberg Foundation are acknowledged for financial support. Funding sources had no role in the design of the study, analysis, and interpretation of the results, or writing and submission of the manuscript for publication.

CONFLICT OF INTERESTS

Dr. Grinstaff reports a patent pending on CA4+ composition. The other co-authors declare no conflict of interests.

AUTHOR CONTRIBUTIONS

AB, BP, and JT designed the study. HK applied for ethical approval to obtain the cartilage samples. AB, MP, and, MH conducted the biomechanical measurements and analyses. RS, MP and, MH performed digital densitometry measurements and analyses. CA4+ was prepared in the laboratory of MG. Contrast agent diffusion measurements were conducted by AB and BP in the laboratory of HHW. AB, JM, and JT were involved in data analysis and interpretation of the results. AB drafted the manuscript and all co-authors contributed to the critical revision of the manuscript. All authors have read and approved the final version of the submitted manuscript.

ORCID

Abhisek Bhattarai http://orcid.org/0000-0003-3713-1349
Behdad Pouran https://orcid.org/0000-0003-1585-4917
Janne T. A. Mäkelä https://orcid.org/0000-0002-6123-1262
Rubina Shaikh https://orcid.org/0000-0003-4184-8254
Miitu K. M. Honkanen http://orcid.org/0000-0002-2548-4457
Mithilesh Prakash https://orcid.org/0000-0002-3853-4126
Heikki Kröger https://orcid.org/0000-0003-4245-8186
Mark W. Grinstaff http://orcid.org/0000-0002-5453-3668
Jukka S. Jurvelin https://orcid.org/0000-0001-6317-6685
Juha Töyräs https://orcid.org/0000-0002-8035-1606

REFERENCES

1. Ali TS, Prasadam I, Xiao Y, Momot KI. Progression of post-traumatic osteoarthritis in rat meniscectomy models: comprehensive monitoring using MRI. *Sci Rep*. 2018;8(1):6861.
2. Walker JA. Osteoarthritis:pathogenesis, clinical features, and management. *Nurs Stand*. 2009;24(1):35-40.
3. Olson SA, Furman BD, Kraus VB, Huebner JL, Guilak F. Therapeutic opportunities to prevent post-traumatic arthritis: lessons from the natural history of arthritis after articular fracture. *J Orthop Res*. 2015;33(9):1266-1277.
4. Bay-Jensen A-C, Hoegh-Madsen S, Dam E, et al. Which elements are involved in reversible and irreversible cartilage degradation in osteoarthritis? *Rheumatol Int*. 2010;30(4):435-442.
5. Mow VC, Ratcliffe A, Poole AR. Cartilage and diarthrodial joints as paradigms for hierarchical materials and structures. *Biomaterials*. 1992;13(2):67-97.
6. Saarakkala S, Julkunen P, Kiviranta P, Makitalo J, Jurvelin JS, Korhonen RK. Depth-wise progression of osteoarthritis in human articular cartilage: investigation of composition, structure and biomechanics. *Osteoarthr Cartil*. 2010;18(1):73-81.
7. Kaleva E, Saarakkala S, Jurvelin JS, Viren T, Toyras J. Effects of ultrasound beam angle and surface roughness on the quantitative ultrasound parameters of articular cartilage. *Ultrasound Med Biol*. 2009 Aug;35(8):1344-1351.
8. Matzat SJ, Kogan F, Fong GW, Gold GE. Imaging strategies for assessing cartilage composition in osteoarthritis. *Curr Rheumatol Rep*. 2014;16(11):462. Nov.
9. Gilbert ES. Ionising radiation and cancer risks: what have we learned from epidemiology? *Int J Radiat Biol [Internet]*. 2009;85(6):467-482. https://www.ncbi.nlm.nih.gov/pubmed/19401906

10. Jang J, Jung SE, Jeong WK, et al. Radiation doses of various CT protocols: a multicenter longitudinal observation study. *J Korean Med Sci*. 2016;31(suppl 1):S24-S31.
11. Kallioniemi AS, Jurvelin JS, Nieminen MT, Lammi MJ, Töyräs J. Contrast agent enhanced pQCT of articular cartilage. *Phys Med Biol*. 2007; 52(4):1209-1219.
12. Kokkonen HT, Jurvelin JS, Tiitu V, Töyräs J. Detection of mechanical injury of articular cartilage using contrast enhanced computed tomography. *Osteoarthr Cartil*. 2011;19(3):295-301.
13. Kokkonen HT, Aula AS, Kröger H, et al. Delayed computed tomography arthrography of human knee cartilage in vivo. *Cartilage*. 2012; 3(4):334-341.
14. Joshi NS, Bansal PN, Stewart RC, Snyder BD, Grinstaff MW. Effect of contrast agent charge on visualization of articular cartilage using computed tomography: exploiting electrostatic interactions for improved sensitivity. *J Am Chem Soc*. 2009;131(37):13234-13235.
15. Stewart RC, Bansal PN, Entezari V, et al. Contrast-enhanced CT with a high-affinity cationic contrast agent for imaging ex vivo bovine, intact ex vivo rabbit, and in vivo rabbit cartilage. *Radiology*. 2013;266(1):141-150.
16. Bansal PN, Joshi NS, Entezari V, et al. Cationic contrast agents improve quantification of glycosaminoglycan (GAG) content by contrast enhanced CT imaging of cartilage. *J Orthop Res*. 2011;29(5):704-709.
17. Lakin BA, Snyder BD, Grinstaff MW. Assessing cartilage biomechanical properties: techniques for evaluating the functional performance of cartilage in health and disease. *Annu Rev Biomed Eng*. 2017;19:27-55.
18. Bansal PN, Stewart RC, Entezari V, Snyder BD, Grinstaff MW. Contrast agent electrostatic attraction rather than repulsion to glycosaminoglycans affords a greater contrast uptake ratio and improved quantitative CT imaging in cartilage. *Osteoarthr Cartil*. 2011;19(8):970-976.
19. Lakin BA, Ellis DJ, Shelofsky JS, Freedman JD, Grinstaff MW, Snyder BD. Contrast-enhanced CT facilitates rapid, non-destructive assessment of cartilage and bone properties of the human metacarpal. *Osteoarthr Cartil*. 2015;23(12):2158-2166.
20. Weatherley ND, Eaden JA, Stewart NJ, et al. Contrast-enhanced computed tomography scoring system for distinguishing early osteoarthritis disease states: a feasibility study. *J Orthop Res*. 2019;74:611-619.
21. Adair GS. On the Donnan equilibrium and the equations of Gibbs. *Science*. 1923;58(1488):13.
22. Silvast TS, Kokkonen HT, Jurvelin JS, Quinn TM, Nieminen MT, Töyräs J. Diffusion and near-equilibrium distribution of MRI and CT contrast agents in articular cartilage. *Phys Med Biol [Internet]*. 2009; 54(22):6823-6836. http://www.ncbi.nlm.nih.gov/pubmed/19864699
23. Silvast TS, Jurvelin JS, Tiitu V, Quinn TM, Toyras J. Bath concentration of anionic contrast agents does not affect their diffusion and distribution in articular cartilage in vitro. *Cartilage*. 2013;4(1):42-51.
24. Bhattarai A, Honkanen JTJ, Myller KAH, et al. Quantitative dual contrast CT technique for evaluation of articular cartilage properties. *Ann Biomed Eng*. 2018;46(7):1038-1046.
25. Saukko AEA, Turunen MJ, Honkanen MKM, et al. Simultaneous quantitation of cationic and non-ionic contrast agents in articular cartilage using synchrotron microCT imaging. *Sci Rep*. 2019;9(1):7118.
26. Honkanen MKM, Matikka H, Honkanen JTJ, et al. Imaging of proteoglycan and water contents in human articular cartilage with full-body CT using dual contrast technique. *J Orthop Res*. 2019;37:1059-1070.
27. Mirahmadi F, Koolstra JH, Fazaeli S, et al. Diffusion of charged and uncharged contrast agents in equine mandibular condylar cartilage is not affected by an increased level of sugar-induced collagen cross-linking. *J Mech Behav Biomed Mater*. 2019;90:133-139.
28. Lattanzi R, Petchprapa C, Ascani D, et al. Detection of cartilage damage in femoroacetabular impingement with standardized dGEMRIC at 3 T. *Osteoarthr Cartil*. 2014;22(3):447-456.
29. Rautiainen J, Nieminen MT, Salo E-N, et al. Effect of collagen cross-linking on quantitative MRI parameters of articular cartilage. *Osteoarthr Cartil*. 2016;24(9):1656-1664.
30. Julkunen P, Korhonen RK, Herzog W, Jurvelin JS. Uncertainties in indentation testing of articular cartilage: a fibril-reinforced poroviscoelastic study. *Med Eng Phys*. 2008;30(4):506-515.
31. Hayes WC, Keer LM, Herrmann G, Mockros LF. A mathematical analysis for indentation tests of articular cartilage. *J Biomech*. 1972; 5(5):541-551. Sep.
32. Makela JTA, Han S-K, Herzog W, Korhonen RK. Very early osteoarthritis changes sensitively fluid flow properties of articular cartilage. *J Biomech*. 2015;48(12):3369-3376.
33. Fick JM, Huttu MRJ, Lammi MJ, Korhonen RK. In vitro glycation of articular cartilage alters the biomechanical response of chondrocytes in a depth-dependent manner. *Osteoarthr Cartil [Internet]*. 2014;22(10):1410-1418. http://linkinghub.elsevier.com/retrieve/pii/S1063458414011935
34. Kiviranta P, Rieppo J, Korhonen RK, Julkunen P, Toyras J, Jurvelin JS. Collagen network primarily controls Poisson's ratio of bovine articular cartilage in compression. *J Orthop Res*. 2006;24(4):690-699.
35. Lakin BA, Grasso DJ, Stewart RC, Freedman JD, Snyder BD, Grinstaff MW. Contrast enhanced CT attenuation correlates with the GAG content of bovine meniscus. *J Orthop Res*. 2013;31(11):1765-1771.
36. Kiviranta I, Jurvelin J, Tammi M, Saamanen AM, Helminen HJ. Microspectrophotometric quantitation of glycosaminoglycans in articular cartilage sections stained with Safranin O. *Histochemistry*. 1985; 82(3):249-255.
37. Mankin HJ, Dorfman H, Lippiello L, Zarins A. Biochemical and metabolic abnormalities in articular cartilage from osteo-arthritic human hips. II. Correlation of morphology with biochemical and metabolic data. *J Bone Joint Surg Am*. 1971;53(3):523-537.
38. Buschmann MD, Grodzinsky AJ. A molecular model of proteoglycan-associated electrostatic forces in cartilage mechanics. *J Biomech Eng*. 1995;117(2):179-192.
39. Bashir A, Gray ML, Boutin RD, Burstein D. Glycosaminoglycan in articular cartilage: in vivo assessment with delayed Gd(DTPA)(2-)-enhanced MR imaging. *Radiology*. 1997;205(2):551-558.
40. Honkanen MKM, Saukko AEA, Turunen MJ, et al. Synchrotron microCT reveals the potential of the dual contrast technique for quantitative assessment of human articular cartilage composition. *J Orthop Res*. 2019.
41. Canal Guterl C, Hung CT, Ateshian GA. Electrostatic and non-electrostatic contributions of proteoglycans to the compressive equilibrium modulus of bovine articular cartilage. *J Biomech*. 2010;43(7):1343-1350.
42. Peters AE, Comerford EJ, Macaulay S, Bates KT, Akhtar R. Micromechanical properties of canine femoral articular cartilage following multiple freeze-thaw cycles. *J Mech Behav Biomed Mater*. 2017;71: 114-121.
43. Albert Einstein. In: Furth R, On the movement of small particles suspended in a stationary liquid demanded by the molecular kinetic theory of heat. ed. *Investigations on the Theory of the, Brownian Movement*. Dover Publications, Inc; 1956.

SUPPORTING INFORMATION

Additional supporting information may be found online in the Supporting Information section.

How to cite this article: Bhattarai A, Pouran B, Mäkelä JTA, et al. Dual contrast in computed tomography allows earlier characterization of articular cartilage over single contrast. *J Orthop Res*. 2020;38:2230–2238. https://doi.org/10.1002/jor.24774

Paper **III**

Bhattarai A, Mäkelä JTA, Pouran B, Weinans H, Kröger H, Grinstaff MW, Töyräs J, Turunen MJ. "Effect of Human Articular Cartilage Constituents on Simultaneous Diffusion of Cationic and Non-ionic Contrast Agents."

Journal of Orthopaedic Research, 2020 in press.

Received: 4 April 2020 | Accepted: 5 August 2020

DOI: 10.1002/jor.24824

RESEARCH ARTICLE

Journal of Orthopaedic Research®

Effects of human articular cartilage constituents on simultaneous diffusion of cationic and nonionic contrast agents

Abhisek Bhattarai[1,2] | Janne T. A. Mäkelä[1] | Behdad Pouran[3] | Heikki Kröger[4] | Harrie Weinans[3,5] | Mark W. Grinstaff[6] | Juha Töyräs[1,2,7] | Mikael J. Turunen[1,8]

[1]Department of Applied Physics, University of Eastern Finland, Kuopio, Finland

[2]Diagnostic Imaging Center, Kuopio University Hospital, Kuopio, Finland

[3]Department of Orthopaedics, University Medical Center Utrecht, Utrecht, The Netherlands

[4]Department of Orthopedics, Traumatology and Hand Surgery, Kuopio University Hospital, Kuopio, Finland

[5]Department of Biomechanical Engineering, Faculty of Mechanical, Maritime, and Materials Engineering, Delft University of Technology (TU Delft), Delft, The Netherlands

[6]Departments of Biomedical Engineering, Chemistry, and Medicine, Boston University, Boston, Massachusetts

[7]School of Information Technology and Electrical Engineering, The University of Queensland, Brisbane, Australia

[8]SIB Labs, University of Eastern Finland, Kuopio, Finland

Correspondence
Abhisek Bhattarai, Department of Applied Physics, University of Eastern Finland, P.O. Box 1627, 70211 Kuopio, Finland.
Email: abhisek.bhattarai@uef.fi

Funding information
Academy of Finland, Grant/Award Number: 307932; State Research Funding of the Kuopio University Hospital Catchment Area, Grant/Award Number: 5041757 and 5041769; Instrumentariumin Science Foundation

Abstract

Contrast-enhanced computed tomography is an emerging diagnostic technique for osteoarthritis. However, the effects of increased water content, as well as decreased collagen and proteoglycan concentrations due to cartilage degeneration, on the diffusion of cationic and nonionic agents, are not fully understood. We hypothesize that for a cationic agent, these variations increase the diffusion rate while decreasing partition, whereas, for a nonionic agent, these changes increase both the rate of diffusion and partition. Thus, we examine the diffusion of cationic and nonionic contrast agents within degraded tissue in time- and depth-dependent manners. Osteochondral plugs ($N = 15$, $d = 8$ mm) were extracted from human cadaver knee joints, immersed in a mixture of cationic CA4+ and nonionic gadoteridol contrast agents, and imaged at multiple time-points, using the dual-contrast method. Water content, and collagen and proteoglycan concentrations were determined using lyophilization, infrared spectroscopy, and digital densitometry, respectively. Superficial to mid (0%-60% depth) cartilage CA4+ partitions correlated with water content ($R < -0.521$, $P < .05$), whereas in deeper (40%-100%) cartilage, CA4+ correlated only with proteoglycans ($R > 0.671$, $P < .01$). Gadoteridol partition correlated inversely with collagen concentration (0%-100%, $R < -0.514$, $P < .05$). Cartilage degeneration substantially increased the time for CA4+ compared with healthy tissue (248 ± 171 vs 175 ± 95 minute) to reach the bone-cartilage interface, whereas for gadoteridol the time (111 ± 63 vs 179 ± 163 minute) decreased. The work clarifies the diffusion mechanisms of two different contrast agents and presents depth and time-dependent effects resulting from articular cartilage constituents. The results will inform the development of new contrast agents and optimal timing between agent administration and joint imaging.

KEYWORDS

collagen, contrast-enhanced, proteoglycan, water

1 | INTRODUCTION

Articular cartilage is avascular, and its metabolic function is regulated via diffusion and convection of charged and uncharged solutes between the synovial fluid and the constituents of the cartilage extracellular matrix (ECM).[1] Cartilage ECM is a heterogeneous structure, mainly consisting of interstitial water (60%-85%), collagen fibrils (50%-80% of dry content), and negatively charged proteoglycans (PGs; 20%-30% of dry content).[2,3] Changes in the tissue composition alter the interstitial fluid flow [2,4] and mechanical properties.[5-7] The diffusion of a contrast agent inside the tissue, followed by subsequent contrast-enhanced imaging, provides information on the health status of the cartilage tissue.[8-12] For example, contrast-enhanced computed tomography (CECT) is used to evaluate osteoarthritis (OA)-related degeneration of cartilage and the associated alterations in the composition and morphology.[13-16]

CECT diffusion studies of articular cartilage typically employ a single contrast agent.[11,13,14,17] In diffusion equilibrium, the partition of a nonionic agent follows the depth-wise profile of the interstitial water content.[3,15] However, since OA-related degeneration of cartilage affects all cartilage constituents, as well as the structure, sensitive quantification of cartilage health based on the partition of only a nonionic agent, is challenging. Anionic agents similarly suffer from low sensitivity, as they diffuse against the fixed negative charge that prevails inside healthy articular cartilage. In contrast, cationic contrast agents molecules are attracted into the tissue through electrostatic attraction and are used to directly quantify cartilage PG concentration.[12,14,18]

Unhealthy articular cartilage possesses a disorganized collagen fibril network and increased permeability; thus facilitating agent diffusion.[19,20] However, the fixed charge density is concurrently reduced, because of the decrease in PG concentration, which slows down the diffusion of cationic agents. The combination of the two simultaneous and opposite effects complicates the interpretation of the acquired results, which in turn reflects the overall tissue health. To address this challenge, we recently introduced a dual-contrast agent technique. In this technique, two CT-based contrast agents (iodine I-based cationic, CA4+)[21] and gadolinium Gd-based nonionic agent [gadoteridol]) are employed simultaneously (Figure 1) and the molar concentrations of the agents are quantified using a dual-energy CT scan.[12,22,23] The premise is that normalization of the cationic contrast agent partition with that of the nonionic contrast agent allows early diagnostics, as the changes in the tissue's steric hindrance are accounted for. The dual-contrast method shows improved sensitivity and assessment of cartilage properties.[12,22,23] However, questions still remain regarding the effects of the cartilage constituents and its hierarchical structure on the diffusion, for example, how the contrast agent flux in the superficial zone of cartilage differs from that in the deep cartilage, and how agent diffusion relates to the variation in the depth-wise organization of the cartilage constituents?

In this study, we characterized the effects of the main cartilage constituent content, that is, PGs, collagen, and water, and their changes during OA-related cartilage degradation, on the simultaneous diffusion of cationic and nonionic contrast agents. We evaluated the composition of the human articular cartilage samples via microscopy and spectroscopy and measured the diffusion of the contrast agents by dual-contrast CECT.

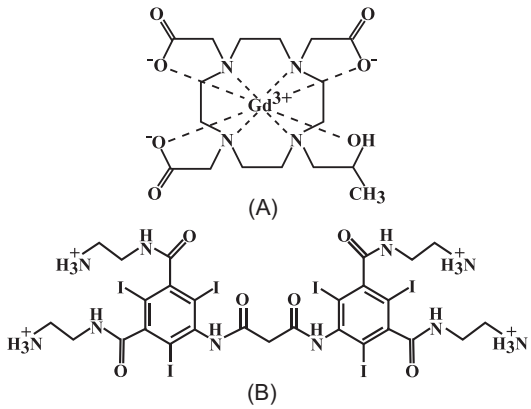

FIGURE 1 Molecular structure of (A) gadoteridol and (B) CA4+

2 | MATERIALS AND METHODS

2.1 | Sample extraction and microCT imaging

Human osteochondral plugs ($N = 15$, $d = 8$ mm) were extracted from the proximal tibiae and distal femora of left and right knee joints of four cadavers (male 1: 68 years, male 2: 68 years, male 3: 69 years, and female 1: 79 years of age). The research committee of the North Savo Hospital District (Kuopio University Hospital, Finland) gave a favorable opinion (statement number: 134/2015 [58/2013]) for the sample collection. After the extraction, the plugs were halved to separately conduct diffusion experiments and reference measurements (Figure 2). For the CECT experiment, diffusion of the contrast agent mixture was allowed only through the articulating surface by sealing the edges using cyanoacrylate (Superglue Precision, Loctite, Düsseldorf, Germany). The plugs were immersed in a contrast agent bath (5 mL, osmolality: 297 mOsm/kg, 4°C) comprising of CA4+, which is a hydrochloride salt of 5,5′-(malonylbis[azanediyl])bis(***N*^1^,*N*^3^**-bis(2-aminoethyl)-2,4,6-triiodoisophthalamide) (molecular formula: $C_{27}H_{36}C_{l4}I_6N_{10}O_6$, $q = +4$, $M = 1499$ g/mol, 10 mgI/mL) and gadoteridol (molecular formula: $C_{17}H_{29}GdN_4O_7$, Prohance, Bracco International B V, Amsterdam, The Netherlands, $q = 0$, $M = 559$ g/mol, 20 mgGd/mL), diluted in phosphate-buffered saline (PBS). The estimated molecular length and width of CA4+ is 29 Å and 18 Å, respectively.[24] The molecular size of gadoteridol was measured with a freely available open-source web-application to be ~11 Å long and ~6 Å wide (MolView, 2015).[25] The osmolality of the contrast agent bath was selected to be similar to physiological saline, which is safe for clinical application.[26] The bath was supplemented with following proteolytic

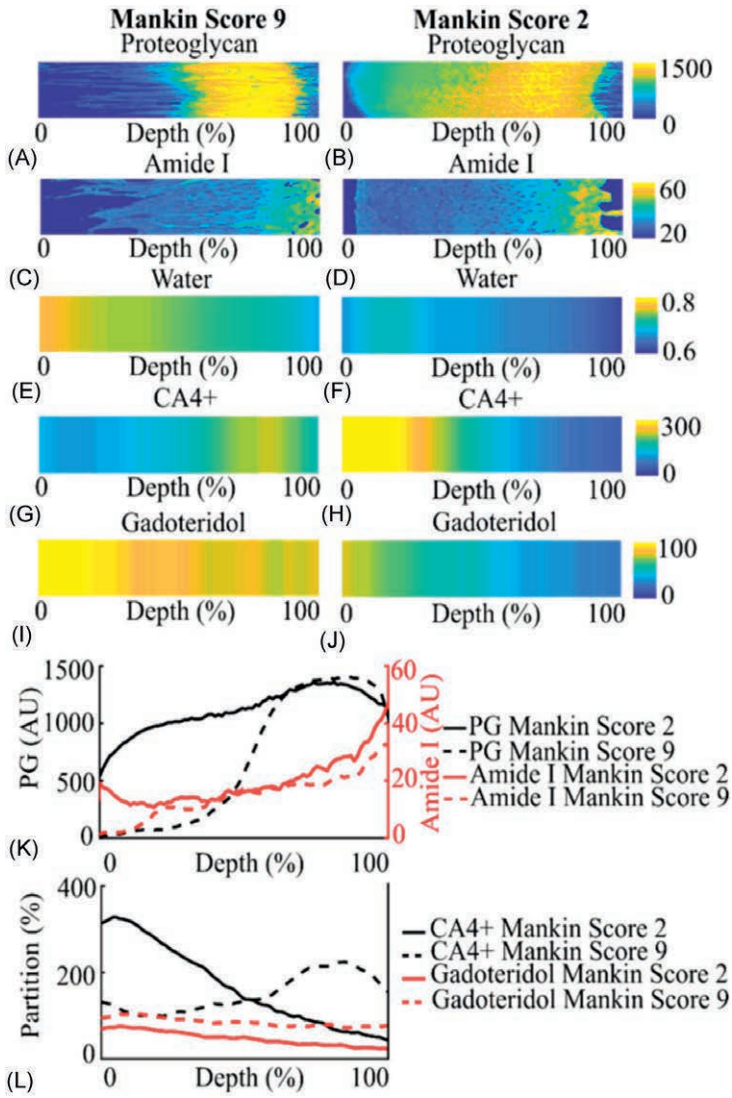

FIGURE 2 Depth-wise proteoglycan (A, B, and K) concentration, amide I (C, D, and K) concentration, and water (E and F) content in the human articular cartilage samples. CA4+ (G, H, and L), and gadoteridol (I, J, and L) partitions in samples with Mankin scores of 9 and 2 after 10 hour of contrast agent diffusion (not in equilibrium). [Color figure can be viewed at wileyonlinelibrary.com]

inhibitors: 5 mM of ethylenediaminetetraacetic acid (VWR International, France), 5 mM of benzamidine hydrochloride hydrate (Sigma-Aldrich Inc), and penicillin-streptomycin-amphotericin (antibiotic antimycotic solution, stabilized, Sigma-Aldrich Inc, St. Louis, MO). Plugs were imaged in the air with a high-resolution microCT scanner (Quantum FX, Perkin Elmer) using an isotropic voxel size of 40 × 40 × 40 µm and 20 × 20 mm field of view at two X-ray energies (tube voltages of 90 kV and 50 kV). Similarly, after 10 minute, 30 minute, and 1, 2, 3, 4, 6, 10, 21, 32, 50, and 72 hour of the immersion the samples were removed from the bath and imaged. During the immersion in the contrast agent, the baths were constantly stirred and kept at a temperature of 4°C.

2.2 | Image analysis

From the microCT images of the osteochondral plugs, the cartilage surface and the cartilage-bone interface were defined manually using a segmentation software (Seg3D, version 2.4.0, The University of Utah, Salt Lake City, UT). Depth-wise X-ray attenuation inside a selected cartilage volume of interest (2800 × 2000 µm × cartilage thickness) was analyzed using Matlab (R2018b, The Mathworks Inc, Natick, MA). The depth-wise concentration profiles of I and Gd-based contrast agents within the cartilage were resolved from the X-ray attenuation profiles (90 kV and 50 kV), based on the Beer-Lambert law and Bragg's additive rule of mixtures.[12,22,27,28] Time-dependent

contrast agent diffusion curves were determined for 20% thick sections (0%-20%, 20%-40%, 40%-60%, 60%-80%, and 80%-100% of cartilage depth) by fitting the following equation to the diffusion data $C = C_{max} \times [1 - \exp(-t/T)]$, where C_{max} is the contrast agent concentration maximum, t is the diffusion time, and T is the time required for the contrast agent to reach 63.2% of the maximum concentration.[18] The diffusion of the contrast agents was examined separately for five 20% thick cartilage sections with a partition threshold of 20%. This threshold was chosen to ensure sufficient temporal and spatial resolutions for determination of the contrast agent diffusion times.

2.3 | Reference methods

Water content measurements were carried out on the osteochondral halves used in the diffusion experiments. The contrast agents were washed out by immersing the halves in PBS solution, supplemented with proteolytic inhibitors and penicillin-streptomycin-amphotericin for 5 days, while constantly stirred and refrigerated at a temperature of 4°C. The samples were then embedded (LAMB-OCT, Thermo Fisher Scientific, Waltham, MA), fixed onto a frozen metallic sample holder, and placed inside a cryomicrotome (Leica CM3050 S, Leica Biosystems, Weltzar, Germany) chamber maintained at −21°C. To allow depth-dependent characterization, 200 µm thick cartilage sections were cut along the transverse plane from the articulating surface until the cartilage-bone interface, corresponding to an average of 11 slices per sample. The average thickness of the plugs was 2.35 ± 0.55 mm. The cut slices were freeze-dried inside a lyophilizer chamber (Christ, Alpha 1-2, B. Braun Biotech International, 37520 Osterode, Germany) for 48 hour by maintaining pressure 610.61 Pa. Each slice was weighed three times before and after the lyophilization and averaged. Depth-wise water content was then obtained by subtracting the dry weight with the wet weight of the slice.

To determine the PG concentration distribution, 3-µm thick sections were cut from the second half of the plug allocated for the reference measurements. The sections were stained with Safranin-O, and quantitative digital densitometry (DD) measurements (Figure 2A,B) were conducted using a light microscope (Nikon Microphot-FXA, Nikon Co, Japan) equipped with a monochromatic light source ($\lambda = 420 \pm 5$ nm) and a 12-bit CCD (ORCA-ER, Hamamatsu Photonics K.K., Japan).[29] Before the DD measurements, the system was calibrated using neutral density filters (Schott, Germany) with an OD range between 0 and 3. From the DD measurements, depth-wise OD profiles from the cartilage surface to cartilage-bone interface were calculated (Figure 2K).

Collagen concentration distribution was determined using Fourier Transform Infrared (FTIR) microspectroscopy system (Agilent Cary 670/620, Agilent Technologies Inc, Santa Clara, CA). For this, 3-µm thick sections were prepared from an area adjacent to the sections prepared for Safranin-O staining. Before the measurements, paraffin was removed, and the sections were moved onto Zinc-Selenide windows. Similar regions of interest were selected from three sections per sample covering the full thickness of cartilage (Figure 2C-D). The pixel size of 5.5 ×5.5 µm, spectral resolution 8 cm^{-1}, and eight repeated scans were selected to measure the spatially resolved infrared spectra of the cartilage. The infrared light absorption spectrum in each pixel was collected within the wavelength range of 3800 to 750 cm^{-1} and, amide I concentration was measured from the peak area ranging from 1720 cm^{-1} to 1595 cm^{-1}.[30] The depth-wise amide I concentration profiles were averaged from three sections per sample.

Histopathological Mankin score was assigned for the Safranin-O stained cartilage sections by four independent observers.[31] The grading (three sections per sample) is based on: (a) staining (0-4), (b) tidemark integrity (0-1), (c) abnormality in structure (0-6), and (d) cellularity (0-3). The Mankin score of the sections assigned by all the observers was finally averaged (Figure 2K).

2.4 | Statistical analysis

To evaluate the effect of cartilage degeneration on contrast agent diffusion the samples were grouped based on the Mankin score ("more degenerated": Mankin score > 5, $n = 8$, average score = 6.9 ± 1.1; "less degenerated": Mankin score ≤ 5, $n = 7$, average score = 4.6 ± 1.3). Depth-wise PG and collagen concentrations, and water content profiles were normalized to the length of 100 points and averaged (Figure 3). The association between the contrast agent partitions and the cartilage reference parameters was evaluated using Pearson's correlation. For all statistical tests, $P < .05$ was set as the limit of statistical significance. The significance of the difference in correlation coefficients between groups was tested with the Zou's method.[32] Throughout this paper, the average descriptive values of the sample properties are presented as mean ± SD. All statistical analyses were conducted using SPSS (ver 23.0 SPSS Inc, IBM Company, Armonk, NY).

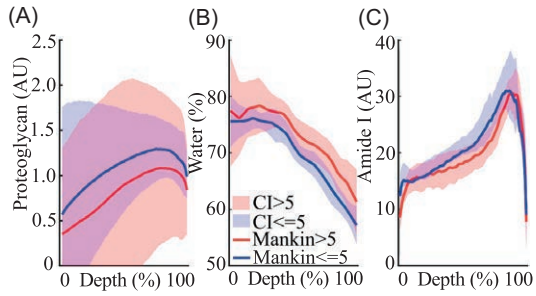

FIGURE 3 Depth-wise profiles with confidence intervals (CIs) of (A) proteoglycan concentration, (B) water content, and (C) collagen (amide I) concentration in human articular cartilage samples with Mankin score ≤5 and Mankin score > 5. [Color figure can be viewed at wileyonlinelibrary.com]

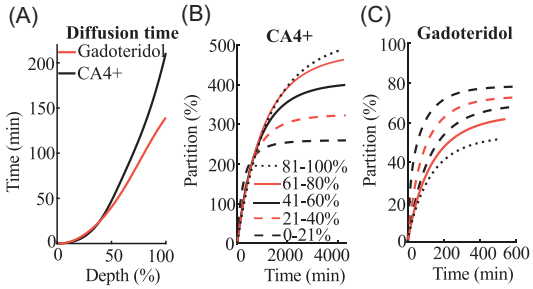

FIGURE 4 (A) The time required for the contrast agents partition to reach 20% of the bath concentration in each cartilage section. (B) CA4+ and, (C) gadoteridol partitions as a function of diffusion time at different 20% thick cartilage depths (sections). The initiation of diffusion in each section is assumed to begin when the contrast agent partition in the section reaches 20% of the contrast agent bath concentration. [Color figure can be viewed at wileyonlinelibrary.com]

3 | RESULTS

Histological analyses showed that PG and amide I concentrations predominantly increased while water content decreased as a function of cartilage depth (Figure 3).[30,33-35] The differences between the distributions of collagen (amide I) and PG concentration between more (Mankin score > 5) and less degenerated samples (Mankin score ≤ 5) were not statistically significant.

3.1 | Diffusion as a function of cartilage depth

The rate of diffusion was similar for CA4+ and gadoteridol until the agents reached 40% of the cartilage depth (Figure 4A). The average time (all the samples) for gadoteridol to reach the cartilage-bone interface was 141 ± 83 minute and for the CA4+ it was 216 ± 165 minute. This difference was statistically significant ($P < .01$) for the more degenerated samples where the time for gadoteridol was 111 ± 63 minute and for CA4+ 248 ± 171 minute. For the less degenerated samples, the times were 179 ± 163 minute and 175 ± 95 minute, respectively.

3.2 | Effects of cartilage constituents to the diffusion

The correlation between the cartilage constituents and the contrast agent partitions were studied at three time-points: 10, 21, and 72 hour. CA4+ concentration maximum ($C_{CA4+\ max}$, 72 hour) correlated significantly with the PG concentration ($R > 0.671$, $P < .01$) in the deeper cartilage (40%-100% of cartilage thickness) (Figures 5A and 6). At 72 hour, we observed a significant inverse correlation ($R < -0.521$, $P < .05$) with water content from the surface until 60% of cartilage depth (Figures 5B and 6). The maximum gadoteridol concentration ($C_{Gd\ max}$) correlated inversely with collagen concentration ($R < -0.514$, $P < .05$) at 21 hour of diffusion throughout the cartilage thickness (Figures 5C and 7). At the 72 hour time-point, $C_{Gd\ max}$ correlated inversely with the collagen concentration ($R < -0.705$, $P < .01$) at the superficial 40% of cartilage depth and correlated positively ($R > 0.567$, $P < .01$) with PG concentration from 40% depth until the cartilage-bone interface (Figures 5A and 7).

4 | DISCUSSION

In this study, we evaluate the effects of human articular cartilage constituents and structure on the simultaneous diffusion of cationic and nonionic contrast agents. By correlating the depth-wise composition of cartilage with the maximum contrast agent partitions, we show that the CA4+ partition in the superficial (0%-20%) and initial middle zone (20-40) is governed by the PG concentration and to a greater extent by the tissue water content ($R = 0.4$ vs $R = 0.54^*$ and $R = 0.45$ vs $R = 0.61^*$, respectively, $^*P < .05$). However, the differences in the correlations are not significant (Zou's method).[32] In the later middle (40%-60%) and deep (60-80 and 80%-100%) zones, the CA4+ partition strongly and significantly correlates with the PG concentration ($R = 0.67^*$, $R = 0.82^*$, and $R = 0.92^*$, respectively, $^*P < .05$). This finding is

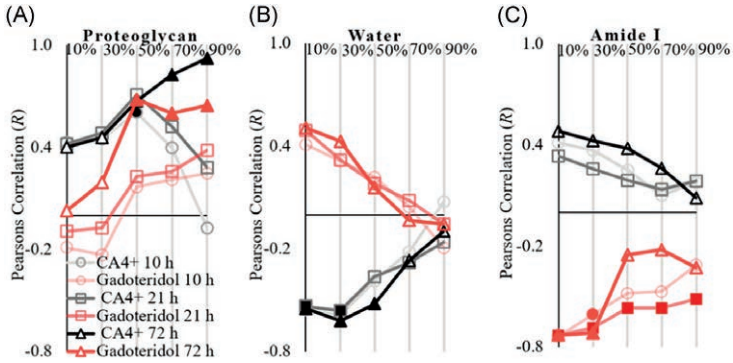

FIGURE 5 Pearson's correlation coefficients between maximum contrast agent concentration ($C_{CA4+\ max}$ and $C_{Gd\ max}$) and cartilage (A) proteoglycan concentration, (B) water content, and (C) collagen (amide I) concentration after 10, 21, and 72 hour of diffusion. Solid markers indicate a statistically significant correlation ($P < .05$) [Color figure can be viewed at wileyonlinelibrary.com]

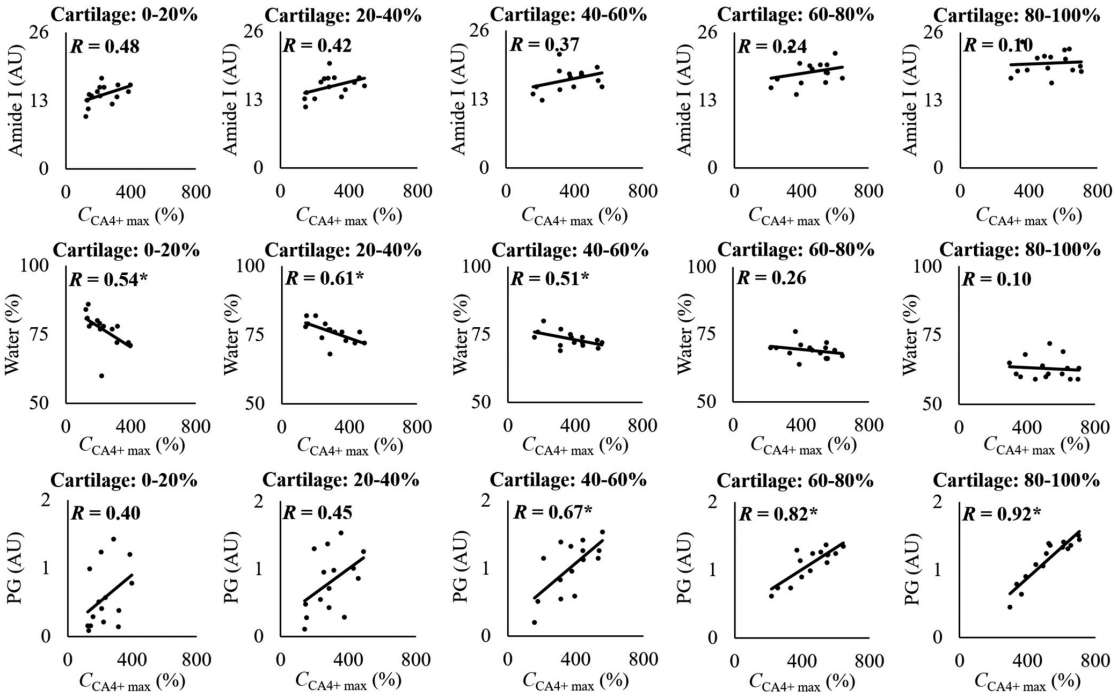

FIGURE 6 Scatterplots showing linear Pearson's correlations (*R*) between CA4+ maximum concentration at 72 hour (the time point closest to the diffusion equilibrium) and collagen (amide I), water, and proteoglycan (PG) concentrations at different 20% thick cartilage sections. Statistical significance is indicated with * when $P < .05$

consistent with the lower concentration of PG in the superficial/middle zones and the PG gradient present in cartilage.[36,37] In addition, contrary to the general perception,[15,36] the gadoteridol partition did not correlate with the water content. Instead, we observed a strong inverse relationship with the collagen concentration.

PG concentration governs CA4+ diffusion via the electrostatic attraction induced by the fixed negative charge.[38] A positive correlation between $C_{CA4+\ max}$ and the PG concentration exists in the middle to deep cartilage (ie, 40% depth to the calcified cartilage layer) (Figures 5A and 6). However, based on the current results, the PGs alone does not govern the diffusion of CA4+ in the superficial and middle zones (ie, from the articulating surface to ~40% of the cartilage depth). The $C_{CA4+\ max}$ inversely correlates with cartilage water content. This might be due to the loss of PGs or an increase in the water content in the superficial and middle zones, resulting from the loss of collagen integrity.[2] As expected, the collagen concentration had no direct effect on $C_{CA4+\ max}$ (Figures 5C and 7). Even though the depth-wise gadoteridol partition resembles the water distribution in cartilage (Figure 3B), the expected association between the water content and $C_{Gd\ max}$[3,39] are not statistically significant. Instead, $C_{Gd\ max}$ inversely correlates with the collagen concentration. This relation is a result of the collagen being the main solid constituent of the cartilage. In degenerated cartilage, the resulting collagen fibrillation allows more free fluid flow, that is, increased permeability and allowing swifter diffusion of contrast agents.[20,40] However, an inverse correlation exists between the water content and collagen concentration ($R = -0.62$, $P < .05$; Figure S1).

Structural degradation of cartilage, that is, collagen fibrillation and an increase in water content are important factors affecting the diffusion of the contrast agents (Figure 2). Our results show that the diffusion of the contrast agents is nonuniform throughout the thickness of the cartilage (Figure 4). The time required to reach 20% partition in the deep cartilage is longer for CA4+ than for gadoteridol (Figure 4A), and the time increases with advancing cartilage degeneration (ie, increased Mankin score). We surmise that this result is due to: (a) the larger molecule size of CA4+ (29 × 18 Å) compared with gadoteridol (11 × 6 Å); (b) degradation related decrease in PG concentration, reducing the electrostatic attraction, which is especially pronounced in the superficial and middle regions (Figure 3); and/or (c) the multivalent electrostatic interactions between CA4+ and PGs as it traverses the tissue, slowing the diffusion. All of the aforementioned factors result in increased time for the agent to reach deeper into the cartilage-bone interface. Previous studies reported a decrease in permeability towards the deep cartilage, due to the gradual increase in PG concentration, and similar findings are reported herein (Figures 3A and 3C).[41,42] As revealed in the present study, in the more degenerated samples the time for the cationic agent to reach the cartilage-bone interface is twice that of

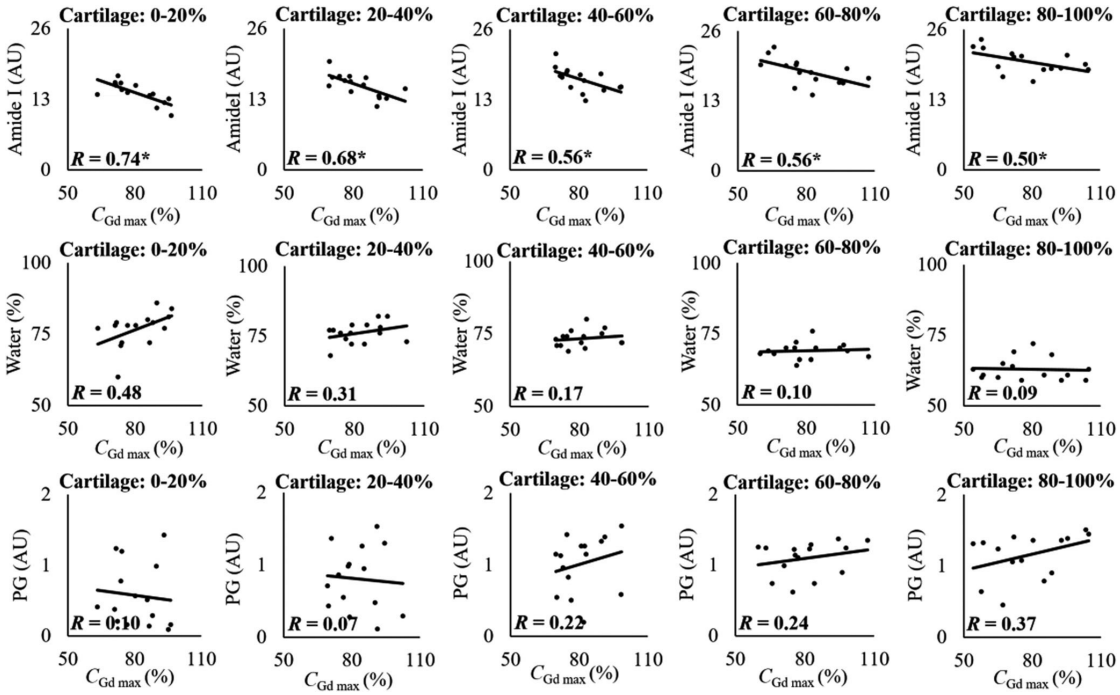

FIGURE 7 Scatterplots showing linear Pearson's correlations (*R*) between gadoteridol maximum concentration at 21 hour (the time point closest to the diffusion equilibrium) and collagen (amide I), water, and proteoglycan (PG) contents at different 20% thick cartilage sections. Statistical significance is indicated with * when $P < .05$

the nonionic agent, while no difference is seen with the less degenerated samples. These results add to the literature and further demonstrate that OA-related degradation of cartilage and associated compositional variations affect the contrast agent's partitions and their diffusion rates.[43,44]

The diffusion of cationic contrast agent (CA4+) in cartilage is governed by negatively charged PGs, tissue permeability, and water content. There were no significant correlations between amide I concentration and CA4+ partition in any diffusion time point or cartilage depth, and the correlations are similar between the diffusion time points (10, 21, and 72 hour) (Figure 5C). Gadoteridol reaches diffusion equilibrium between the 21 and 32 hour measurement time points (1745 minute). At this time-point, no correlation exists between the gadoteridol partition and the PG concentration. However, at the 72 hour diffusion time point, the gadoteridol partition strongly correlates with the PG concentration, whereas the correlation with collagen (amide I) concentration observed in the 21 hour time point is not present in the mid to deep cartilage sections. High diffusion flux of CA4+ has been suggested to cause drag influencing diffusion of gadoteridol.[45,46] However, current data and experiments are not sufficient to state whether the high uptake of CA4+ in deep cartilage influenced gadoteridol diffusion and decrease in correlation between amide I concentration and gadoteridol partition at 72 hour time point. Authors suspect the high partition and diffusion flux of CA4+ affected gadoteridol partition at 72 hour diffusion time point. Hence, we presented the correlation between gadoteridol partition and cartilage constituent content earlier, that is, at 21 hour diffusion time point (when gadoteridol diffusion was near equilibrium).

There are some limitations associated with the current study. The diffusion experiments and the reference (histological and spectroscopic) measurements were performed on the adjacent regions of the halved plugs. This might add error to the comparison between the diffusion properties and the reference data. However, since the regions were adjoining, we assume the state of samples to be relatively homogeneous across the halved plugs. The diffusion in cartilage was examined in a time- and depth-dependent manner, which required intact cartilage. The samples could not be sliced for water content measurement prior to the diffusion experiment. Even after washing out the contrast agents from the sample for 120 hours remnants of CA4+ might have persisted, adding to the weight of the slices. However, any remaining contrast agent would also stay attached during and after lyophilization, adding only a minimal error to the determined water content. The FTIR measurements provided the depth-dependent concentration of collagen (amide I) content in cartilage. Fibrillation and alteration in collagen fiber orientation precede the loss in collagen.[47] The present samples were mostly arthritic (average Mankin score = 5.6) with eroded superficial zones

(Figure 3C), which affects contrast agent diffusion. The information on the collagen fibril organization would have added to the interpretation contrast agents' diffusion properties, and lack of this information is acknowledged as a limitation of this study. The diffusion of the contrast agents was examined separately for five 20% thick cartilage sections. The concentration of contrast agents in every section depends on the concentration of the preceding cartilage section and the values are related to the equilibrium concentration. Thus, the extraction of diffusion coefficients will be a premise of future study requiring finite element modeling.[48]

To conclude, the diffusion of cationic contrast agents depends not only on the PG concentration but also on the water content, especially in the superficial and middle zones of cartilage. The diffusion of nonionic agents inversely relates to cartilage collagen concentration. The degenerative state of the cartilage governs contrast agent's diffusion rates; with cartilage degeneration, the diffusion rates of nonionic and cationic contrast agents increase and decrease, respectively. The results presented in this study increase the knowledge base and understanding of how the contrast agent diffusion and the resulting partitions depend on the composition and OA-related degradation of the articular cartilage. Furthermore, the present results will inform the timing between the contrast agent administration and the tomographic image acquisition.

ACKNOWLEDGMENTS

E Rahunen is acknowledged for assistance in cartilage section preparation for infrared spectroscopy, FTIR, and water content measurement. Academy of Finland (Project 307932), State Research Funding of the Kuopio University Hospital Catchment Area (projects 5041757 and 5041769), and Instrumentarium Science Foundation are acknowledged for financial support. Funding sources had no role in the design of the study, analysis, and interpretation of the results, or writing and submission of the manuscript for publication.

CONFLICT OF INTERESTS

The authors declare that there are no conflict of interests.

AUTHOR CONTRIBUTIONS

AB, JTAM, JT, and MJT designed the study. HK applied for ethical approval to obtain the cartilage samples. AB and BP performed the contrast agent diffusion experiment in the laboratory of HW. AB conducted water content measurements and digital densitometry analyses. AB and MJT conducted collagen content measurements and analyses. CA4+ was prepared in the laboratory of MG. AB, JTAM, JT, and MJT were involved in data analysis and interpretation of the results. AB drafted the manuscript, and all coauthors contributed to the critical revision of the manuscript. All authors have read and approved the final version of the submitted manuscript.

ORCID

Abhisek Bhattarai http://orcid.org/0000-0003-3713-1349
Janne T. A. Mäkelä https://orcid.org/0000-0002-6123-1262
Behdad Pouran https://orcid.org/0000-0002-1986-3741
Heikki Kröger https://orcid.org/0000-0003-4245-8186
Harrie Weinans https://orcid.org/0000-0002-2275-6170
Mark W. Grinstaff https://orcid.org/0000-0002-5453-3668
Juha Töyräs https://orcid.org/0000-0002-8035-1606
Mikael J. Turunen https://orcid.org/0000-0003-1093-1178

REFERENCES

1. Arbabi V, Pouran B, Weinans H, Zadpoor AA. Multiphasic modeling of charged solute transport across articular cartilage: application of multi-zone finite-bath model. *J Biomech*. 2016;49(9):1510-1517.
2. Mow VC, Holmes MH, Lai WM. Fluid transport and mechanical properties of articular cartilage: a review. *J Biomech*. 1984;17(5):377-394.
3. Mow VC, Ratcliffe A, Poole AR. Cartilage and diarthrodial joints as paradigms for hierarchical materials and structures. *Biomaterials*. 1992;13(2):67-97.
4. Makela JTA, Han S-K, Herzog W, Korhonen RK. Very early osteoarthritis changes sensitively fluid flow properties of articular cartilage. *J Biomech*. 2015;48(12):3369-3376.
5. Bank RA, Bayliss MT, Lafeber FP, Maroudas A, Tekoppele JM. Ageing and zonal variation in post-translational modification of collagen in normal human articular cartilage. The age-related increase in non-enzymatic glycation affects biomechanical properties of cartilage. *Biochem J*. 1998;330(Pt 1):345-351.
6. Walker JA. Osteoarthritis:pathogenesis, clinical features and management. *Nurs Stand*. 2009;24(1):35-40.
7. Maroudas A, Bullough P, Swanson SA, Freeman MA. The permeability of articular cartilage. *J Bone Joint Surg Br*. 1968;50(1):166-177.
8. Kokkonen HT, Aula AS, Kröger H, et al. Delayed computed tomography arthrography of human knee cartilage in vivo. *Cartilage*. 2012;3(4):334-341.
9. Lakin BA, Patel H, Holland C, et al. Contrast-enhanced CT using a cationic contrast agent enables non-destructive assessment of the biochemical and biomechanical properties of mouse tibial plateau cartilage. *J Orthop Res*. 2016;34(7):1130-1138.
10. Silvast TS, Jurvelin JS, Tiitu V, Quinn TM, Toyras J. Bath concentration of anionic contrast agents does not affect their diffusion and distribution in articular cartilage in vitro. *Cartilage*. 2013;4(1):42-51.
11. Honkanen JTJ, Turunen MJ, Freedman JD, et al. Cationic contrast agent diffusion differs between cartilage and meniscus. *Ann Biomed Eng*. 2016;44(10):2913-2921.
12. Bhattarai A, Honkanen JTJ, Myller KAH, et al. Quantitative dual contrast CT technique for evaluation of articular cartilage properties. *Ann Biomed Eng*. 2018;46(7):1038-1046.
13. Kokkonen HT, Suomalainen J-S, Joukainen A, et al. In vivo diagnostics of human knee cartilage lesions using delayed CBCT arthrography. *J Orthop Res*. 2014;32(3):403-412.
14. Joshi NS, Bansal PN, Stewart RC, Snyder BD, Grinstaff MW. Effect of contrast agent charge on visualization of articular cartilage using computed tomography: exploiting electrostatic interactions for improved sensitivity. *J Am Chem Soc*. 2009;131(37):13234-13235.
15. Silvast TS, Kokkonen HT, Jurvelin JS, Quinn TM, Nieminen MT, Töyräs J. Diffusion and near-equilibrium distribution of MRI and CT contrast agents in articular cartilage. *Phys Med Biol*. 2009;54(22):6823-6836.
16. Lakin BA, Ellis DJ, Shelofsky JS, Freedman JD, Grinstaff MW, Snyder BD. Contrast-enhanced CT facilitates rapid, non-destructive assessment of cartilage and bone properties of the human metacarpal. *Osteoarthr Cartil*. 2015;23(12):2158-2166.
17. Shafieyan Y, Khosravi N, Moeini M, Quinn TM. Diffusion of MRI and CT contrast agents in articular cartilage under static compression. *Biophys J*. 2014;107(2):485-492.

18. Stewart RC, Bansal PN, Entezari V, et al. Contrast-enhanced CT with a high-affinity cationic contrast agent for imaging ex vivo bovine, intact ex vivo rabbit, and in vivo rabbit cartilage. *Radiology*. 2013;266(1):141-150.
19. Ewers BJ, Jayaraman VM, Banglmaier RF, Haut RC. Rate of blunt impact loading affects changes in retropatellar cartilage and underlying bone in the rabbit patella. *J Biomech*. 2002;35(6):747-755.
20. Kokkonen HT, Jurvelin JS, Tiitu V, Töyräs J. Detection of mechanical injury of articular cartilage using contrast enhanced computed tomography. *Osteoarthr Cartil*. 2011;19(3):295-301.
21. Stewart RC, Patwa AN, Lusic H, et al. Synthesis and preclinical characterization of a cationic iodinated imaging contrast agent (CA4+) and its use for quantitative computed tomography of ex vivo human hip cartilage. *J Med Chem*. 2017;60(13):5543-5555.
22. Honkanen MKM, Matikka H, Honkanen JTJ, et al. Imaging of proteoglycan and water contents in human articular cartilage with full-body CT using dual contrast technique. *J Orthop Res*. 2019;37:1059-1070.
23. Saukko AEA, Turunen MJ, Honkanen MKM, et al. Simultaneous quantitation of cationic and non-ionic contrast agents in articular cartilage using synchrotron microCT imaging. *Sci Rep*. 2019;9(1):7118.
24. Bansal PN, Stewart RC, Entezari V, Snyder BD, Grinstaff MW. Contrast agent electrostatic attraction rather than repulsion to glycosaminoglycans affords a greater contrast uptake ratio and improved quantitative CT imaging in cartilage. *Osteoarthr Cartil*. 2011;19(8):970-976.
25. Bergwerf H MolView [Internet]. 2015. http://molview.org/. Accessed July 7, 2020.
26. Turunen MJ, Töyräs J, Lammi MJ, Jurvelin JS, Korhonen RK. Hyperosmolaric contrast agents in cartilage tomography may expose cartilage to overload-induced cell death. *J Biomech*. 2012;45(3):497-503.
27. Saukko AEA, Honkanen JTJ, Xu W, et al. Dual contrast CT method enables diagnostics of cartilage injuries and degeneration using a single CT image. *Ann Biomed Eng*. 2017;45:2857-2866.
28. Rangacharyulu C. *Physics of Nuclear Radiations Concepts, Techniques and Applications*. Park Drive, UK: Taylor and Francis; 2013:130.
29. Rieppo J, Töyräs J, Nieminen MT, et al. Structure-function relationships in enzymatically modified articular cartilage. *Cells Tissues Organs*. 2003;175(3):121-132.
30. Rieppo L, Kokkonen HT, Kulmala KAM, et al. Infrared microspectroscopic determination of collagen cross-links in articular cartilage. *J Biomed Opt*. 2017;22(3):35007.
31. Mankin HJ, Dorfman H, Lippiello L, Zarins A. Biochemical and metabolic abnormalities in articular cartilage from osteo-arthritic human hips. II. Correlation of morphology with biochemical and metabolic data. *J Bone Joint Surg Am*. 1971;53(3):523-537.
32. Zou GY. Toward using confidence intervals to compare correlations. *Psychol Methods*. 2007;12(4):399-413.
33. Makela JTA, Huttu MRJ, Korhonen RK. Structure-function relationships in osteoarthritic human hip joint articular cartilage. *Osteoarthr Cartil*. 2012;20(11):1268-1277.
34. Mow VC, Wang CC, Hung CT. The extracellular matrix, interstitial fluid and ions as a mechanical signal transducer in articular cartilage. *Osteoarthr Cartil*. 1999;7(1):41-58.
35. Cockman MD, Blanton CA, Chmielewski PA, et al. Quantitative imaging of proteoglycan in cartilage using a gadolinium probe and microCT. *Osteoarthr Cartil*. 2006;14(3):210-214.
36. Maroudas A. Distribution and diffusion of solutes in articular cartilage. *Biophys J*. 1970;10(5):365-379.
37. Silvast TS, Jurvelin JS, Lammi MJ, Toyras J. pQCT study on diffusion and equilibrium distribution of iodinated anionic contrast agent in human articular cartilage--associations to matrix composition and integrity. *Osteoarthr Cartil*. 2009;17(1):26-32.
38. Maroudas A. Physicochemical properties of cartilage in the light of ion exchange theory. *Biophys J*. 1968;8(5):575-595.
39. Kulmala KAM, Karjalainen HM, Kokkonen HT, et al. Diffusion of ionic and non-ionic contrast agents in articular cartilage with increased cross-linking: contribution of steric and electrostatic effects. *Med Eng Phys*. 2013;35(10):1415-1420.
40. Maleki M, Hashlamoun K, Herzog W, Federico S. Effect of structural distortions on articular cartilage permeability under large deformations. *Biomech Model Mechanobiol*. 2020;19:317-334.
41. Rieppo J, Hyttinen MM, Halmesmaki E, et al. Changes in spatial collagen content and collagen network architecture in porcine articular cartilage during growth and maturation. *Osteoarthr Cartil*. 2009;17(4):448-455.
42. Palmer AW, Guldberg RE, Levenston ME. Analysis of cartilage matrix fixed charge density and three-dimensional morphology via contrast-enhanced microcomputed tomography. *Proc Natl Acad Sci USA*. 2006;103(51):19255-19260.
43. Correa D, Lietman SA. Articular cartilage repair: Current needs, methods and research directions. *Semin Cell Dev Biol*. 2017;62:67-77.
44. Bay-Jensen A-C, Hoegh-Madsen S, Dam E, et al. Which elements are involved in reversible and irreversible cartilage degradation in osteoarthritis? *Rheumatol Int*. 2010;30(4):435-442.
45. Honkanen MKM, Saukko AEA, Turunen MJ, et al. Synchrotron microCT reveals the potential of the dual contrast technique for quantitative assessment of human articular cartilage composition. *J Orthop Res*. 2019;38(3):563-573.
46. Bhattarai A, Pouran B, Mäkelä JTA, et al. Dual contrast in computed tomography allows earlier characterization of articular cartilage over single contrast [published online ahead of print June 11, 2020]. *J Orthop Res*. 2020. https://doi.org/10.1002/jor.24774
47. Mäkelä JTA, Rezaeian ZS, Mikkonen S, et al. Site-dependent changes in structure and function of lapine articular cartilage 4 weeks after anterior cruciate ligament transection. *Osteoarthr Cartil*. 2014;22(6):869-878.
48. Arbabi V, Pouran B, Weinans H, Zadpoor AA. Transport of neutral solute across articular cartilage: the role of zonal diffusivities. *J Biomech Eng*. 2015;137(7):071001.

SUPPORTING INFORMATION

Additional supporting information may be found online in the Supporting Information section.

How to cite this article: Bhattarai A, Mäkelä JTA, Pouran B, et al. Effects of human articular cartilage constituents on simultaneous diffusion of cationic and nonionic contrast agents. *J Orthop Res*. 2020;1–9.
https://doi.org/10.1002/jor.24824

ABHISEK BHATTARAI

Current diagnostic tools lack sensitivity in detecting lesions and early post-traumatic degeneration in cartilage. To improve the diagnostics of the cartilage injuries, this thesis presents a novel computed tomography technique that simultaneously utilizes cationic and non-ionic contrast agents. The dual-contrast technique allows swifter characterization of cartilage structural and functional status, compared to a single contrast agent, and displays potential for sensitive diagnostics of joint and cartilage health.

UNIVERSITY OF
EASTERN FINLAND

uef.fi

**PUBLICATIONS OF
THE UNIVERSITY OF EASTERN FINLAND**
Dissertations in Forestry and Natural Sciences

ISBN 978-952-61-3576-2
ISSN 1798-5668